

**EFFECTS OF PLANT-DERIVED OLEANOLIC ACID
IN AN IN-VITRO MODEL OF HYPERGLYCAEMIA-
INDUCED OXIDATIVE STRESS**

By

Dlamini I. N (200301318)

**Submitted in fulfilment of the requirements for the degree of Master of Medical Science in
Human Physiology in the Discipline of Human Physiology, School of Medical Sciences, Faculty
of Health Sciences**

Supervisor: Dr M Zungu

Co-Supervisor: Prof M F Essop



**UNIVERSITY OF
KWAZULU-NATAL**

Declaration

I, Immaculate Nonkululeko Dlamini (200301318), hereby declare that the dissertation entitled **“Effects of plant-derived oleanolic acid in an in-vitro model of hyperglycaemia-induced oxidative stress”**

is the result of my own investigation and research and that it has not been submitted in part or in full for any other degree or to any other university. Where use was made of the work of others, it is duly acknowledged in the text.

Signatures:

H.O.D.....

Date.....

Supervisor.....

Date.....

Co-Supervisor.....

Date.....

Supervisee.....

Date.....

Acknowledgements

First and foremost to GOD: this project would not have been a success without you, indeed you deserve all the Glory.

To Dr Makhosazane Zungu, the encouragement, for believing in me guidance, advice supervision, and mostly your perseverance thank you so much may God bless your future. NRF and MRC for all the funding. I owe much to my co-supervisor Prof Essop it is a great blessing to have you as a supervisor, for I have received constant and committed guidance. To Dr Uthra Rajamani for everything, you were more than a supervisor to me your expertise, training, patience I couldn't have asked for more, Thank you.

My family oMalandela, mfolozi emnyama ikhetha abaweli, iNkosazane iyabonga iyanconcoza.

To Mark Magwaza, the moral support, strength, and a shoulder to cry on. I will not have made it this far, thank you Yengwayo.

To Rudo Mapanga and Mangazile Jawuza, thank you so much guys 2009 and 2010 would not be what it was if you two were not there.

CMRG research group, Dr Ben Loos (for all the technical assistance) Physiology department in Stellenbosch thank you guys for the warm welcome and sharing you space with me you made it easy for me to work in the Lab, wish you guys all the best in your studies.

To my research group at UKZN (Prof Musabayane, Prof Shode, Damien, Mark Tufts, Dennis Makhubela, Refiole, Sethu and Pretty). There is no end without the start; this project will have not started if you guys were not there. A special thank you to Mrs September and Family especially Crezelda Simons this project would not have been a reality, you were truly a God's sent for my breakthrough for the year.

My friends Audry, Lihle, Zama, Nhlakanipho, Resident life team 2010 (Westville and Edgewood campus), Dept of Career counselling Westville, you guys kept me going. Rev M Ximba, Mrs T Yaka your prayers and advice kept me grounded and focus.

Dedication

To my grandmother, MaNkosi ngeculo 111 kwawase-Sheshi

Table of contents

Chapters	Pages
Cover page	i
Declaration	ii
Acknowledgements	iii
Dedication	iv
Table of content	v-viii
Abbreviations	ix-xiii
List of tables and Figures	xiv-xvi
Abstract	xvii-xviii
Chapter 1	
1.1 Diabetes mellitus	1-2
1.2 Complications of diabetes mellitus	2
1.2.1 Acute Complications	3
1.2.2 Chronic Complications	3-4
1.2.3 Macrovascular Complications	4-5
1.3 Diabetes mellitus and cardiovascular diseases	5
1.3.1 Cardiac metabolism	5-8
1.3.2 Diabetic cardiomyopathy	8-11
1.4 Treatment and management of diabetes mellitus	11-12
1.4.1 Phytomedicine	12-13
1.4.2 <i>Syzygium aromaticum</i> (Hochst.) [Myrtaceae]	13-15

1.4.3 Bioactive compounds	16
1.4.4 Triterpenoids	16-19
1.5 Aim	19
1.5.1 Objectives	19
 Chapter 2	
2.1 Introduction	20-22
2.2 Materials and Methods	23
2.2.1 Plant Material	23
a) Isolation of oleanolic acid	23
b) Chromatographic Fractionation	23-25
c) Structure elucidation of oleanolic acid	26
2.2.2 Cell culture	26
a) High glucose and bioactive compound treatment	27-27
b) Measurement of intracellular reactive oxygen species	28-30
c) Seeding and staining for microscopy	31
d) Seeding and staining for flow cytometer	32
e) Statistical analysis	33
2.3 Results	34
2.3.1 Structural elucidation of oleanolic acid	34-37
2.3.2 <i>In- vitro</i> model of hyperglycaemia-induced oxidative stress in cardiac myocytes	38-40
2.3.3 Effects of oleanolic treatment acid on glucose-exposed H9C2 cell line	41-48

2.4 Discussion	49
2.4.1 <i>Syzigium aromaticum</i> (cloves) derived oleanolic acid	49
2.4.2 <i>In- vitro</i> model of hyperglycaemia-induced oxidative stress	49-51
2.4.2 Effects of plant derived triterpene (oleanolic acid) on treated H9C2 cell line	51-53

Chapter 3

3.1 Introduction	54-55
3.1.1. The extrinsic cell death pathway	55-56
3.1.2 The intrinsic cell death pathway	56-57
3.1.3 Apoptosis and diabetic cardiomyopathy	58
3.2 Materials and Methods	59
3.2.1 Cell culture	59
3.2.2 Cell Treatment	59-60
3.2.3 <i>In- vitro</i> model of high glucose induced apoptosis in H9C2 cell line	61-69
a) Caspase activity assay	61-63
b) Western blots for Caspase 3	63-65
i) Electrophoresis (SDS-PAGE)	64
c) Annexin-V staining	65-66
d) Mitochondrial membrane potential	66-67
i) Seeding and staining for microscopy	67-68

ii) Seeding and staining for flow cytometer	68-69
3.3 Statistical analysis	69
3.4 Results	70
3.4.1 Caspase 3 assay	70-72
3.4.2 Western blots for Caspase3	73-76
3.4.3 Mitochondrial membrane potential	77-80
3.4.4 Annexin V- FITC staining	81-83
3.5 Discussion	84
3.5.1 Annexin V-FITC staining	84-85
3.5.2 Mitochondrial membrane potential	85-86
3.5.3 Western blots for Caspase 3	86-87
3.5.4 Caspase 3 assay	87-88
Chapter 4	
4.1 General discussion	89-90
4.2 Limitations and recommendations for future studies	90
Chapter 5	
5.1 References	91-104

Abbreviations

μM	micromolar
ACC	Acetyl-CoA carboxylase
AGE	Advanced glycation end-product
AIF	Apoptotic inducing factor
AMPK	Adenosine monophosphate protein kinase
ANOVA	One way analysis of variance
Apo B	Apolipoprotein B
ATP	Adenosine triphosphate
C ₂₀	Carbon 20
Ca ²⁺	Calcium
cAMP	Cyclic adenosine monophosphate
CC	Column chromatography
CMXRos	Chloromethyl- X-rosamine
CO ₂	Carbon dioxide
Cyt c	Cytochrome c
DAG	Diacylglycerol
DAPI	4'-6' diamidino-2-phenylindole
DCF	Dichloro fluorescein
DCFDA	Dichloro fluorescein diacetate
DCM	Dichloromethane soluble
DM	Diabetes mellitus
DMEM	Dulbecco's Modified Eagle's medium

DMSO	Dimethyl sulphoxide
DNA	Deoxy ribonucleic acid
EAS	Ethyl acetate solubles
FA	Fatty acids
FADH ₂	Flavin adenine dinucleotide
FBS	Foetal bovine serum
FFA	Free fatty acids
FITC	Fluorescein isothiocyanate
FSC	Forward scatter
GADPH	Glyceraldehyde-3-phosphate dehydrogenase
GLUT (s)	Glucose Transporter(s)
GLUT-1	Glucose transporter-1
GLUT-4	Glucose transporter-4
H ₂ DCFDA	1, 2 dihydroxydichloro fluorescein diacetate
H ₂ O ₂	Hydrogen peroxide
H ₂ SO ₄	Sulphuric acid
HCl	Hydrochloric acid
HMQC	Heteronuclear multiple quantum coherence
ICAM-1	Intracellular cell adhesion molecule-1
IR	Insulin receptor
JC-1	5,5,6,6-tetrachloro-1,1,3,3-tetraethylbenzimidazolcarbocyanine-
I	Iodine
K ⁺	Potassium

K_{ATP}	Adenosine-5'- triphosphate sensitive potassium channels
KCl_2	Potassium chloride
Kg	kilogram
l	litre
LDL	Low density lipoprotein
LTD	limited
M	Molar
MAP	Mean arterial pressure
MAPK	Mitogen-activated protein kinase
mg	milligram
MHz	millihertz
mM	millimoler
mRNA	messenger ribo-nucleic acid
Mv	micromolar volts
NaCl	Sodium chloride
NAD^+	Oxidised nicotinamide dinucleotide
NADH	Nicotinamide adenine dinucleotide hydrogen
NADPH	Nicotinamide adenine dinucleotide phosphate hydrogen
NF- $\kappa\beta$	Nuclear factor-kappa beta
NMR	Nuclear Magnetic Resonance
NOs	Nitric oxide synthase
O_2^-	Superoxide
O_2	Oxygen

OA	Oleanolic acid
OH	Hydroxyl radical
ONOO ⁻	Peroxynitrite
PAGE	Polyacrylamide gel electrophoresis
PBS	Phosphate buffer solution
PDH	Pyruvate dehydrogenase
PDK	PDH kinase
PFK	Phosphofructokinase
PGC	PPAR coactivator
PKC	Protein kinase C
PPAR's	Peroxisome proliferator-activated receptor(s)
PPAR- α	Peroxisome proliferator-activated receptor alpha
PPAR- γ	Peroxisome proliferator-activated receptor gamma
PPAR- δ	Peroxisome proliferator-activated receptor delta
ppm	parts per million
PS	Phosphatidyl serine
RAGE	Receptor for advanced glycation end product
ROS	Reactive oxygen species
<i>S aromaticum</i>	<i>Syzigium aromaticum</i>
SDS	Sodium dodecyl sulphate
SEM	Standard error of mean
SGLT-2	Sodium glucose transporter-2
SOD	Superoxide dismutase

STZ	Streptozotocin
TCA	Tricarboxylic acid
TGF- β	Transforming growth factor beta
TLC	Thin layer chromatography
TMB	3,3',5,5' Tetramethylbenzidine
TMRM	Tetramethylrhodaminemethylester
TNF- α	Tumour necrosis factor alpha
TZD	Thiazolidinediones
UA	Ursolic acid
UDP	Uridine diphosphate
UDP-GlycNac	Uridine diphosphate acetylglucosamine
UK	United Kingdom
UKPDS	United Kingdom Prospective Diabetes Study
UKZN	University of KwaZulu-Natal
USA	United States of America
VCAM-1	Vascular cell adhesion molecule-1
VEGF	Vascular endothelial growth factor
WHO	World health organisation
α	Alpha
β	Beta
μ	micro
μg	microgram
μl	microlitre

List of tables and figures

Page no. **Figure no**

Chapter 1

- 14 Figure 1: *Syzygium aromaticum* leaves with green flower buds (Top
Tropicals.com)
- 15 Figure 2: Sun dried unopen flower buds (Cloves) (Top Tropicals.com)
- 17 Figure 3: The chemical structure of ursolic acid and oleanolic acid

Chapter 2

- 25 Figure 4: A schematic representation of chromatographic fractionation
- 27 Figure 5: A schematic representation of the experimental procedure
- 30 Figure 6: Illustration of flow cytometer instrumentation.
- 35 Figure 7: Chemical structure (A) and carbon numbering (B) of oleanolic acid
- 36 Figure 8: One dimensional ^1H and ^{13}C - NMR spectra of oleanolic acid isolated
from *Syzygium aromaticum* (cloves) (A-B) and two dimensional ^1H and ^{13}C -
NMR spectra by Distortion Enhancement Proton Transfer (DEPT) (C) and
heteronuclear multiple quantum coherence (HMQC) (D).
- 37 Table 1: ^{13}C (100.64 MHz) Bruker Avance III NMR spectral data of plant-derived
OA and documented OA
- 39 Figure 9: Effects of 54 hrs high glucose treatment on ROS production in H9C2
cell line.
- 40 Figure 10: Effects of 72 hrs high glucose treatment on ROS production in H9C2
cell line.

- 42 Figure 11: Effects of 6 hr OA treatment on ROS production in low glucose exposed H9C2 cell line.
- 44 Figure 12: Effects of 6 hr OA treatment on ROS production in high glucose exposed H9C2 cell line.
- 46 Figure 13: Effects of 24 hr OA treatment of low glucose exposed H9C2 cells on ROS production.
- 48 Figure 14: ROS production of 24 hr OA treatment in high glucose exposed H9C2 cells.

Chapter 3

- 57 Figure 15: A schematic representation of intrinsic and extrinsic apoptotic pathways.
- 60 Figure 16: A schematic representation of the experimental procedure.
- 62 Figure 17: A schematic representation of the Caspase-Glo[®] 3/7 assay.
- 70 Figure 18: Caspase activity for H9C2 cells treated with high glucose.
- 71 Figure 19: Effects of 6 hr OA treatment on caspase activity in H9C2 cell line.
- 72 Figure 20: Effects of 24 hr OA treatment on caspase activity in H9C2 cell line.
- 73 Figure 21: Effect of 6hr OA treatment on caspase-3 protein in A) normal and B) high glucose exposed H9C2 cells.
- 76 Figure 22: Effect of 24 hour OA treatment on caspase-3 protein expression in A) normal or low and B) high glucose exposed H9C2 cells.
- 77 Figure 23: Effect of 6 hrs OA treatment on mitochondrial membrane potential in low glucose exposed H9C2 cells.

- 78 Figure 24: Effect of 6 hrs OA treatment on mitochondrial membrane potential in high glucose treated H9C2 cells.
- 79 Figure 25: Effect of 24 hrs OA treatment on mitochondrial membrane potential in normoglycaemic treated H9C2 cell.
- 80 Figure 26: Effect of 24 hrs OA treatment on mitochondrial membrane potential in hyperglycaemic treated H9C2 cells.
- 81 Figure 27: Effects of OA treatment on apoptosis in H9C2 cell line.
- 82 Figure 28: Effects of 6 hr OA treatment on apoptosis in H9C2 cell lines.
- 83 Figure 29: Effects of 24 hr OA treatment on apoptosis in H9C2 cell lines

Abstract

Introduction

Diabetes mellitus (DM) has become a global threat in developing and developed countries, where diabetic patients are more prone to cardiovascular complications, a condition called diabetic cardiomyopathy. Studies have shown a direct link between hyperglycaemia and an increase in the production of reactive oxygen species in cardiac cells leading to diabetic cardiomyopathy. This study tests oleanolic acid, a bioactive compound from the plant *Syzigium aromaticum* as an antioxidant which could have a potential role in management of DM.

Aims

i) To extract Oleanolic acid (OA) from *Syzigium aromaticum*, ii) Investigate the antioxidant effects of plant derived OA in an *in-vitro* model of hyperglycaemia induced oxidative stress.

Methods

The flower buds of the *Syzigium aromaticum* [(Linnaeus) Merrill & Perry] (Myrtaceae) plant (commonly called cloves) were used to isolate OA. The ethyl acetate solubles from the cloves were subjected to chromatographic fractionation to yield OA powder. Spectroscopic analysis was done using 1D and 2D ^1H and ^{13}C NMR techniques for the identification of the structure of the compound. This compound was then used *in vitro* to test for its antioxidative properties. H9C2 cardiac myoblasts were employed which were treated with normoglycaemic (5.5 mM) and hyperglycaemic (33 mM) glucose conditions. The cells were then treated with oleanolic acid to test for its antioxidant properties. We looked at a dose-dependent (0, 20, 50 μM) and time-dependent effects of OA treatment (6 and 24 hrs) following 48 hours glucose exposure. ROS levels were measured using $\text{H}_2\text{DCF-DA}$ fluorescence staining using microscopy and flow cytometry techniques for analysis.

Results

Recrystallisation of the powder with ethanol and inspection of the 1 and 2- dimensional ^1H - and ^{13}C -NMR spectra of the compound with comparison to literature data confirmed OA molecular structure and IUPAC numbering similar to that of literature characterized and confirmed the structure of oleanolic acid.

In cell specific data high glucose treatments on H9C2 cells showed increased ROS production ($22 \pm 6 \%$ and $20 \pm 7 \%$ $n=3$ $p<0.01$) for 6 and 24 hrs treatments, respectively, compared to their normoglycaemic control groups. The 6 h OA treated group showed a decrease in ROS production with $26.6 \pm 17.4 \%$ for the $20 \mu\text{M}$ while for $50 \mu\text{M}$ there was a $37.7 \pm 14.3\%$ decrease. A ROS reduction trend was observed in the normoglycaemic group, but this was significant at 24 hrs with $46.8 \pm 45.3\%$ and $57.3 \pm 9 \%$ for both 20 and $50 \mu\text{M}$ treatments, respectively. The 24 hrs OA treated group showed a dose-dependent decrease in ROS with $50 \mu\text{M}$ more pronounced ($80.7\% \pm 4.5 \%$). The $20 \mu\text{M}$ OA treatments also showed a $15.7 \pm 19 \%$ decrease in ROS.

Discussion

In the present study, we have evaluated the antioxidant effects of OA *in vitro* following extraction of the compound from *Syzigium aromaticum*. The oxidative stress induced by hyperglycaemia was attenuated by oleanolic acid and this also translated into decreased ROS suggesting its use as an antioxidant in alleviating cardiovascular complications associated with diabetes mellitus.

Chapter 1

1.1 Diabetes mellitus

Diabetes mellitus (DM) is an endocrine disorder mainly characterised by insufficient secretion or receptor insensitivity to the endogenous insulin thereby resulting in hyperglycaemia (Brownlee, 2001; Rolo and Palmeira 2006). Hyperglycaemia is a prominent feature in DM (Pacher *et al.*, 2007). Classical symptoms of DM include polydipsia, polyuria, polyphagia, blurred vision and weight loss (Brownlee 2001; Dinneen, 2006). DM is also associated with obesity and dyslipidemia (Pacher *et al.*, 2007). A steady blood glucose level is maintained by the secretion of insulin from the β cells of the pancreas (Dinneen, 2006; William *et al.*, 2008). DM is classified into three different types according to this hormonal effect and these are discussed below.

Type 1 DM is characterized by loss of the β cells in the pancreas as a consequence of an autoimmune attack by the T- cells (William *et al.*, 2008). This loss of β cells is associated with prolonged hyperglycaemia which occurs as a consequence of reduced glucose uptake by the liver and skeletal muscle and a relative increase in glucagon secretion and gluconeogenesis (Pacher *et al.*, 2007). Type 1 DM is diagnosed early in life and is therefore referred to as juvenile DM. Type 1 DM is also referred to as insulin dependent as it is managed by insulin replacement therapy to supplement the insufficiently produced insulin or assist β cells response to external stimuli (Palters *et al.*, 2004).

Type 2 DM is characterised by peripheral insulin resistance in skeletal muscle and the liver causing an increased glucose output. In addition, there might be pancreatic β cell dysfunction

which leads to a relative decrease of insulin secretion (Hall and Davies 2008; Rao, 2007). Frequently diagnosed in matured patients, Type 2 DM is associated with high calorie nutrition and obesity. Genetic inheritance is another crucial factor in the development of Type 2 DM. For instance, approximately $\leq 20\%$ new cases of Type 2 DM have been diagnosed in children and adolescents (Prosch *et al.*, 2004; Greenspan and Gardner 2004). Good management of diet in conjunction with frequent exercise and medication for lowering hyperglycaemia are vital in potentiating insulin sensitivity.

Gestational diabetes mellitus manifests in about 2%-5% of all pregnancies (Rao, 2007). Complications in pregnant women results in hypertension, pre-eclampsia and increased risk of developing Type 2 DM, while 20%-50% of these women may develop Type 2 DM later in life (Buchanan and Xiang, 2005). The precise mechanisms for the development of gestational DM are still obscure. However, changes in metabolism during pregnancy occur to support nutritional requirements for the developing foetus. In addition to insulin, hormones secreted during pregnancy may also play a role in the metabolic changes. For instance, increased fat deposition together with placental hormones (cortisol and progesterone) during pregnancy mediates insulin resistance by promoting β cell hyperplasia and increased insulin release leading to peripheral insulin resistance (Buchanan *et al.*, 2002; Carr and Gabbe 1998).

1.2 Complications of diabetes mellitus

Numerous acute and chronic complications are manifested with diabetes mellitus (Rao, 2007). Hyperglycaemia is an independent risk factor that induces acute and chronic diabetic complications (Cai *et al.*, 2002).

1.2.1 Acute Complications

Some of the acute complications associated with DM are known to lead to frequent admission into intensive care units (Williams *et al.*, 2008). These include hypoglycaemia, non-ketotic hyperosmolar diabetic coma and ketoacidosis (Fong, 2002; Williams *et al.*, 2008). Diabetic ketoacidosis is prevalent in patients with Type 1 DM and correlates with disturbances in acid-base fluid and electrolyte balance (Dhatariya, 2008). Normally, insulin suppresses lipolysis in adipocytes and skeletal muscle by inhibiting hormone sensitive lipase (Rodrigues *et al.*, 1995; Fong, 2002). However, insulin deficiency leads to accelerated lipid break down releasing free fatty acids (FFA) into the circulatory system. The FFA are metabolised in the liver into ketone bodies, i.e. primarily β -hydroxybutarate and acetoacetate. These metabolites are found in excess in the blood circulation and urine of patients with metabolic disorders (Rodrigues *et al.*, 1995; Fong, 2002; Williams *et al.*, 2008).

1.2.2 Chronic Complications

Sustained hyperglycaemia due to carbohydrates, lipid and protein metabolism leads to chronic complications in diabetic individuals (Pacher *et al.*, 2007). High glucose triggers alteration in vascular tissues resulting in atherosclerosis (Aronson and Rayfield 2002). Non-enzymatic glycosylation of protein and lipids impedes the normal function of vascular tissues by disrupting molecular conformation, altering enzymatic activity; reducing degradative capacity and interfering with receptor recognition. For example, glycosylation of LDL (low-density lipoprotein) apo B reduces its recognition by the low-density lipoprotein LDL receptor; this further alters LDL clearance and high susceptibility to oxidative modification (Aronson and Rayfield 2002). LDL transportation to various vascular tissues occurs via apolipoprotein B which serves as a basic

apolipoprotein for LDL. Apo B is a ligand for LDL receptors in vascular tissues. High levels of ApoB are observed in vascular tissues and lead to plaque formation causing vascular and heart disease (Chumakova *et al.*, 2006; Itakura and Matsumoto 1995; Mahley, 1985). Moreover, glycosylated proteins interact with a specific receptor expressed on all cells relevant to the atherosclerotic process. These cell types include monocyte-derived macrophages, endothelial cells and smooth muscle cells (Aronson and Rayfield 2002; Hansson, 2005; Sadeghi, 2006). This interaction promotes induction of oxidative stress and a pro-inflammatory response which entails promotion of advanced glycation end-product (AGE) and also activation of protein kinase-c (PKC) (Aronson and Rayfield 2002). Alteration in the vascular walls such as increased vascular permeability and growth of new blood vessels may also result in end organ damage (Hansson, 2005; Sadeghi, 2006).

1.2.3 Macrovascular Complications

Macrovascular complications are associated with the damage in blood vessels of the brain, heart, and extremities (Pacher *et al.*, 2007). Cardiovascular complications are the most significant damaging health outcome of diabetes mellitus (Rao, 2007). There are numerous mechanisms responsible for progression of cardiovascular disease in DM (Pacher *et al.*, 2007). The increased risk for developing vascular disease may be due to high circulating levels of insulin which have been shown to stimulate the atherogenic process by inducing smooth muscle cell proliferation and cholesterol synthesis. Subsequently, the diabetic state has been shown to alter platelet function, increase platelet aggregation and increase levels of fibrinogen, resulting in clot formation in the vasculature, a major step in the pathogenesis of cardiovascular disease (Rao, 2007).

Studies have shown that diabetes mellitus is associated with increased oxidative stress (Finkel *et al.*, 2000). Progression of DM and cardiovascular disease are therefore underlined by metabolic disturbances (Rajamani and Essop, 2010) Hyperglycaemia triggers oxidative stress by disturbing the cellular redox state thereby generating reactive oxygen species (Cai *et al.*, 2002). The perturbed redox state results in altered metabolic pathways such as polyol signalling resulting in increased oxidative stress and apoptosis (Pacher *et al.*, 2007). This will be further discussed in Chapter 2.

1.3 Diabetes mellitus and cardiovascular diseases

1.3.1 Cardiac metabolism

During the foetal stage the heart relies primarily on glucose metabolism as source of energy. However, with age the heart shares its metabolic needs between glucose lactate and fatty acids (Lopaschuck *et al.*, 2006; Feuvray and Darmellah 2008). Fatty acids are the dominant substrates supplying almost 60-80 % of the hearts metabolic needs (Opie 1969; Sharma and McNeill 2006; Essop, 2009). The remaining 20-40 % is shared between the carbohydrates such as glucose and lactate (Huss and Kelly 2005; Sharma and McNeill 2006). The metabolic switch to a multi-substrate usage during the adult stage is required for a healthy metabolic state (Feuvray and Darmellah 2008). Insulin is vital in the regulation of myocardial glucose uptake and usage. However, in DM glucose uptake is impaired due to 90- 100% reliance of the myocardium on fatty acid utilization (Avogaro *et al.*, 2004; Lashin, 2006; Huang *et al.*, 2005). Reduced cardiac glucose metabolism results in increased fatty acid oxidation due to impaired insulin action in adipocytes and liver (Wang *et al.*, 2006; Fang *et al.*, 2009; Brownlee, 2005).

High circulating fatty acids and triglycerides increase the uptake and oxidation of fatty acids in the cardiomyocytes. In addition peroxisome proliferator-activated receptor (PPAR) are up-regulated in the diabetic heart resulting in increased expression of target genes involved in cardiac fatty acid uptake and oxidation (Avogaro, 2004). PPARs are members of the nuclear hormone receptor super family of peroxisome proliferator-activated receptors (Brun, 1996; Kudzma, 2002). There are three isoforms 1. PPAR α , is highly distributed in the heart, liver and kidneys where its role entails regulation of genes implicated in lipid metabolism, more specifically the enzymes involved in β -oxidation of fatty acids 2. PPAR γ is predominantly distributed in adipose tissue and are involved in gene expression and differentiation and 3. PPAR δ , is expressed in insulin sensitive tissues, its expression stimulated by the inhibition of cell growth at confluence. Thus PPARs are responsible for regulation of lipid metabolism and further serve as lipid sensors (Brun, 1996; Kudzma, 2002; Bar-Tana, 2001; Rotondo and Davidson 2002).

Increased free fatty acid utilization contributes to the progression of diabetes by inhibiting glucose breakdown, pyruvate oxidation, and uptake of lactate and subsequently increasing NADH/ NAD⁺ and acetyl-CoA (Sharma and Mc Neill 2006; Hayat *et al.*, 2004). Moreover, increased FA oxidation results in high intracellular fatty acids which can damage the mitochondria. The increased FA oxidation may also lead to the conversion of palmitate to ceramide, thereby stimulating apoptosis in cardiomyocytes. Lastly, dependence of the diabetic myocardium on fatty acid metabolism causes impairment in cardiac energy efficiency (Wang *et al.*, 2006). Triglyceride aggregation is vital in the progression of diabetic cardiomyopathy. Elevated FA flux and oxidation in the diabetic myocardium leads to cardiac dysfunction and subsequently heart failure (Huang *et al.*, 2005).

Cardiomyocytes regulate their own glucose uptake via the transmembrane glucose gradient and this aids in alleviating complications associated with hyperglycaemia (Rodrigues *et al.*, 1995; Young *et al.*, 2002). During the postprandial state blood glucose levels increase in relation to insulin levels. However, during the fasted state, the rate of glucose uptake is slower than its degree of phosphorylation (Young *et al.*, 2002; Hue *et al.*, 1995; Feuvray and Darmellah 2008).

Glucose transport in cardiomyocytes is regulated by glucose transporters (GLUTs). The two cardiac isoforms are GLUT 1 and GLUT 4 (Barnard and Youngren 1992; Bouché *et al.*, 2004; Wiernsperger, 2005). Insulin and exercise are the main triggers for translocation of GLUT 4 from the cytosol to the cell membrane (Barnard and Youngren 1992; Bouché *et al.*, 2004; Wiernsperger, 2005; Carvalho *et al.*, 2005). GLUT4 is highly expressed in skeletal muscle, the heart as well as white and brown adipose tissues (Carvalho *et al.* 2005). GLUT 4 is insulin-dependent and is the main glucose transporter that is highly expressed in the membrane surface of cardiomyocytes (Bouché *et al.*, 2004). It is usually found internalized within vesicles in the cytosol, and upon stimulation by insulin translocates to the sarcolemma (Barnard and Youngren 1992; Bouché *et al.*, 2004; Wiernsperger, 2005). The expression of the GLUT 4 transporter ensures proper maintenance of cardiac function and its depletion results in alterations in hearts function (Feuvray and Darmellah 2008). Altered GLUT 4 activity leads to decreased glucose uptake in skeletal muscle and adipose tissues leading to obesity and Type 2 DM. Gene knock-out studies showed that removal of one allele of the murine GLUT-4 gene reduced its expression in adipose and skeletal tissues and abruptly the progression of hyperglycaemia and hyperinsulinemia (Stenbit, 1997)

Hyperinsulinemia is associated with reduced free fatty acid supply to the heart and also with cardiac hypertrophy (Belke *et al.*, 2002; Stenbit, 1997). These studies were supported by Kodowaki (2000), who showed that GLUT 4 deficiency in cardiomyocytes results in marked reduction in FFA levels in both fasted and postprandial state. GLUT 4 *-/-* mice had reduced body weight and developed cardiac hypertrophy whereas the GLUT 4 *+/-* suffered peripheral resistance of striated muscle and no effect on the hepatic insulin resistance. Histopathological studies in the latter knockout model showed diabetic cardiomyopathy and liver stenosis (as observed in clinical studies) due to alterations in whole body glucose disposal (Kodowaki, 2000). GLUT 1 is expressed abundantly in most tissues including the pancreatic β -cells intestine, liver, kidneys and the myocardium, and is a foetal phenotype. GLUT 1 is a non-insulin dependent transporter that is responsible for the basal glucose uptake required for cell homeostasis (Bouché *et al.*, 2004; Wiernsperger, 2005).

1.3.2 Diabetic cardiomyopathy

Cardiomyopathy is a specific disease of the myocardium, which often results in heart failure (Hayat *et al.*, 2004; Ashgar *et al.*, 2009). Rubler (1972) described this pathological condition for the first time based on the postmortem analysis of four diabetic patients who suffered from heart failure (Sharma and McNeill 2006; Wang *et al.*, 2006; Hayat *et al.*, 2004; Wold *et al.*, 2005). The known factors that contribute to cardiac heart failure include hypertension, coronary artery disease, valvular or congenital heart diseases (Wold *et al.*, 2005; Hayat *et al.*, 2004; Ashgar *et al.*, 2009; Fang *et al.*, 2004). Studies have shown that diabetic cardiomyopathy can trigger heart failure

independently of other cardiovascular complications (Sharma and McNeill 2006; Boudina and Abel 2007).

Diabetic cardiomyopathy arises due to the diabetic state affecting the cardiac structure and function with no changes in blood pressure and coronary artery disease (Rodrigues and McNeill 1992; Lashin and Romani 2003; Ashgar *et al.*, 2009; Boudina and Abel 2007). This has been confirmed by clinical studies which showed that diabetic cardiomyopathy occurs without any major vascular lesions (Trost and LeWinter 2001; He *et al.*, 2007). Diabetes mellitus leads to myocardial structural abnormalities and functional changes which progress from the asymptomatic diastolic to systolic dysfunction (Ballano *et al.*, 2007; Dallack *et al.*, 2008) and ultimately to left ventricular hypertrophy. Metabolic derangements are the fundamental factors contributing to diabetic cardiomyopathy (King and Loeken 2004; Rolo and Palmero 2006).

Although glucose is the second major myocardial fuel substrate, with diabetes its transport and oxidation are altered and hence myocardial energy generation is almost entirely dependent on fatty acid catabolism (King and Loeken 2004; Shipoor *et al.*, 2008). In addition to increased fatty acid metabolism, the disturbed uptake of glucose due to insulin resistance by fat and muscle tissues leads to chronic hyperglycaemia which has a role in predisposing cardiac cells to programmed cell death. Subsequently there is still elevated glucose uptake by insulin-independent tissues (due to high concentration gradient) and an increased flux alters the antioxidant defence in the myocardium (King and Loeken 2004.) Therefore, a direct correlation between diabetic cardiomyopathy and hyperglycaemia exists (Cai *et al.*, 2002).

Two basic components are known to precede the progression of diabetic cardiomyopathy. Physiological adaptation to metabolic alterations is a short-term component which initiates the pathology (Boudina and Abel 2007). With the progression of the disease, degenerative changes to the myocardium have been shown to induce irreversible damage. The changes are attributed to the effects of hyperglycaemia as a mediator of the diabetic complications and originator of mechanisms regulating diabetic cardiomyopathy (Sharma and McNeill 2006). Clinical manifestations of the disease vary from patient to patient, and this is mainly due to the risk factors that affect the development of the disease (Fang *et al.*, 2004).

The diabetic cardiomyopathy is primarily induced by hyperglycaemia. The earliest pathophysiological characteristic observed in this metabolically disturbed environment is a reduction in GLUT 4 mRNA and protein levels (Rodrigues, 1995; Feuvray and Darmellah 2008; Kaczmarczyk *et al.*, 2003). Oxidative stress is induced as a result of insulin resistance leading to an increase in free fatty acids, carnitine deficiency and altered calcium homeostasis (Boudina and Abel 2009; Fang *et al.*, 2004; Sharma and McNeill 2006). There are little or no structural changes to the myocardium at this point, although sub-structural changes in cardiomyocytes may be present (Fang *et al.*, 2004; Sharma and Mc Neill, 2006). The changes in metabolism and development of myocardial fibrosis characterize the micro-vascular changes (Fang *et al.*, 2004; Sharma and Mc Neill 2006).

Metabolic alterations are often preceded by cellular changes involving apoptosis and necrosis. Apoptosis and necrosis manifest secondary to the defects in calcium transport and fatty acid metabolism (Fang *et al.*, 2004). The changes are supported by minute structural features to the left

ventricular mass and wall thickness (Fang *et al.*, 2004; Sharma and Mc Neill 2006). Diastolic dysfunction and ejection fraction with a large increase in left ventricular size and wall thickness are part of the functional and structural features observed during the progression of the disease (Fang *et al.*, 2004; Sharma and Mc Neill 2006).

1.4 Treatment and management of diabetes mellitus

The pharmaceutical agents available in the market have provided better management of diabetes mellitus. These agents include insulin, metformin and sulfonylureas (DeWitt and Dugdale 2003). Synthetic drugs such as troglitazones have been shown to introduce further complications in diabetic patient's e.g. liver toxicity. Rosiglitazones have been shown to exacerbate the symptoms and risk factors of cardiomyopathies (Tiwari and Rao, 2002). Unlike the more affluent developed countries, in developing countries patients have limited access to the conventional drugs due to socio-economic conditions (Durcorps *et al.*, 1996; Tiwari and Rao 2002; Musabayane *et al.*, 2005). Therefore, a need for new alternative treatments for treating diabetes mellitus is needed (Tiwari and Rao 2002).

Medication, exercise, and diet are the cornerstone in diabetic care, and in the past these components were part of traditional lifestyle (Alberti and Zimmet, 1998). Under physiological conditions the body synthesizes a wide range of antioxidants as part of defence against damage induced by free radicals (Natali *et al.*, 1999). However, high intracellular glucose levels result in loss of anti-oxidant reducing equivalents (Rolo and Palmera, 2006; Brownlee, 2005). The Mediterranean diet which consists mainly of vegetables, fruits and plant derived beverages (fruit

juice, red wine tea and coffee) may, however, counter this since it is a useful exogenous source of antioxidants (Nuttall *et al.*, 1999; Scalbert *et al.*, 2005).

1.4.1 Phytomedicine

Traditional medicine is currently providing new therapies owing to its active principles and properties (Tiwari and Rao, 2002). For example, the World Health Organization (WHO) has mandated scientific evaluation of these medicinal plants (WHO, 2002). Over the years, medicinal approaches in diabetes management have been made, which include herbs and plant derived extracts taken as food supplements (Teodoro *et al.*, 2008). Previous studies have shown that 85 % of the 295 documented plants used for management of diabetes possess hypoglycaemic (Mc Cune and Johns 2002) and antioxidant properties (Arulrayan *et al.*, 2007).

In Asian and South American countries there is increased prevalence in the usage of cheap and easily accessible Phytomedicine from medicinal plants of the genus *Syzygium* (Prasad *et al.*, 2005). This *genus* is used for the treatment of toothache, respiratory ailments, and digestive ailments, in significance to this study diabetes mellitus, (Banerjee *et al.*, 2006). For instance, *Syzygium cumini* (L.) Skeels (Myrtaceae) and *Syzygium alternifolium* (Wright) Walp. (Myrtaceae), have been shown to possess hypoglycaemic properties (Prince *et al.*, 1998; Teixeira *et al.*, 1997; Rao and Rao 2001). In Indian folk medicine *Syzygium cumini* is widely used to manage diabetes while in Brazil tea prepared from *Syzygium cumini* is also used to treat this disease (Prince *et al.*, 1998; Teixeira *et al.*, 1997; Prasad *et al.*, 2005). Recently, *Syzygium cordatum* crude leaf extract was shown to exert hypoglycaemic effects in an *in vivo* model of streptozotocin-induced Type 1 DM in rats (Musabayane *et al.*, 2005 Mapanga *et al.*, 2009).

Besides *Syzygium*, other plant extracts have also been used in the management of DM. For example, seed extracts of *Bauhinia candicans* (Benth) [Caesalpinaceae] and procyanidins from *Vitis vinifera* (Linnaeus) [Vitaceae] have been shown to possess insulin-mimetic effects on glucose uptake in insulin sensitive cell lines (Pinent, *et al.*, 2004; Fuentes and Alarcón, 2006). Moreover, aqueous extract of the seed from *Tamarindus indica* (Linnaeus) [Fabaceae] lowered blood glucose levels by increasing hepatic glycogen concentrations (Maiti *et al.*, 2005). *Asparagus racemosus* (Willdenow) [Asparagaceae] root extracts have also been shown to increase insulin secretion in isolated β -cells and perfused pancreas via the cyclic adenosine monophosphate (cAMP) pathway (Hannan *et al.*, 2007). In addition, *Momordica charantia* has been reported to alter the activities of glucose-6-phosphatase and fructose-1, 6-bisphosphatase in diabetic rats (Garau *et al.*, 2003). This depression of key enzymes in glycogen synthesis was associated with regeneration of pancreatic β -cell function (Garau *et al.*, 2003). Lastly, *Hypoxis hemerocallidea* (commonly referred to as African potato) (Musabayane *et al.*, 2006; Ojewole, 2006) has been shown to exhibit hypoglycaemic properties in an *in vivo* model of streptozotocin -induced DM in rats (Mohamed and Ojewole, 2003; Musabayane *et al.*, 2006; Ojewole, 2006).

1.4.2 *Syzygium aromaticum* (Hochst.) [Myrtaceae]

Syzygium aromaticum (*S. aromaticum*), formerly known as *Eugenia caryophyllata*, is an evergreen tree 8-30 m tall; consisting of numerous semi-erect branches and a medium-sized crown base. The leaves are glabrous with a number of oil glands on its lower surface, and the flowers and leaves are triangular projection (Figure 1). The fruits are olive-like shaped with one seed commonly referred to as cloves. With time the un-open buds are sun dried (Figure 2). The plant grows in

warm climates and is cultivated commercially in Tanzania, Sumatra, the Maluku (Molucca) Islands and South America (Bisset, 1994; Agbaje *et al.*, 2009). *S. aromaticum* is not cultivated in South Africa (Agbaje *et al.*, 2009). However, *S. cordatum* species grow on forest margins or in swampy spots from KwaZulu-Natal to Zimbabwe and Mozambique (Van Wyk *et al.*, 1997).



Figure 1: *Syzigium aromaticum* leaves with green flower buds (Top Tropicals.com).



Figure 2: Sun dried unopened flower buds (Cloves) (Top Tropicals.com).

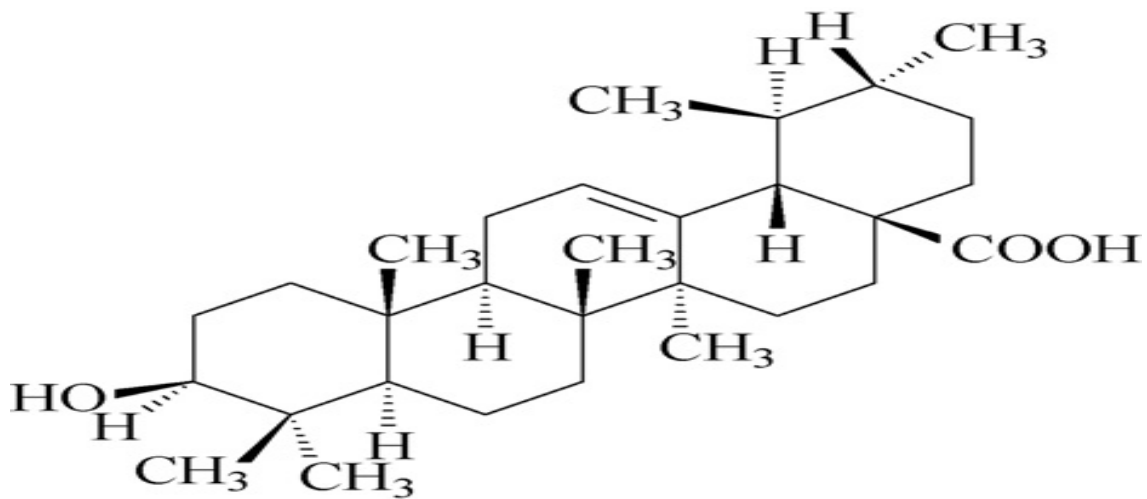
In India, cloves are often used as a spice (*Syzygium aromaticum* L.) to add flavour to exotic food preparations (Abdel-Rahman and El-Megeid 2006; Orwa *et al.*, 2009). Cloves are also used by Ayurvedic healers in India for the treatment of respiratory and digestive ailments (Abdel-Rahman and El-Megeid 2006). Aqueous clove preparation inhibits the growth of germinated spores of several fungus and bacterial species, suggesting antiseptic and antibiotic properties (Orwa *et al.*, 2009). In addition, aqueous extracts of clove have been shown to exhibit inhibitory effects on hepatitis C virus protease (Banerjee *et al.*, 2006; Orwa *et al.*, 2009). Moreover, *Syzygium aromaticum* has been shown to be a potential chemo-preventive agent for treatment of lung cancer (Banerjee *et al.*, 2006).

1.4.3 Bioactive compounds

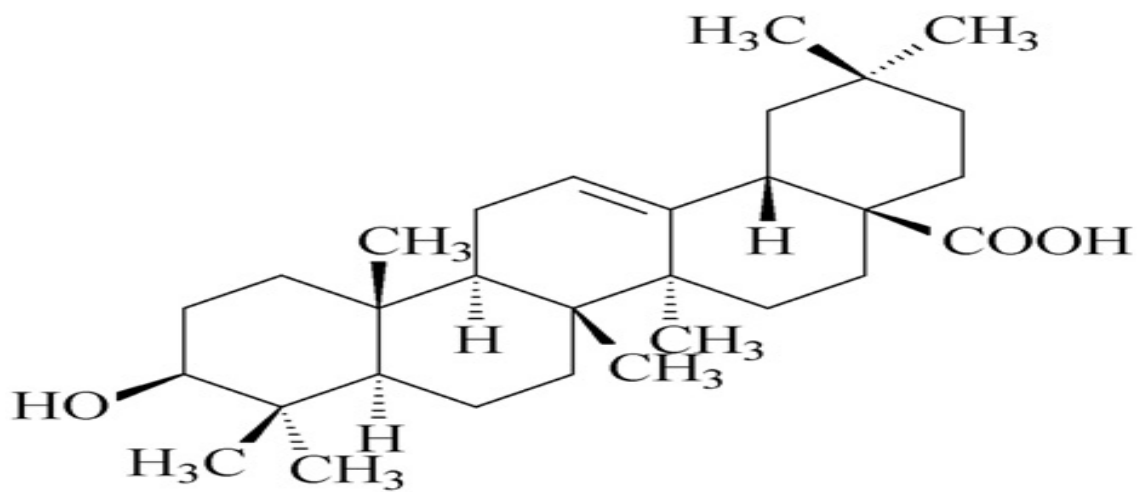
Bioactive compounds are plant-derived natural products which exist widely in nature, the most common compounds include glycosides, alkaloids, (Somova *et al.*, 2003; Khan *et al.*, 2007) polyphenolic, flavonoids, squalene, anti-oxidants and triterpenes (Liu, 1995; Senthil *et al.*, 2007). The main focus of our study is the plant-derived active ingredients belonging to a class of compounds called triterpenoids.

1.4.4 Triterpenoids

More than 120 plant species have been found to possess triterpenoids (Somova *et al.*, 2003). Triterpenoids are widely distributed in the vegetation in the form of saponins or glycosides and free acids (aglycone or genin) attached to carbohydrate residues (Liu, 1995; Somova *et al.*, 2003). The occurrence of the acids differs within the same genus and in different species (Dzubak *et al.*, 2006). As early as 1981 researchers have established a range of therapeutic effects attributed to the triterpenoids. These include anti-inflammatory, anti-tumour, anti-diabetic, anti-hypertensive and antimicrobial activity with varying potencies, (Ghosh *et al.*, 1981; Liu, 1995; Somova *et al.*, 2003; Dzubak *et al.*, 2006; Lee *et al.*, 2006; Jung *et al.*, 2007). Other examples of triterpenoids include ursolic acid, corosolic acid, gallic acid, masilinic acid and oleanolic acid (Liu, 1995; Shishodia *et al.*, 2003; Dzubak *et al.*, 2006). Oleanolic acid (OA) was chosen as a triterpenoid of choice for our study based in studies conducted in our laboratories with oleanolic acid. OA has been shown to have potential in diabetes management where it reduced mean arterial pressure in STZ- induced diabetic rats therefore alleviating cardiovascular disorders (Mapanga, *et al.*, 2009). However, in literature no evidence of plant-derived oleanolic acid and potential antioxidant effects in cardiomyocytes (H9C2) is currently available; this prompted us to conduct this study.



$C_{30}H_{48}O_3$
Ursolic acid



$C_{30}H_{48}O_3$
Oleanolic acid

Figure 3: The chemical structure of ursolic acid and oleanolic acid (Wang *et al.*, 2008).

The chemical structure of oleanolic acid is formed by cyclization of squalene (Figure 3). The pentacyclic rings are composed of 30 carbons with two methyl groups located on carbon 20 (C20) (Stangeland *et al.*, 2008). Ursolic acid (UA) is an isomer of OA. Unlike OA, UA has methyl groups on carbon 19 and 20 (Liu, 1995; Musabayane *et al.*, 2005, Wang *et al.*, 2008). Oleanolic acid has been shown to possess anti-arrhythmic, cardiotoxic and anti-hypertensive effects in experimental studies (Liu, 1995; Wang *et al.*, 2008). OA exhibited anti-oxidant, anti-arrhythmic, and cardiotoxic effects in a rat model of isoprenaline-induced myocardial ischemia (Senthil *et al.*, 2007). Furthermore, OA has been shown to possess anti-apoptotic, antioxidant effects in various models (Huang *et al.*, 2005; Ovesná *et al.*, 2006; Bai *et al.*, 2007; Teodoro *et al.*, 2008). For example, improved insulin secretion in isolated rat islets and pancreatic β -cells were observed, demonstrating that OA possesses insulin secretagogue properties. Similar effects were observed under basal and high glucose environments in cultured cells (Teodoro *et al.*, 2008).

OA derived from pomegranate flowers promoted PPAR- α resulting in cardiac metabolic improvement in diabetes and obesity in *in vivo* studies (Huang *et al.*, 2005). Oleanolic acid isolated from Glossy privet fruit, showed antioxidant properties in relation to glucose-induced oxidation of plasma and low density lipoprotein (LDL) in human (Wang *et al.*, 2009). Other antioxidant properties of OA were observed in a model of H₂O₂ induced DNA damage in HL-60 cell lines (Ovesná *et al.*, 2006). Moreover, OA isolated from *Olea europaea* (olive) leaf extract exhibited antioxidant effects *in vitro* and hepatoprotective properties in an *in vivo* model of carbon tetrachloride induced liver injury (Bai *et al.*, 2007). However, despite these advances the precise mechanisms underlying OA-induced effects on the diabetic heart remain unclear. We believe this is an important area to study since the identification of novel anti-oxidants may help to attenuate

diabetes-induced damage to the heart and thereby alleviate the overall burden of disease in developed and especially developing countries.

1.5 Aim

To investigate the effects of plant-derived oleanolic acid in an *in vitro* heart model of hyperglycaemia-induced oxidative stress. We are employing this model to simulate the damaging effects of hyperglycaemia on heart cells (e.g. cell death) and to subsequently determine whether OA is able to blunt this.

1.5.1 Objectives:

1. To isolate OA from *Syzygium aromaticum*.
2. To investigate whether OA inhibits hyperglycaemia-induced oxidative stress in cardiac-derived H9C2 cells.
3. To determine whether OA would abolish hyperglycaemia-induced apoptosis in H9C2 cells.

Chapter 2

2.1 Introduction

Diabetes mellitus-induced hyperglycaemia can trigger reactive oxygen species (ROS) and nitrogen species production (Hayat *et al.*, 2004; Dallack *et al.*, 2008). This is one of the initial and most detectable effects of hyperglycaemia in cardiomyocytes which further contributes to the development of diabetic cardiomyopathy (Cai and Kang 2001; He *et al.*, 2008). ROS-induced damage is postulated to occur as a consequence of an imbalance between cellular generation and elimination of ROS (Fiordaliso *et al.*, 2006), or high cellular glucose levels resulting in the loss of anti-oxidant reducing equivalents (Bonnetfont-Rousselot, 2002; Rolo and Palmera 2006; Brownlee, 2005). Hyperglycaemia triggers oxidative stress by disturbing the cellular redox state (Kuyvenhoven and Menders 1999; Pacher *et al.*, 2007). Multiple sources of oxidative stress exist in diabetes mellitus; these include non-enzymatic, enzymatic and mitochondrial pathways.

By definition a free radical is an atom or molecule that contains one or more unpaired electrons in its outer orbital. ROS include hydroxyl radical (OH^\cdot), peroxynitrite (ONOO^-) and superoxide anion (O_2^-) (Kuyvenhoven and Menders 1999; Stephens *et al.*, 2009). Hyperglycaemia-induced ROS generation occurs via glucose auto-oxidation with transition metals such as *trans*-dihydrodiol which generates OH^\cdot radicals (Goetz and Luch 2008). Another source of non-enzymatic oxidative stress is through reaction-specific receptors with proteins, thereby leading to development of early glycosylated products (Amadori products) and subsequently the formation of advanced glycosylation end products (AGE) (Aronson and Rayfield 2002). This pathway of ROS production occurs via multiple steps where hyperglycaemia augments glucose metabolism through sorbitol resulting in O_2^- production (Johansen *et al.*, 2005; Bonnetfont-Rousselot, 2002). Nitric oxide

synthase (NOS), NAD (P) H oxidase, and xanthine oxidase are enzymes that potentiate generation of ROS in diabetes (Johansen *et al.*, 2005). ROS generated in this way is dependent on the presence of L-arginine nitric oxide synthase co-factor which is required for superoxide generation. However, in the absence of NOS cofactor uncoupled ON^- is produced (Johansen *et al.*, 2005).

During the progression of diabetes, cardiomyocytes are exposed to high glucose, thereby increasing the rate of glucose oxidation via the tricarboxylic acid (TCA) cycle to generate reducing equivalents, i.e. nicotinamide adenine dinucleotide (NADH) and flavin adenine dinucleotide (FADH_2), that donate electrons to Complex I and Complex II of the mitochondrial electron transport chain. Complex I and Complex II donate their electrons to Co-enzyme Q which then transfers electrons to Complex III. From Complex III electrons are transferred to cytochrome-c and to Complex IV. Moreover, in Complex IV superoxide donates an electron resulting in the formation of a water molecule. Electron transfer to Complex III is attenuated in the hyperglycaemic state due to a blockade of electron transfer inside Complex III, resulting in back-transfer of electrons to Co-enzyme Q (Allen *et al.*, 2005). Complex III and Complex IV electrons are donated one at a time to the superoxide molecule and form oxygen and nitrogen reactive species (Huss and Kelly 2005; Khavandi *et al.*, 2009). Superoxide anions play a vital role in the pathology of diabetic cardiomyopathy (Aronson and Rayfield, 2002; Johansen *et al.*, 2005). Increased glucose-induced superoxide generation induces DNA breakage and poly ADP ribose polymerase (PARP) production which in turn induces the poly (ADP-ribosyl) action of glyceraldehyde-3-phosphate dehydrogenase (GAPDH). This alters the metabolism of polyol pathway by the aldose reductase enzyme leading to increased oxidative stress (Pacher *et al.*, 2007; Dallack *et al.*, 2008).

Studies at the University of Kwa-Zulu Natal Physiology department have been conducted using different plants distributed in this province including *Syzygium cordatum*, *Hypoxis hyperocallidea*, *Ficus thonningi*, and some of them have shown to have cardioprotective effects (Musabayane *et al.*, 2005). Musabayane (2005) reported that extracts mixtures of oleanolic acid (OA) and ursolic acid (UA) from *Syzygium cordatum* (Hochst.) [Myrtaceae] were responsible for the hypoglycaemic effects observed in streptozotocin (STZ)-induced diabetic rats. As mentioned earlier hyperglycaemia can trigger reactive oxygen species (ROS) and nitrogen species production resulting in the loss of anti-oxidant reducing equivalents in cardiomyocytes which contributes to the development of diabetic cardiomyopathy.

However, to our knowledge the effects of plant-derived OA on hyperglycaemia induced oxidative stress in cardiomyocytes have not been investigated. Therefore the aim of this study was to investigate the anti-oxidant potential of oleanolic acid in H9C2 cells exposed to low and high glucose environments in order to test its ability to decrease oxidative stress and apoptosis.

2.2 Materials and Methods

2.2.1 Plant Material

For this study, *Syzigium aromaticum* [(Linnaeus) Merrill & Perry] (Myrtaceae) cloves (purchased from Africa International Food and Cosmetics Technologies, South Africa) (Somova *et al.*, 2003) were employed for the extraction of oleanolic acid.

a) Isolation of oleanolic acid

The cloves (1 kg) were extracted thrice at room temperature at 24 hour intervals i.e. sequentially in 3L each of, dichloromethane and ethyl acetate to yield residues of dichloromethane-solubles (DCMS) and ethyl acetate-solubles (EAS), respectively. Previous studies have shown that OA is mostly concentrated in EAS (Somova *et al.*, 2003; Musabayane *et al.*, 2005). Thereafter filtration was performed with 30 cm filter paper (0.2 µm pore size) (Whatman, England). The filtrates were then concentrated *in vacuo* using a rotary evaporator, at 60±1°C using a laboratory 4000 efficient rotary evaporator (supplied by Laboratory Consumables and Chemical Supplies, South Africa) resulting in 29.37g crude ethyl-acetate extract.

b) Chromatographic Fractionation

For the separation of different solubles, thin layer chromatography was used to analyse the crude ethyl acetate extract for the different compounds present in the extracts. The crude extracts were analyzed by thin layer chromatography (TLC) on pre-coated aluminium plates Merck Si gel F254 (Merck, Darmstadt, Germany) to reveal the type of chemical constituents they contained. This was done by spotting a diluted portion of the crude extract on a TLC plate with authentic oleanolic acid. The TLC plate was developed with ethyl acetate/hexane (7:3) in a TLC tank. The developed

TLC plate was visualised by exposure to ultraviolet light at 254 nm to 366 nm and then sprayed with anisaldehyde /sulphuric acid/ alcohol solution and heated at 110°C. Appearance of a blue or violet blue colouration indicated the presence of triterpenoids. The non-polar compounds were discarded and the semi-polar to polar compounds subjected to chromatographic fractionation (Hostettmann and Marston 1995; Mapanga *et al.*, 2009).

The EAS of *S. aromaticum* contained triterpenoids, the solubles were, therefore, subjected to further purification processes. A portion of EAS (2 g) was fractionated on silica gel (70-230 mesh, 3.5 x 45 cm) by open column chromatography using a step gradient of n-hexane-ethyl acetate 90:10 (250 ml), 80:20 (250 ml), and 70:30 (800 ml). Data from collected fractions analyzed by TLC were compared with authentic OA purchased from Sigma (St Louis, Missouri, USA). Fractions were pooled according to similar TLC profiles and concentrated *in vacuo* using a rotary evaporator at 55°C. The concentrates were reconstituted using minimal amounts of chloroform and allowed to air dry in pre-weighed vials. Measured eluates were collected and combined into fractions on the basis of their TLC similarities. The eluates with similar TLC profiles to oleanolic acid were combined and subjected to further chromatographic purification (Figure 4).

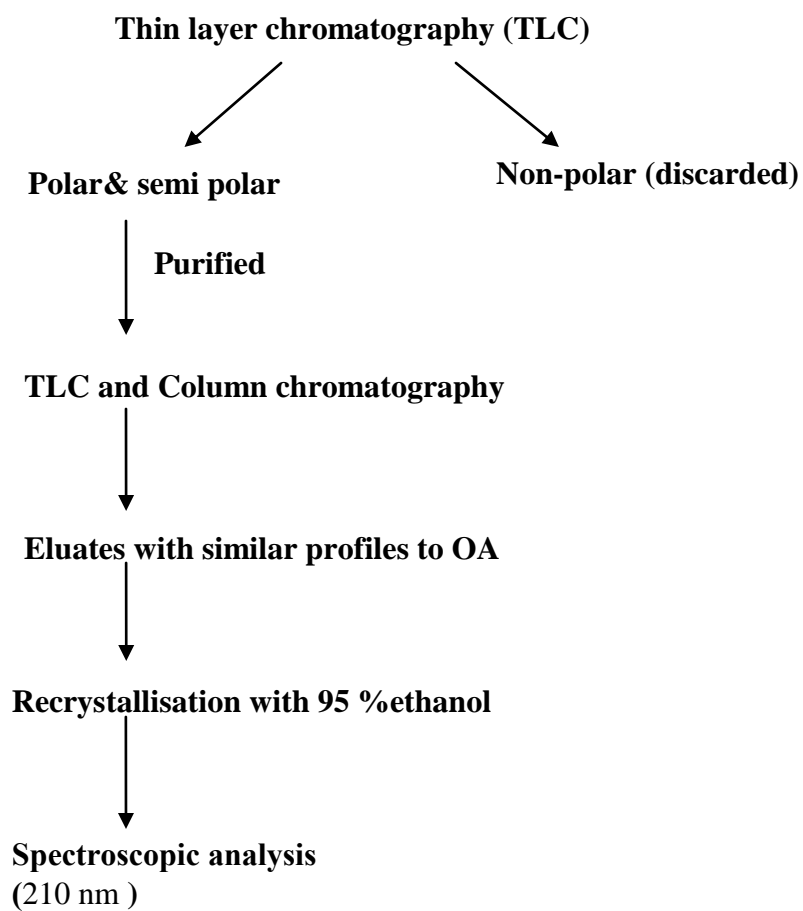


Figure 4: A schematic representation of chromatographic fractionation.

c) Structure elucidation of oleanolic acid

Pure OA was obtained by recrystallisation with 95% ethanol and its structure confirmed by spectroscopic analysis using 1D and 2D, ^1H and ^{13}C Nuclear Magnetic Resonance (NMR) (400MHz, Bruker ,Germany) techniques with the purity of about 98%.

2.2.2 Cell culture

We employed H9C2 cells, an embryonic rat heart-derived cell line that was obtained from Sigma-Aldrich, (Steinheim, Germany). The cells were cultured in T 75 flasks (Greiner, Krensmunster, Australia) and incubated at 37° C in 95% O₂ and 5% CO₂ in Dulbecco's modified Eagle's medium (DMEM) (Sigma-Aldrich, Steinheim, Germany) supplemented with 10% foetal bovine serum (FBS) (Invitrogen, Carlsbad, CA) and a normal glucose concentration of 5.5 mM in DMEM. Sub-culturing was done at a confluency of 80% and the media was changed every third day.

a) High glucose and bioactive compound treatment

On day 1 H9C2 cells were split and sub-cultured for experiments on 5.5 mM glucose in DMEM and allowed to plate for 24 hours. Cells cultured in a media of the same concentration (a) 5.5 mM glucose served as a control group and (b) 33 mM glucose as a high glucose treated group. H9C2 cells were further exposed for 48 hours under these conditions followed by dose-dependent treatment with 0, 20, 50 μM oleanolic acid for 6 hours and 24 hours, respectively (Figure 5). For the H9C2 exposed to normal and high glucose with 0, 20, 50 μM OA treatment our time points were 54 and 72 hours.

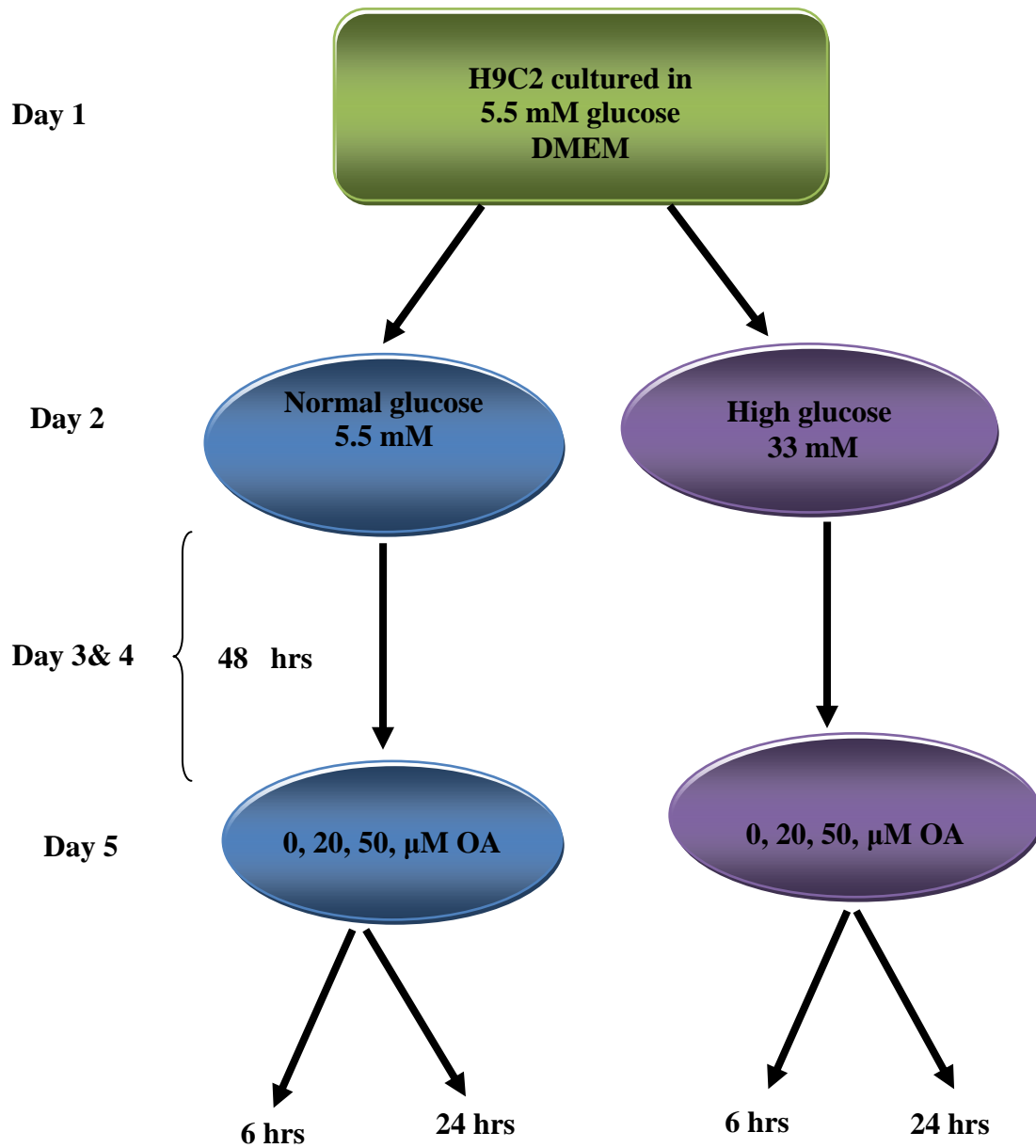


Figure 5: A schematic representation of the experimental procedure.

b) Measurement of intracellular reactive oxygen species

Several methods have been established for qualitative and quantitative measurement of intracellular reactive oxygen species. Different types of fluorescent probes (fluorophores) have been described for the detection of radical species (Hafer *et al.*, 2008). The principle is based on secondary antibodies that are conjugated to a fluorophore. Excitation of the fluorophore with a photon of a particular wavelength triggers emission of light by a photon, its wavelength is proportional to the energy released after excitation (Heginbotham *et al.*, 2004) For this study we used the H₂-DCFDA fluorophore. Oxidation of H₂-DCFDA by reactive oxygen species results in the formation of the fluorescent compound fluorescein and calcein. Quantification of cell specific data was conducted with an Olympus Cell^R fluorescence 1 X 81 inverted microscope (Olympus Biosystems, Germany).

Measurement of intracellular ROS was performed with cell culture suspensions of the fluorescent dye using flow cytometry. Flow cytometry is made of three functional systems, viz., fluidics, optics and electronics (BD Biosciences, 2000). The fluidic system delivers cells of a fluid stream singly to a particular region that is intersected by an illuminating beam. The flow cytometric tubes containing cells are placed in the centre of an enclosed chamber through which the sample flows into a flowing stream of sheath fluid (BD Biosciences, 2000). Particles are restricted to the centre of the fluid stream by hydrodynamic focusing (BD Biosciences, 2000; Alvarez-Barrientos *et al.*, 2000). Detectors collect either light scatter or fluorescence emissions of each particle and transmitted to a computer for dispersion of population with respect to several parameters (Alvarez-Barrientos *et al.*, 2000). Scatter light is collected in the same direction as the incident of light. Forward scatter (FSC) light measures the cell surface area or size; this is relative to diffracted

light of the axis of the incident in the forward direction. FSC is responsible for detecting particles greater than a given size independent of their fluorescence. The side-scatter light is the measurement for the internal complexity, and it evaluates refracted and reflected light occurring at an interface within the cell. At approximately 90 degrees the beam collects lenses and redirects them using a splitter to relevant detectors (BD Biosciences, 2000; A´lvarez-Barrientos *et al.*, 2000). Absorption of light causes an electron to be raised to a higher energy level, decaying of the excited electron back to its ground state cause an emission of energy by the fluorescence of a compound (A´lvarez-Barrientos *et al.*, 2000).

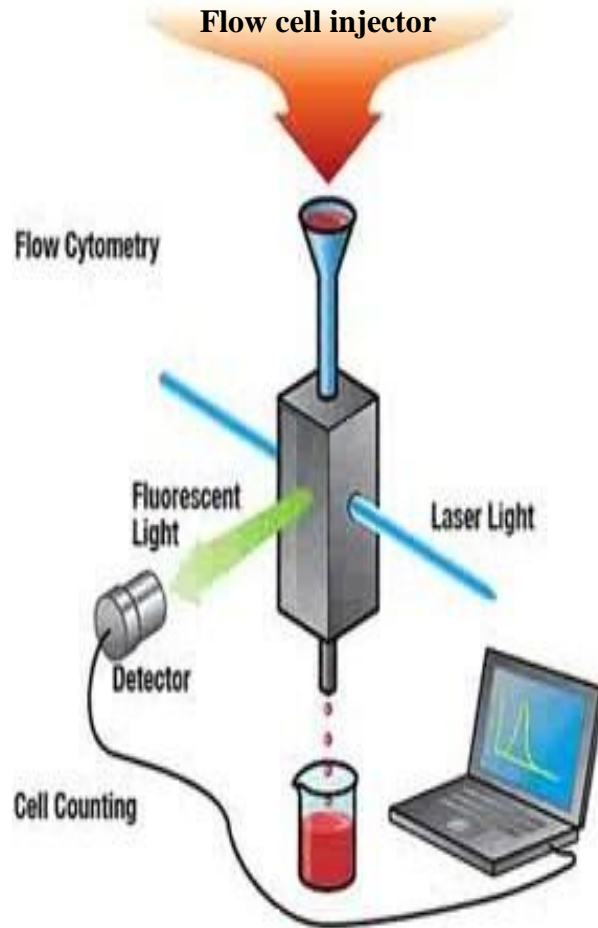


Figure 6: Illustration of flow cytometer instrumentation. Suspensions are passed through the fluidic system and the light scattered by cells is collected by photo detectors. Signals are digitized and captured on the computer for analysis (Los Alamos National Laboratory).

Cells were cultured in a T75 flask and upon confluency trypsinised and washed with 1 X PBS [137 mM NaCl₂, 2.7 mM KCl, 10 mM Na₂HPO₄ · 7H₂O, 1.8 mM KH₂PO₄, pH 7.4] and pelleted before being re-suspended in DMEM. Cell count was performed using a haemocytometer (LASEC, South Africa) and cells were seeded for microscopy and flow cytometry.

c) Seeding and staining for microscopy

500 μL of DMEM with 10% FBS were added to eight well NuncTM chamber cover glass slides (Nalge Nunc, Rochester, NY). For each well 15 000 cells (15 μL) were seeded and re-suspended 3 to 4 times, followed by incubation for 24 hrs at 37°C. DMEM was removed by suction pump following exposure of H9C2 cells to high glucose exposure and bioactive compound treatment. The wells were rinsed 3 times with 1X PBS (300 μL). 100 μL DCF dye was added at dilution of 1:200 of the stock solution (10 mM) in 1X PBS to each well. The plates were covered in foil and incubated at 37°C in the dark for 10 minutes. The dye was then removed and discarded. The cells were further stained with Hoechst dye in PBS at a ratio of 1:200 for 3 to 5 min and discarded. To avoid stressing the cell, 100 μL of 1X PBS was added to the cells prior to viewing with the light microscope. An Olympus Cell^R fluorescence 1 X 81 inverted microscope (Olympus Biosystems, Germany) with an F-view II camera (Olympus Biosystems, Germany) was used for image acquisition and Cell^R software (Olympus Biosystems, Germany) for processing images. The temperature of the microscope was maintained at 37°C for live cell imaging using a Solent Scientific microscope incubator chamber (Solent Scientific, UK). The green intensity of all cells expressing DCF signal was measured, generating a numerical value corresponding to ROS levels and oxidative stress. Three independent experiments were conducted and 3 images per experiment acquired. Thus n=9 was generated for each experiment.

d) Seeding and staining for flow cytometer

T25 flasks were used to seed approximately 1×10^5 cells (100 μ L) in each flask containing 5 ml of DMEM in 10% FBS. Seeding was performed for all different treatment groups (0, 20 and 50 μ M OA) under normoglycaemic (5.5 mM) and hyperglycaemic (33 mM) conditions. At the end of the experimental protocol DMEM was removed using a pipette and the cells were washed 3 times with 1 X PBS (300 μ L). To dislodge cardiomyoblasts from the flasks, cells were trypsinised with 2 ml trypsin for 3min followed by 4 ml DMEM in 10% FBS and centrifuged into a pellet. Trypsin/DMEM mixture was discarded. Initially we prepared a 1M H₂DCFDA stock by dissolving it in 210 μ L dH₂O. Subsequently, several aliquots of 10 mM stocks were made by diluting the 1 M stock in DMSO. 100 μ L DCF dye was added at the ratio of 1:200 of the stock solution (10 mM) in 1X PBS to each well. The dye-treated cell pellet was suspended without clumps and incubated in the dark for 20 minutes at 37°C. The cleaved DCF is a fluorescent substrate and any external light affects the signal causing background and hence the staining was performed in the dark. The cells were then run through FACS Aria flow cytometer (Becton-Dickinson, CA) and population data obtained.

Cells not treated with H₂DCFDA were used as negative controls, and stained cells treated with 100 μ L hydrogen peroxide (30% w/v hydrogen peroxide) incubated for 10 minutes served as positive controls. Four independent experiments were conducted for each condition investigated. The mean of the fluorescence of a cell population represented the numerical value of the experiment which was used for analysis.

e) Statistical analysis

All data were expressed as means \pm standard error of the mean (S.E.M). Statistical analysis was done using GraphPad InStat Software (version 4.00, GraphPad Software, San Diego, California, USA) using one-way analysis of variance (ANOVA), followed by Turkey-Kramer multiple comparison test multiple comparison test. A p value < 0.05 was considered significant.

2.3.1 Results

2.3.1 Structural elucidation of oleanolic acid

A yield of 7.03 g from 1kg cloves white powder with the molecular formula $C_{30}H_{48}O_3$ confirmed the chemical structure (Fig 7A) and IUPAC numbering of oleanolic acid (Fig 7B).

To ascertain the chemical formula of oleanolic acid recrystallisation of the powder with 95% ethanol and inspection of the 1D 1H - and ^{13}C -NMR spectra of the compound confirmed the presence of the 48 hydrogen and the 30 carbon atoms present in the molecule as depicted by distortion enhancement of proton transfer (Fig 8A, Fig 8B).

Comparison of the resonance frequencies of all carbon atoms is shown in Table 1. Of note are the signals at carbon 12 and 13 which correspond to that of 1- dimensional ^{13}C -NMR spectra. Carbon 12 and 13 with 143.6 and 122.7 parts per minute, respectively, depicted the presence of the carbon-carbon double olefinic bond which is a major structural feature of the triterpenoids. For the determination of complex components within the molecule two- dimensional 1H - and ^{13}C -NMR spectra of OA was conducted see figure Fig 8C. The lines at the bottom represent peaks for all the carbon-hydrogen bonds, middle line represents carbon attached to one hydrogen atoms. In the uppermost line CH_2 are presented by the downward signal peaks and the upward signal or peaks presenting the CH_3 . Carbon 18 has a β methyl group further downstream of the two (CH_3) methane groups in Carbon 20 confirmed the chemical structure of oleanolic acid. Figure 8D represents a heteronuclear multiple quantum within the molecule using the 1H - and ^{13}C -NMR spectra of oleanolic acid.

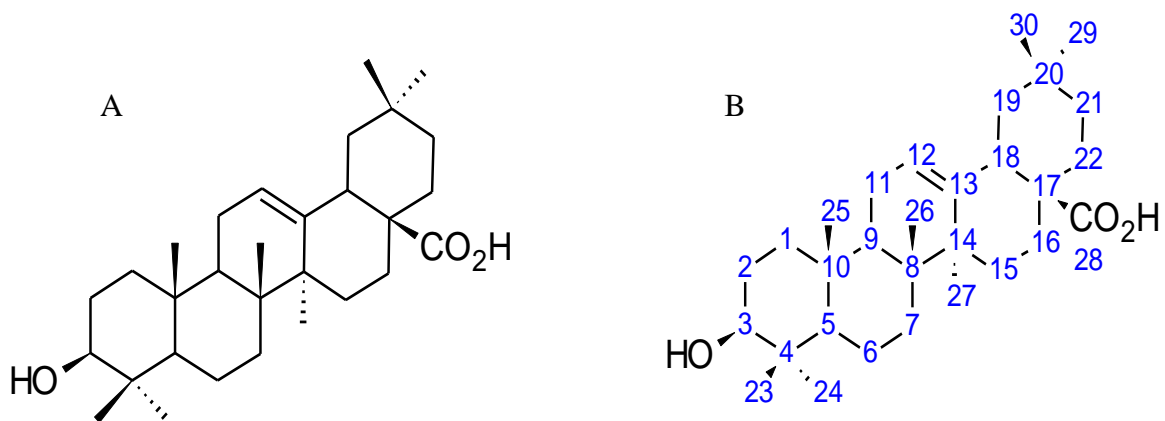


Figure 7: Chemical structure (A) and carbon numbering (B) of oleanolic acid (International Union of Pure and Applied Chemistry, IUPAC).

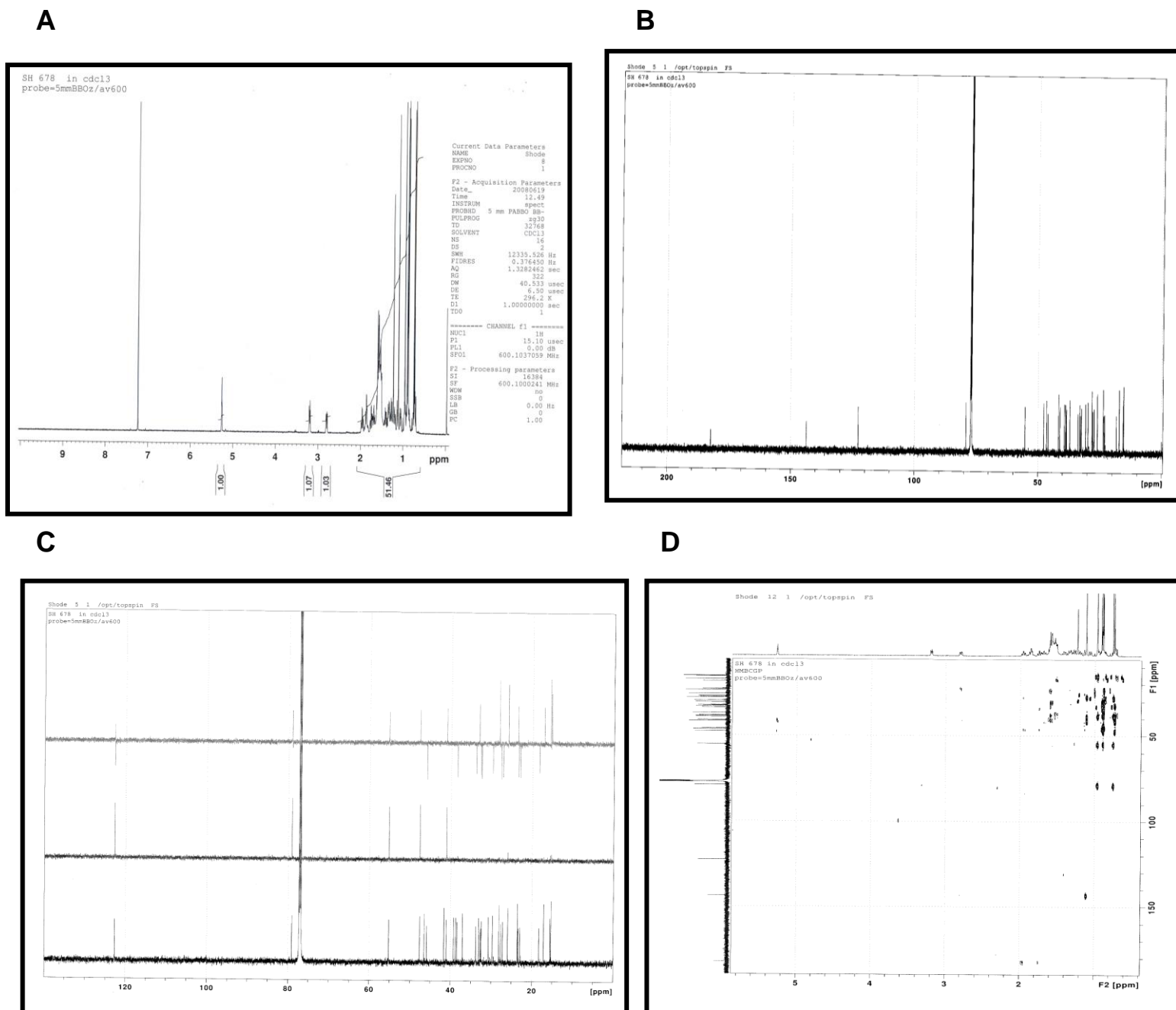


Figure 8: One dimensional ^1H and ^{13}C -NMR spectra of oleanolic acid isolated from *Syzygium aromaticum* (cloves) (A-B) and two dimensional ^1H and ^{13}C -NMR spectra by Distortion Enhancement Proton Transfer (DEPT) (C) and heteronuclear multiple quantum coherence (HMQC) (D).

Table 1: ^{13}C (100.64 MHz) Bruker Avance III NMR spectral data of plant derived OA and documented OA (Mahato and Kundu 1994; Mapanga *et al.*, 2009).

Carbon Position	Plant Derived OA	Reported OA [Mahato and Kundu 1994]
	δC	δC
1	38.4	38.5
2	27.2	27.4
3	79.0	78.7
4	38.8	38.7
5	55.2	55.2
6	18.3	18.3
7	32.6	32.6
8	39.3	39.3
9	47.6	47.5
10	37.1	37.1
11	23.0	22.9
12	122.7	122.5
13	143.6	143.5
14	41.6	41.6
15	27.7	27.7
16	23.4	23.4
17	46.5	46.5
18	41.0	40.9
19	45.9	45.9
20	30.7	30.6
21	33.8	33.8
22	32.4	32.4
23	28.1	28.1
24	15.5	15.5
25	15.3	15.3
26	17.1	17.1
27	25.9	25.9
28	182.2	183.5
29	33.07	33.1
30	23.6	23.6

2.3.2 *In- vitro* model of hyperglycaemia-induced oxidative stress in cardiac myocytes

Qualitatively, we measured ROS production in arbitrary units (AU) as a measure of H₂DCFDA fluorescence with an inverted immunofluorescence microscope. Quantitative analysis of ROS generation was conducted using flow cytometry in parallel to the microscopy data.

Microscope data showed a $22 \pm 6\%$ ($n=9$ $p<0.01$ vs. normal glucose control) increase in ROS production in H9C2 cells exposed to high glucose for 54 hours (Fig 9C). In parallel, we performed flow cytometry for quantitative measurement of ROS production. Here, ROS was increased in high glucose treated cells by $30.4 \pm 8\%$ ($n=4$; $p<0.05$ vs. 5.5mM glucose control) (Fig 9D).

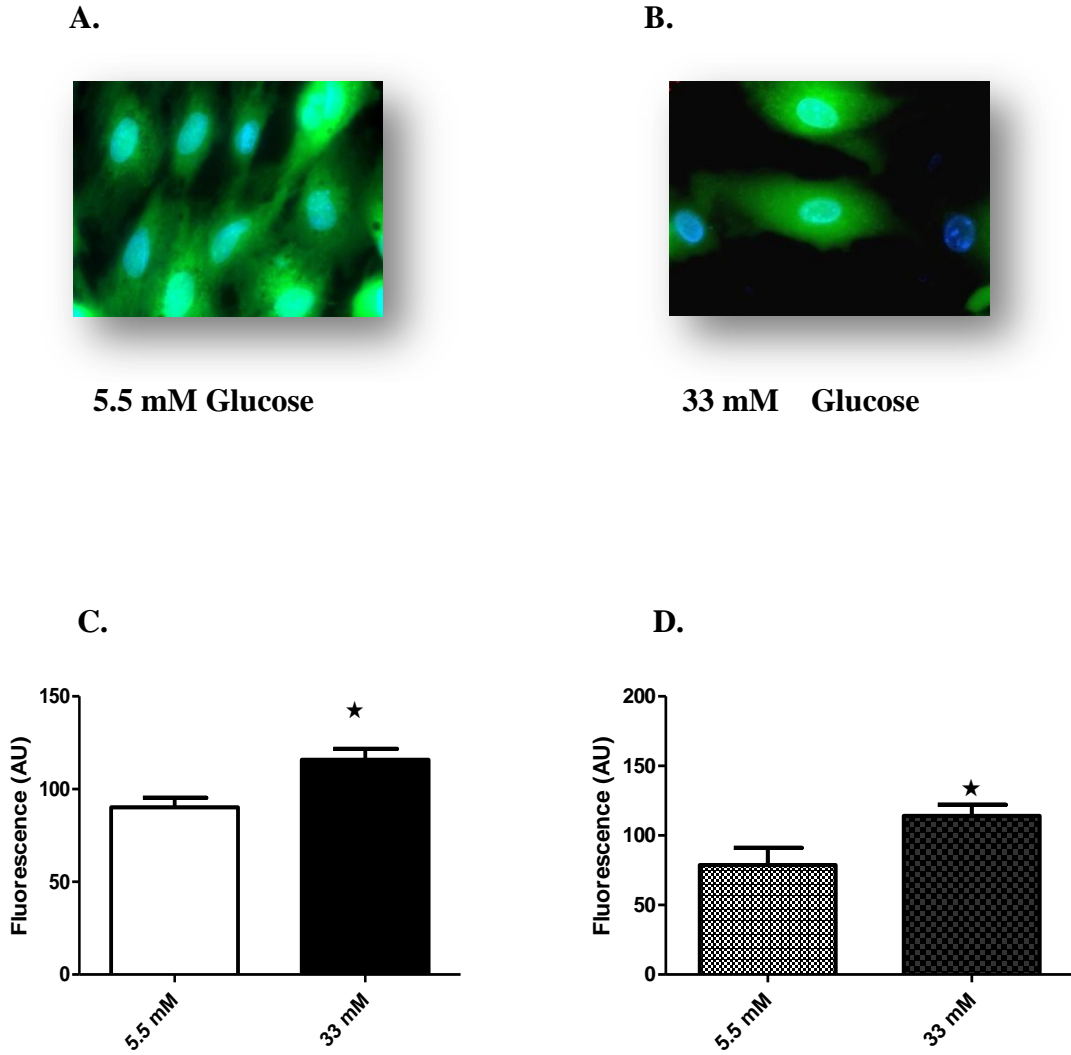


Figure 9: Effects of 54 hrs high glucose treatment on ROS production in H9C2 cells (magnification X60). Green fluorescence of cells treated with (A) 5.5 mM Glucose (B) 33 mM Glucose (C) Fluorescence quantification using Fluorescence microscope and (D) Flow cytometry. Values are expressed as mean \pm SEM (n=9 Fig 9 C and n=4 Fig 9 D). * p< 0.05 vs. 5.5 mM glucose control group.

No significant changes in ROS production was observed following exposure of cells with high glucose for 72 hours as determined by microscopy analysis (Fig 10C). Similar results were obtained with the flow cytometry analysis (Fig 10D).

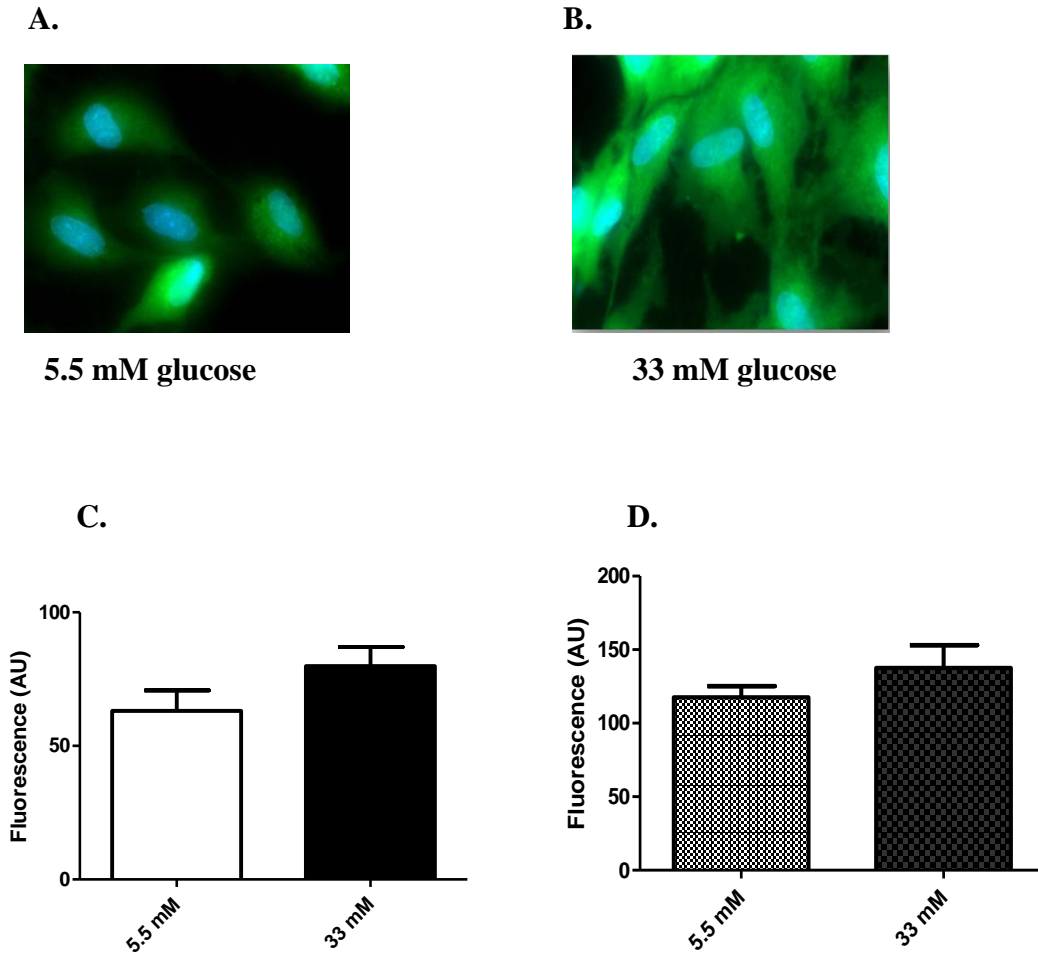


Figure 10: Effects of 72 hrs high glucose treatment on ROS production in H9c2 cells (magnification X60). Green fluorescence of cells treated with (A) 5.5 mM glucose, (B) 33 mM glucose. Fluorescence quantification using (C) Inverted microscopy and (D) Flow cytometry. Values are expressed as mean \pm SEM (n=9 Fig 10C and n=4 Fig 10D). * p < 0.05 vs. 5.5 mM glucose control group.

2.3.3 Effects of oleanolic treatment acid on glucose-exposed H9C2 cell lines

Treatment of low glucose exposed (48 hours) H9C2 cells with 20 μM OA for 6 hours had no significant effects on ROS production as determined by microscopic and flow analysis (Fig 11). However, treatment with 50 μM OA attenuated ROS generation by $32.3 \pm 9.3 \%$ and by $19.6 \pm 6.3\%$ ($n=9$; $p < 0.05$ vs. 5.5 mM glucose control) as determined by microscopy (Fig 11D) and flow cytometry (Fig 11E), respectively.

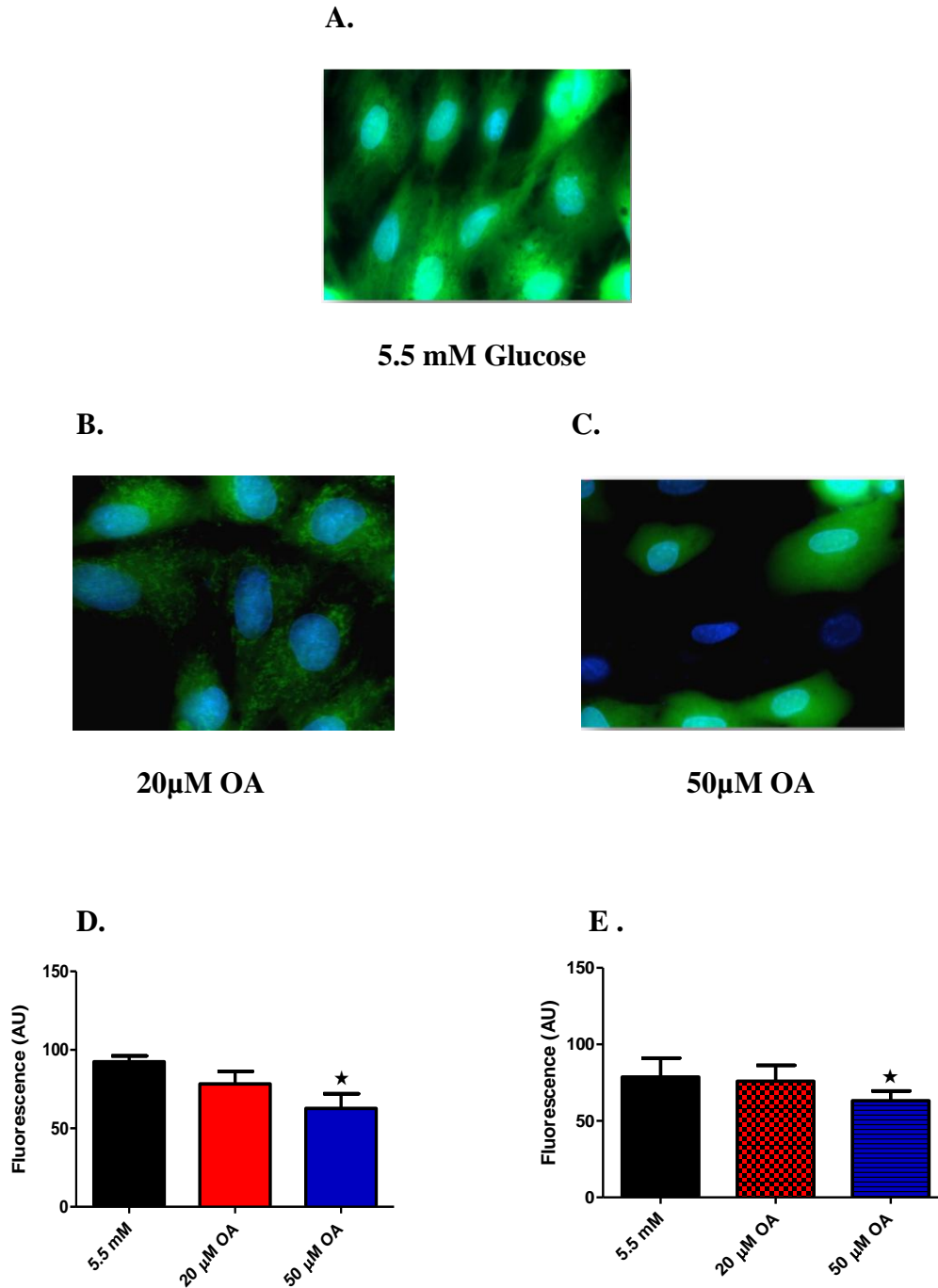


Figure 11: Effects of 6 hr OA treatment on ROS production in low glucose exposed H9C2 cell lines (magnification X60). Green fluorescence of cells treated with (A) 5.5 mM glucose, (B) 20 μM OA, (C) 50 μM OA treated groups. Fluorescence quantification using (D) Inverted microscope and (E) Flow cytometry. Values are expressed as mean ± SEM (n=9 Fig 11D and n=4 Fig 11E). * p < 0.05 vs. 5.5 mM glucose control.

Treatment of high glucose exposed cells for 6 hours with 20 μ M and 50 μ M OA, respectively, showed a marked reduction in ROS production (Fig 12) as shown by microscope and flow cytometry. Here, microscope analysis showed reduction in ROS fluorescence by $26.6 \pm 8.5\%$ and $37.7 \pm 6.2\%$ ($n=9$; $p < 0.005$ vs. high glucose treated control group) (Fig 12D). In parallel, flow cytometry analysis of treatment of high glucose exposed cells with 20 μ M and 50 μ M OA for 6 hours showed a significant reduction in ROS production. Reduction in ROS fluorescence reached $31.8 \pm 6.9\%$ and $40 \pm 6.8\%$, respectively, ($n=4$) $p < 0.005$ vs. 33 mM glucose control group.

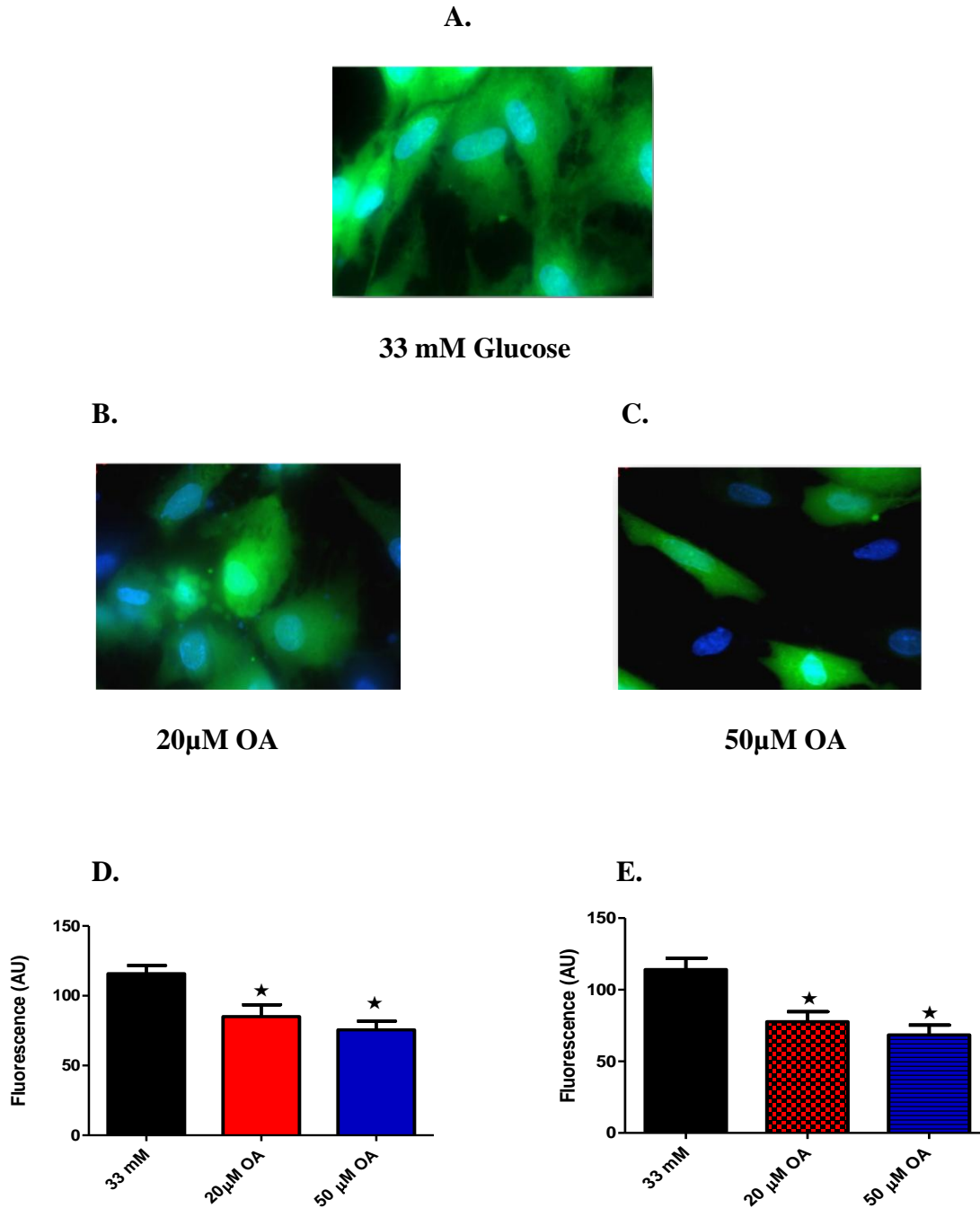


Figure 12: Effects of 6 hr OA treatment on ROS production in high glucose exposed H9C2 cell lines (magnification X60). Green fluorescence of cells treated with (A) 33 mM Glucose (B) 20 μM OA (C) 50 μM OA treated groups. Fluorescence quantification using (D) Inverted microscope and (E) Flow cytometry. Values are expressed as mean ± SEM (n=9 Fig 12D and n=4 Fig 12E)* p < 0.05 vs. 33 mM glucose control.

Next, we investigated the effects of oleanolic acid for 24 hours on ROS generation of low glucose exposed cells. Figure 13 represents the 24 hour treatment of H9C2 cells with normal glucose treated H9C2 cell lines at 24 hours. Microscope analysis showed that 20 μ M and 50 μ M OA caused a dose-dependent reduction in ROS fluorescence signal by $47 \pm 8.5\%$ and by $59.6 \pm 1.9\%$ ($n=9$; $p < 0.005$ vs. 33 mM glucose) (Figure 13 D). Flow cytometry analysis of low glucose exposed cells treated with 20 μ M and 50 μ M OA for 24 hours showed a reduction in ROS fluorescence signal by $44 \pm 3.4\%$ and $46 \pm 6.1\%$ ($n=4$; $p < 0.005$ vs. 33 mM glucose) (Fig 13E).

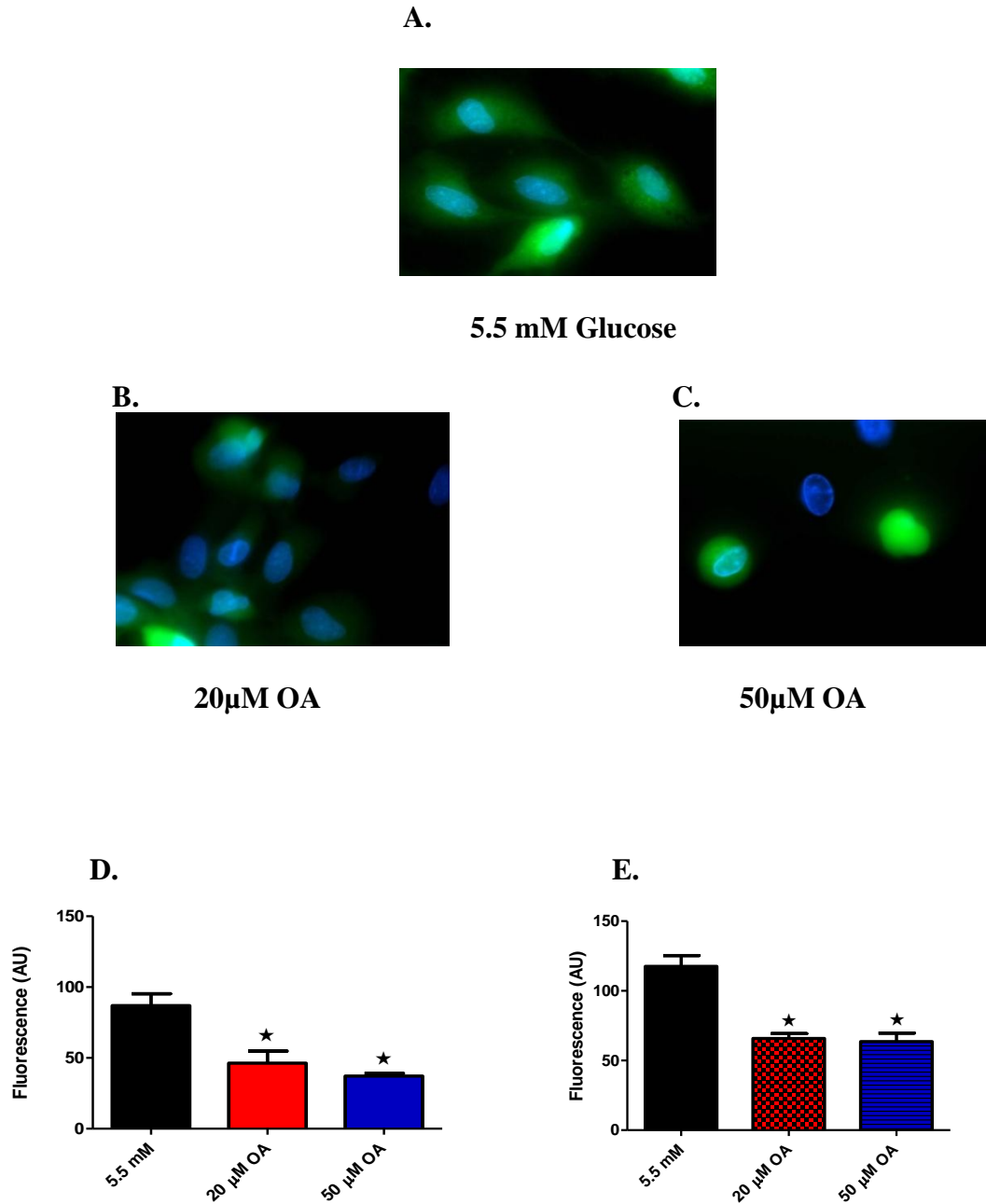


Figure 13: Effects of 24 hr OA treatment of low glucose exposed H9C2 cells on ROS production (magnification x60). Green fluorescence of cells treated with (A) 5.5 mM glucose (B) 20 μM OA (C) 50 μM OA. Fluorescence quantification using (D) Inverted microscopic and (E) Flow cytometry. Values are expressed as mean ± SEM (n=9 Fig 13 D and n=4 Fig 13 E). * p<0.05 vs. 5.5 mM glucose.

The effect of oleanolic acid on high glucose treated H9C2 cells treated for 24 hours was investigated following treatment with 20 μ M and 50 μ M OA. The dose-dependent reduction in ROS fluorescence signal reached $15.7 \pm 5.4\%$ and $80.7 \pm 0.4\%$ ($n=9$; $p < 0.005$ vs. 33 mM glucose) using the inverted microscope analysis for 24 hours on high glucose treated H9C2 cell lines (Fig 14D). Next we performed quantitative analysis using high glucose exposed H9C2 cells treated with 20 μ M and 50 μ M OA, respectively, for 24 hours using flow cytometry. ROS generation showed a significant reduction in ROS fluorescence signal following 24 hour-treatment of high glucose exposed cells with 20 μ M and 50 μ M OA, i.e. by $44.6 \pm 6.7\%$ and $54.4 \pm 12.5\%$, respectively ($n=9$; $p < 0.005$ vs. 33 mM glucose) (Fig 14E).

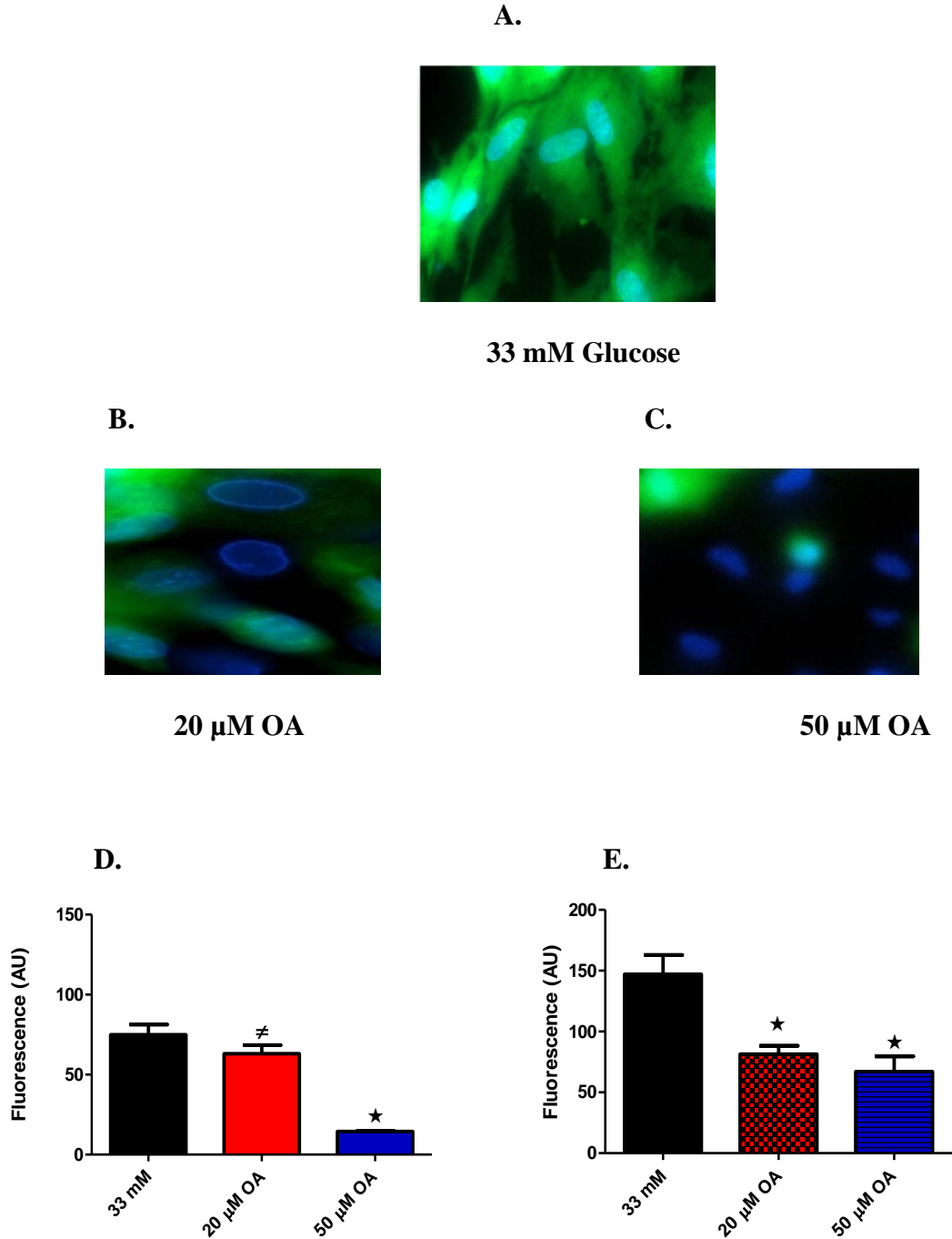


Figure 14: ROS production of 24 hr OA treatment in high glucose exposed H9C2 cells (Magnification X60). Green fluorescence of cells treated with (A) 33 mM Glucose (B) 20 μM OA (C) 50 μM OA treated groups. Fluorescence quantification using (D) Inverted microscope and (E) Flow cytometry. Values are expressed as mean ± SEM (n=9). * p<0.05 vs. 33 mM glucose. # p<0.05 vs 50 μM OA treated group.

2.4 DISCUSSION

2.4.1 *Syzigium aromaticum* (cloves) derived oleanolic acid

In the present study, we isolated OA a triterpenoid from *Syzigium aromaticum*. Recrystallisation of the powder with ethanol and inspection with spectroscopic techniques of 1 and 2- dimensional ¹H- and ¹³C-NMR spectra of the compound confirmed the presence of the 48 Hydrogen and 30 Carbon atoms (Somova *et al.*, 2003; Mapanga, *at al.*, 2009). Carbon 18 has a β methyl group which is common character between the two isomers (oleanolic and ursolic acid). The most distinguishing factor was the presence of the two (CH₃) methane groups in Carbon 20 which are the main character that confirmed the structure of oleanolic acid from the other acids in its class (Mapanga *at al.*, 2009).

2.4.2 *In- vitro* model of hyperglycaemia-induced oxidative stress

Diabetes mellitus-induced hyperglycaemia has been shown to trigger reactive oxygen species (ROS) and nitrogen species production (Hayat, *et al.*, 2004; Dallack, *et al.*, 2008). Several studies have shown that high glucose induces oxidative stress in various *in-vitro* models, for example; human umbilical vein (Meng *et al.*, 2008) and PC12 neuronal cells (Sharifi *et al.*, 2009). Cai *et al.* (2002) showed that 33 mM glucose induces oxidative stress in H9C2 cells. The glucose transport system of the H9C2 cell line is similar characteristics to that isolated from neonatal rats or mouse *in-vivo* (Cai *et al.*, 2002). Recently, Rajamani and Essop (2010) confirmed that 33 mM glucose treatment of H9C2 cells generated reactive oxygen species production.

Our findings were similar to those in literature (Cai, *et al.*, 2002; Rajamani and Essop, 2010), i.e. 54 hours treatment with high glucose (33 mM glucose) caused an increased in levels of

fluorescence signal of the H₂DCF-DA dye which suggests the presence of oxidative stress. However, this burst of ROS generation was only observed following exposure of H9C2 cells to high glucose for 54 hours and not 72 hours. Rajamani and Essop (2010) showed that exposure of H9C2 cells to high glucose for 5 days increased ROS production. Furthermore, Cai *et al.* (2002) showed that these effects occurred in a time-dependent fashion. However, in our study this was not the case. We speculate that the high glucose exposed cells at 72 hours did not exhibit significant fluorescence due to reduced cell density. A similar increasing trend is observed with the 72 hour exposures, although no statistical significance is obtained. Few viable cells exhibiting the fluorescence could account for this increased trend in fluorescence observed. Of note is that the cell specific data (microscope) is in agreement with the population data (flow cytometer) both which are established tools used in cell studies (Ormerod 1998). The cell viability assay is a colorimetric assay used to measure parameters of a viable cell for any metabolic activity (Wayerman *et al.*, 2005). These reactions can only occur in metabolically active cells therefore establishing the cell densitometry (Mosman, 1983; Chiba *et al.*, 1997; Stephanou *et al.*, 2000; Wayerman *et al.*, 2005). However, in our study this assay was not performed but it forms part of future plans.

Peroxynitrite has been shown to be the main inducer of oxidative stress in the myocardium (Levrard *et al.*, 2006). However, in our study we did not specifically measure the different types of ROS. Moreover, several studies suggest that mitochondria are the main source of ROS in glucose-induced models. Therefore, superoxide is suggested to be likely the culprit for ROS-induced damage in our cultured cell line. H₂DCF-DA is an oxyburst dye, which collectively detects all types of ROS. Other studies employed ROS-specific dyes such as dihydrorhodamine for the peroxynitrite, dihydroethidium for superoxide and carboxy H₂DCF-DA for the hydroxyl

species (Kumar and Sisawad, 2009). 1, 2 dihydroxy H₂DCF-DA dye is an oxyburst is specific for hydroxyl compound. The carboxy-DCF-DA was used to detect intracellular ROS mainly H₂O₂ production (Wang *et al.*, 2010). Thus future studies should employ some of these markers to more accurately detect the precise origin of ROS in our experimental system.

2.4.3 Effects of plant derived triterpene (Oleanolic acid) on treated H9C2 cell lines

ROS production in cardiomyocytes contributes to the onset of diabetic cardiomyopathy and subsequent heart failure in diabetic patients (Dallack *et al.*, 2008). The myocardium is known to have low levels of antioxidants (Kumar and Sitasawad, 2009). There are several antioxidants shown to reduce levels of oxidative stress in cardiomyocytes, and this is of utmost clinical significance in management of DM and heart failure (Kumar and Sitasawad, 2009). For example, N-acetylcysteine inhibited glucose-induced oxidative stress in H9C2 cells, and had a protective role in a rat model of streptozotocin-induced diabetes (Kumar and Sisatawad 2009)

OA is a bioactive compound isolated from many medicinal plants such as pomegranate flower, *Syzigium cordatum* leaves and *S aromaticum* (cloves) (Somova *et al.*, 2003; Musabayane, *et al.*, 2005; Huang *et al.*, 2005; Mapanga *et al.*, 2009). The crude clove extract had insulin-like effects on hepatic gene expression (Prasad *et al.*, 2005). Oleanolic acid isolated from Glossy privet fruit (*Ligustrum lucidum*) showed antioxidant properties in relation to glucose-induced oxidation of plasma and low density lipoprotein (LDL) in human cells (Wang *et al.*, 2009). Antioxidant properties of OA were also observed in H₂O₂-induced DNA damage in leukemic cells. OA had antioxidative effects in HL-60 cells (Ovesn'a *et al.*, 2006). Moreover, OA isolated from olive leaves exhibited antioxidant effects *in-vitro* and hepatoprotective effects *in-vivo* in carbon tetrachloride induced liver injury (Bai *et al.*, 2007).

Our study showed that OA had anti - oxidative effects in low glucose treated cardiac cell line. 24 hour treatment of low glucose cells with 20 μM and 50 μM OA inhibited ROS production. Previous studies have shown that OA is not only a free radical-scavenger acting through direct chemical reactions but also a biological molecule, which may enhance the antioxidant defences and restore the lost anti-oxidant reducing equivalents (Bonnetfont-Rousselot, 2002; Rolo and Palmera 2006; Brownlee, 2005). ROS production has a fundamental role in various physiological reactions therefore profuse inhibition could be detrimental (Somova *et al.*, 2003).

OA exhibited ROS alleviating properties in high glucose (33 mM glucose) exposed cells suggesting its protective and antioxidant properties. Such ROS inhibiting effects were more pronounced at 24 hours with the high glucose treated cells suggesting increased ROS. Interestingly, the antioxidant effects of 50 μM OA was more pronounced with the microscope cell specific data. This is in line with the findings from Teodoro (2008) where OA was shown to be more potent at 50 μM treatment. These findings also confirmed the most potent treatment of OA for its ROS inhibiting properties in cardiac cell lines. Furthermore, OA has been shown to have concentration-dependent effects in inflammation, tumour, viral and hepatic studies (Teodoro *et al.*, 2008), and our findings suggest 50 μM OA treatment had the maximal effect in high glucose exposed H9C2 cells.

Several mechanisms by which OA lowers plasma glucose levels in rats have been shown. These include reducing gastric emptying (Yoshikawa and Matsuda 2000), enhancing insulin resistance (Teodoro *et al.*, 2008) and increasing acetylcholine release (Hsu *et al.*, 2006). In the ischemic heart OA modulated energy homeostasis via stimulation of 5' adenosine monophosphate-activated protein kinase (AMPK) signaling pathway which ultimately leads to GLUT 4

translocation to the cell membrane therefore enhancing glucose uptake (Miller *et al.*, 2008). However, these effects were observed in experimental animals. For *in vitro* studies, 50 μ M OA heightened both basal and glucose stimulated insulin secretion in the pancreatic β cells (Teodoro *et al.*, 2008). H9C2 embryonic rat heart-derived cells were employed for the study because they have become an established *in vitro* model to study the effects of ischemia and diabetes on the heart. (Sardao *et al.*, 2007) During differentiation the H9C2 cell line has been shown to maintain several characteristics of the electrical and hormonal signalling pathway of cardiac cells (Sardao *et al.*, 2007)

We therefore speculate that OA may have indirectly facilitated insulin secretion thereby stimulating GLUT 4 release from the vesicles to the membrane leading to glycolysis and increased energy generation. Teodoro (2008) in insulin secretion studies further suggested the mechanism of action of OA to be due to modifying protein activity. The Michael addition which is a chemical reaction between a nucleophile such as –SH group and an unsaturated carbonyl such as those found in OA as initially proposed by Couch using semi-synthetic triterpenoid derived from oleanolic acid in chemo preventive and chemotherapeutic (Couch *et al.*, 2005).

In summary oleanolic acid reduced high glucose induced oxidative stress in myocardial cells; this was shown by reduced fluorescence after 6 and 24 hours treatment with different doses of oleanolic acid. Antioxidants are useful in alleviating oxidative stress implicated in diabetic cardiomyopathy and thus may protect the heart e.g. with ischaemic insult or during heart failure. Clinical and animal models studies are required to confirm these findings and further elucidate mechanism by which OA exerts its antioxidant effects.

CHAPTER 3

3.1 Introduction

Apoptosis or programmed cell death is a morphological transition from an intact metabolically active cellular state into maladaptive shrunken apoptotic bodies (Hotchkiss and Nicholson 2006). Apoptosis is observed both under physiological and pathological conditions (Sharifi *et al.*, 2009; Johansen *et al.*, 2005). Some of the characteristic changes induced by apoptosis include chromatin condensation, nucleosomal DNA fragmentation, and nuclear membrane breakdown, externalization of phosphatidylserine and formation of apoptotic bodies (Schulze-Osthoff *et al.*, 1998; Wang *et al.*, 2001; Regula *et al.*, 2003). Necrotic cell death is characterized by swelling and rupture of injured cells, resulting in inflammation. While apoptosis is an active process, necrosis does not require energy (Rastogi *et al.*, 2009).

Programmed cell death occurs in three stages. These include induction, decision and execution. Induction is dependent on the nature of the death-inducing signal, i.e. the intrinsic or extrinsic signals (Kroemer *et al.*, 2007). Mitochondria play a crucial role in the cell death pathway. Mitochondria are also targets of reactive oxygen species (ROS) and a source for the generation of additional ROS species. Mitochondrial physiology is disrupted in cells undergoing apoptosis. Several mitochondrial proteins are involved in stimulating cellular apoptotic programs directly (Regula *et al.*, 2003). Previous studies have shown that during apoptosis mitochondria undergo specific damages that result in loss of its function (Regula *et al.*, 2003). Cytochrome-c is located between Complex III and Complex IV of the mitochondrial electron transport chain; donate electrons via cyt-c reductase III to cyt-c oxidase IV where oxygen is reduced to a water molecule. Inhibition of this step increases the production of reactive oxygen species with

subsequent peroxidation (Rolo and Palmeria 2006; Regula *et al.*, 2003). Mitochondria have been shown to release cytochrome-*c* in the presence of oxidants (Gill *et al.*, 2002). Cytochrome-*c*, the sole water soluble component of the electron transport chain affects the maintenance of mitochondrial membrane potential and its energy generation (Regula *et al.*, 2003; Kumar, and Sitasawad 2009). Subsequently, the inner mitochondrial membrane permeability is altered resulting in a decrease of the mitochondrial membrane potential (Kumar and Sitasawad 2009). Cytochrome-*c* that is released in the cytoplasm then forms an apoptosome with ATP and apoptotic inducing factor-1.

Biochemical features of an apoptotic cells includes several enzymatic steps. A group of cysteine aspartate-specific proteases (caspases) play a crucial role in the apoptotic cell death. Proteases are present in the cell in their inactive form as procaspases, these are cleaved and stimulated in response to different stimuli which triggers the apoptotic signalling in the cell and may include activation of the caspase cascade. Caspases-8, 9 and 12 are involved in the induction of apoptosis. The second group include caspases-3, 6 and 7 which induce downstream events observed in apoptosis which including degradation of proteins (Sharifi *et al.*, 2009). Caspase-3 and 7 are involved in the downstream apoptosis signalling in the cell cytoplasm due to a cleavage with cytochrome-*c* in mitochondrial mediated pathway or with apoptotic inducing factors such as Bax and Bcl2 in the extrinsic pathway (Figure 15).

3.1.1. The extrinsic cell death pathway

The extrinsic pathway is a receptor-mediated pathway that involves death receptors such as Fas released by other cells. The Fas receptor is required for the formation of death-inducing complex

required for activation of the cascade of caspases leading to apoptosis (Park *et al.*, 2005). Upon binding with the death-inducing complex receptors, tumour necrosis factor (TNF) receptor-1, CD95/Fas (the receptor of CD95L/FasL) are stimulated to bind on the surface (Kroemer, 2007), and accumulate to form an aggregate and recruit procaspase-8 to a death-inducing signal complex. Activation of procaspase-8 to caspase-8 is followed by activation of effector protein (caspase3) which induces degradation of cellular proteins and cell death (Raff, 1998).

3.1.2. The intrinsic cell death pathway

The intrinsic pathway involves mitochondria permeabilisation and occurs due to the release of intrinsic components such as cytochrome-c and other mitochondrial contents such as Smac and apoptotic-inducing factors (Wang, 2001). In diabetes mellitus high glucose serves as an internal apoptotic stimulator by triggering generation of reactive oxygen species. The cardiomyocyte then responds by translocating the pro-apoptotic proteins (AIF) to the cytosol thereby causing mitochondrial depolarisation due to increased oxidative stress as well as release of cytochrome-c and activation of caspases (Allen *et al.*, 2005). Membrane permeabilisation is a key regulatory element in deciding whether a cell survives or undergoes apoptosis (Kroemer, *et al.*, 2007). Several factors are involved in facilitating this process. These include the Bcl-2 protein family that regulates programmed cell death via mitochondrial outer membrane permeability and release of cytochrome-c. Localization of these proteins in the cell membrane may rescue or commit the cell to apoptosis. Anti-apoptotic proteins include Bcl-2 and Bcl-XL which attenuate outer membrane permeabilisation therefore inhibiting release of these proteins from the mitochondria. Moreover, Bax and Bak are known to stimulate outer membrane permeabilisation thereby releasing apoptotic proteins (Armstrong, 2006).

Mitochondrial depolarisation triggers the release of the mitochondrial Bcl-2, Bcl-XL, Bax, Bak and cytochrome-c. Cytochrome-c once released binds to a cytoplasmic protein, Apaf-1. Thereafter, procaspase-9 binds to cytochrome-c and Apaf-1 to form an apoptosome. This activates the initiator caspase-9, which cleaves other executioner caspases (-3 and -7), ultimately leading to apoptosis. The activation of caspase-3 via the extrinsic and intrinsic pathways results in phosphatidylserine externalisation on apoptotic cells, allowing early recognition and phagocytosis of apoptotic cells (Smart and Hoggson 2008).

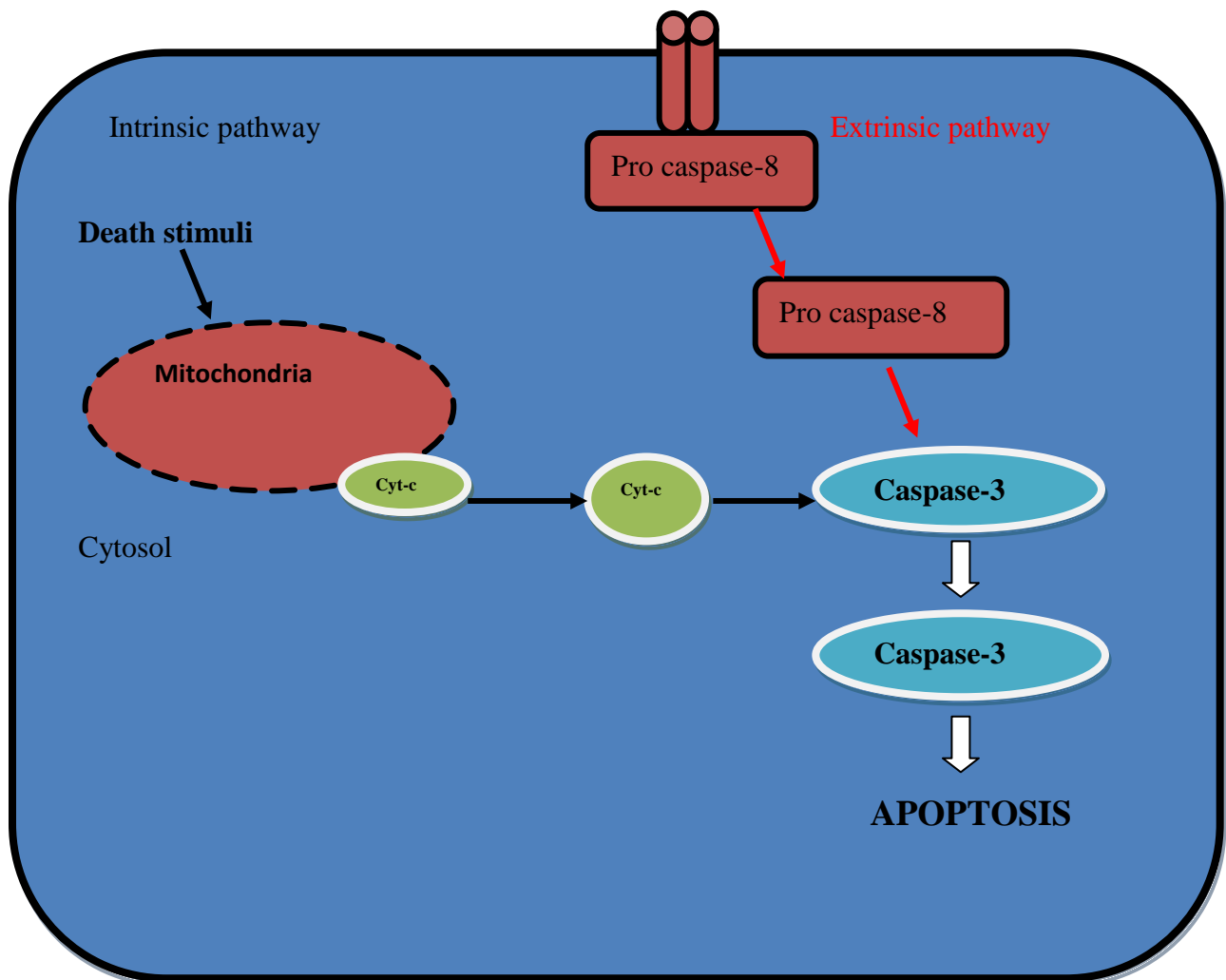


Figure 15: A schematic representation of intrinsic and extrinsic apoptotic pathways.

3.1.3 Apoptosis and diabetic cardiomyopathy

Programmed cell death and ROS generation play a crucial role in the onset of the diabetic cardiomyopathy leading to heart failure in patients with diabetes (Mishra and Rath 2005; Frustaci *et al.*, 2008). In cardiomyopathy, cell death is a resultant effect of the response of myocardial cells to a high glucose insult and is characterised by metabolic remodelling, sub-cellular defects and abnormal expression of genes (Mishra and Rath 2005; Cai *et al.*, 2002). High glucose culturing conditions displayed greater glucose oxidation, increased superoxide production, DNA damage, activation of PPAR, thereby resulting in apoptosis (Zhang *et al.*, 2001; Du *et al.*, 2003; Poornima *et al.*, 2006). Several studies have demonstrated that apoptosis occurs in diabetic myocardium as a consequence of hyperglycaemia-induced oxidative stress (Cai *et al.*, 2002; Dallak *et al.*, 2008). The circulating free radicals seen in diabetic patients have a major role in the progression of heart disease and apoptosis (Dallak *et al.*, 2008; Mishra and Rath, 2005). Reactive oxygen species are known triggers of hyperglycaemia-induced apoptosis in the myocardium implicating them in diabetic cardiomyopathy (Cai *et al.*, 2002). For example, peroxynitrite (ONOO⁻) is the main stimulator of cardiomyocyte apoptosis in diabetic cardiomyopathy both in *in-vitro* and *in-vivo* experimental studies (Levrant *et al.*, 2006; Dallak *et al.*, 2008).

In light of this, the aim of this chapter was to investigate the anti-apoptotic potential of oleanolic acid on H9C2 cells exposed to low and high glucose environments.

3.2 Materials and Methods

3.2.1 Cell culture

We employed H9C2 cells, an embryonic rat heart-derived cell line that was obtained from Sigma-Aldrich, (Steinheim, Germany). The cells were cultured in T75 flasks (Greiner, Krensmunster, Australia) and incubated at 37°C in 95% O₂ and 5% CO₂ in Dulbecco's modified Eagle's medium (DMEM) (Sigma-Aldrich, Steinheim, Germany) supplemented with 10% foetal bovine serum (FBS) (Invitrogen, Carlsbad, CA) and a normal glucose concentration of 5.5 mM in DMEM. Sub culturing was performed at a confluency of 80% and the media changed every third day.

3.2.2 Cell Treatment

On day 1 H9C2 cells were split and sub-cultured for experiments on 5.5 mM glucose in DMEM and allowed to plate for 24 hours. Cells cultured in a media of the same glucose concentration (a) 5.5 mM served as a control group and (b) 33 mM as high glucose treated group. H9C2 cells were further exposed for 48 hours under these conditions followed by dose-dependent treatment with 0, 20, 50 µM oleanolic acid for 6 hours and 24 hours, respectively.

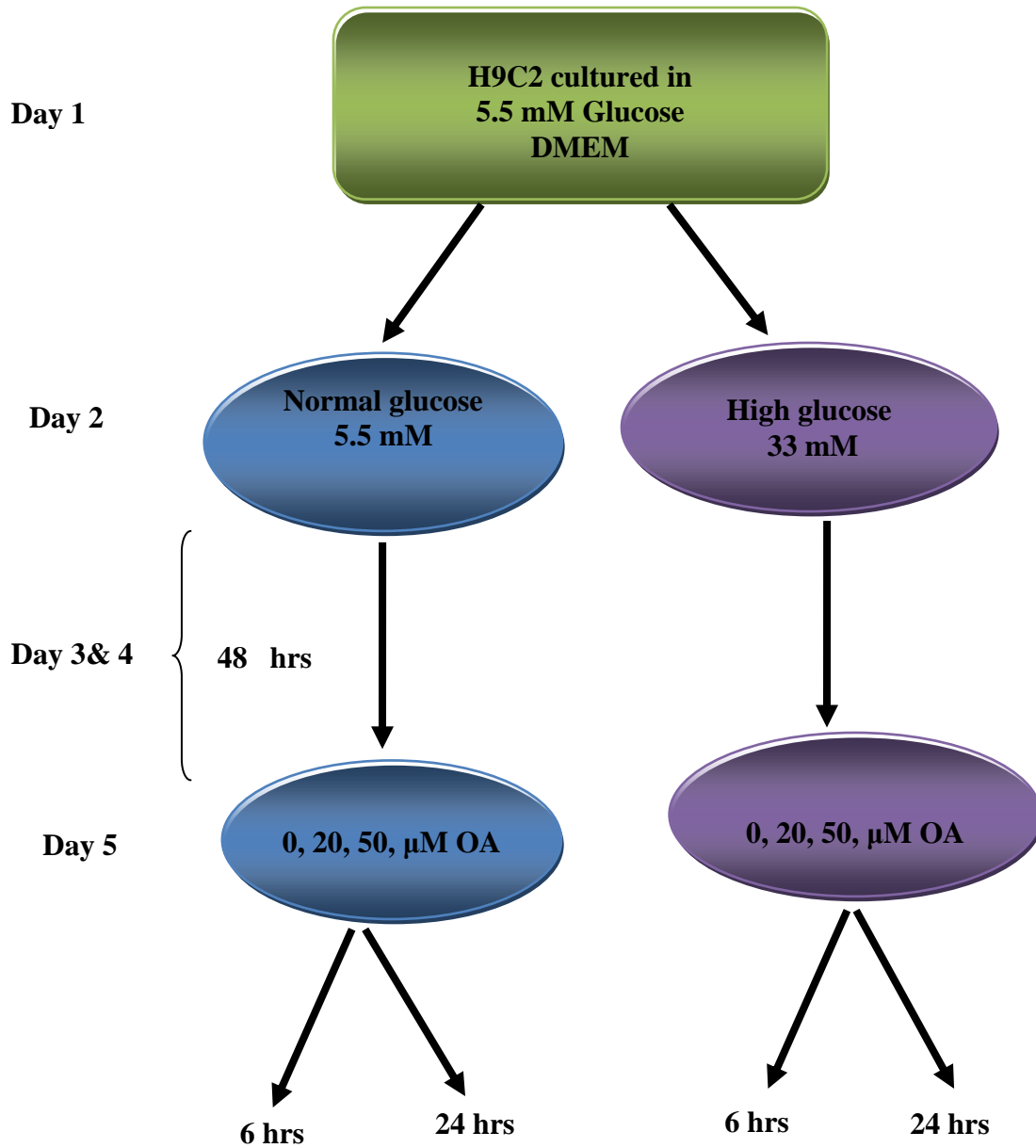


Figure 16: A schematic representation of the experimental procedure.

3.2.3 *In- vitro* model of high glucose induced apoptosis in H9C2 cell line

a) Caspase activity assay

In this study we measured the degree of caspase enzymatic activity which is a marker of apoptosis using the caspase-3/7 glo kit (as described in section 3.2 of this chapter). The process relies on activation of caspase-8 which further stimulates caspase-3 activity (Gill *et al.*, 2002). Caspase-3 is a major effector caspase in the apoptotic process, Western blot for the expression of this protein was also conducted (Varmes *et al.*, 2000).

H9C2 myoblasts were trypsinised and counted in a haemocytometer (LASEC, South Africa). 10×10^3 cells were seeded per well in a 96-well plate (Greiner, Kremsmünster, Austria). Cells were seeded with 300 μ L DMEM. Cells treated with 0.24 μ L DMSO were used as negative controls. Vehicle and DMEM with no cells was used as a blank. For each group, experiments were performed 5 times (n=5).

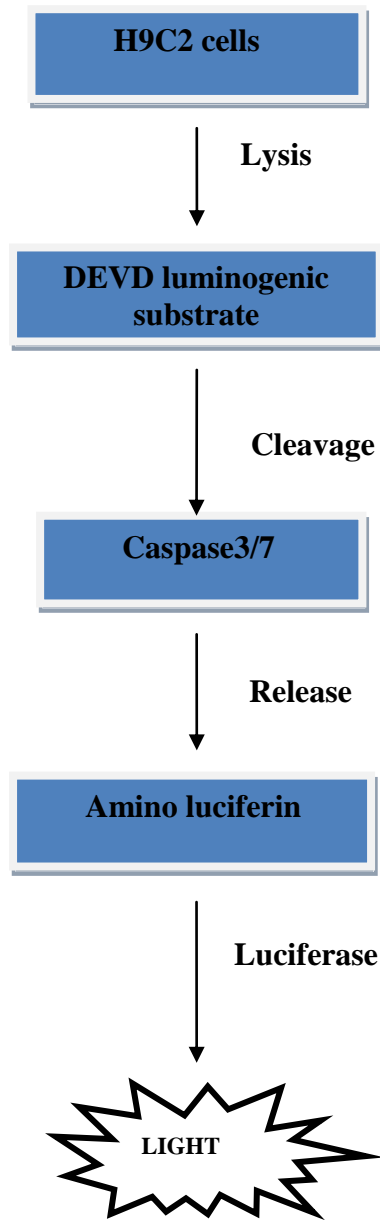


Figure 17: A schematic representation of the Caspase-Glo[®] 3/7 assay.

The Caspase-Glo[®] 3/7 assay (Promega, Madison, WI) was reconstituted as per manufacturer's instructions. Briefly, DMEM was removed and 100 μ L of the reconstituted assay reagent was added onto each well and mixed gently. Cells were then incubated in the dark at room temperature for approximately two hours. The luminescence of the samples was measured using a luminometer. To achieve this, special white-walled 96-well luminometer plates (Amersham, Buckinghamshire, UK) were used. The reagent-treated experiments from the normal 96-well plate were transferred into the white-walled luminometer plate that was then placed in a luminometer and readings taken for each well. The luminescence of each well corresponds to the caspase activity.

b) Western blots for Caspase 3

H9C2 myoblasts were trypsinised and counted. Approximately 3×10^5 cells were seeded in 5 ml DMEM in T25 flasks (Greiner, Kremsmünster, Austria). Following all experimental procedures, proteins were harvested by scrapping cells off the flask using freshly prepared modified Radio Immuno Precipitation Assay (RIPA) buffer. The collected lysate was then sonicated and centrifuged (ALC PK121R Multispeed refrigerated centrifuge) for 10 minutes at 4300 x g at 4°C and the supernatants were stored at -80°C. Total protein was quantified by the Bradford method (Bradford, 1976).

Western blot protein samples were prepared by adding 20 μ g of protein to an equal amount of sample buffer (3x sample buffer: 33.3 ml stacking buffer, 8.8 g SDS, 20 g glycerol and bromophenol blue in 75 ml distilled water; 850 μ L 3x sample buffer + 150 μ L mercaptoethanol

was used as the working sample buffer solution). Samples were subsequently boiled for 5 minutes before being loaded on 10 % sodium dodecyl sulphate- polyacrylamide gel

i) Electrophoresis (SDS-PAGE)

The samples were electrophoresed on a 10% SDS-PAGE (with a 4% stacking gel) at 200 V for one hour at room temperature. 10 μ L of protein marker (Bio-RAD Plus Protein™ Dual Colour Standards, CA) was loaded (Lane 1), with experimental samples loaded in the remaining lanes. After one hour, proteins from the gel were transferred to a PVDF membrane (Immobilon-P, Millipore Corporation, MA) by semi-dry electro transfer. This membrane was used to probe for caspase-3 (Cell Signalling, MA) in order to assess the degree of apoptosis. Caspase-3 primary antibody 1:1000 dilution was probed overnight at 4°C. The incubation was followed by 3-4 times wash with TBS-Tween for 5 min in a shake, incubated for one hour at room temperature with secondary anti-mouse HRP monoclonal antibody (1:4000). The membrane was then washed three to four times in TBS-Tween.

Protein bands were visualised using an ECL kit (700 μ l of reagent 1 and 700 μ l of reagent 2). Sandwich membrane was placed in a cassette, in a dark room. The cassette was closed for 5-8 minutes initially placed on the developer for 3 minutes and washed with water for 15 seconds. The films were also placed on the fixer for 5-6 minutes and finally rinsed with water for 15 seconds these were air dried and bands detected. Protein expression was determined by densitometry. Here the developed film was scanned using an HP Scan jet 3500c scanner (Hewlett Packard, Palo Alto, CA) and densitometry was performed using Un-Scan-It Gel version 5.1 (Silk software, Orem, UT). The densitometry value of the proteins under investigation was

normalised to the densitometry value of the corresponding β -actin. The normalised densitometric value was used for statistical analysis.

c) Annexin-V staining

In the early stages of programmed cell death the translocation of membrane phospholipids phosphatidyl serine (PS) from the inner to the outer leaflet of the plasma membrane occurs. We employed a calcium-dependent phospholipid binding protein, Annexin V, which has a high affinity for PS is conjugated with a fluorescein isothiocyanate (FITC) which emits fluorescence (492-520 nm) as an early marker of apoptosis. PS is an integral part of the apoptotic process, i.e. once committed to die the cell exposes the PS while maintaining the integrity of the plasma (Regula *et al.*, 2003; Dallack *et al.*, 2008). 5×10^5 cells were cultured in a T75 flask and upon confluency, trypsinised, washed with 1 X PBS [137 mM NaCl₂, 2.7 mM KCl, 10 mM Na₂HPO₄-7H₂O, 1.8 mM KH₂PO₄, pH 7.4] pelleted and resuspended in DMEM. Cell count was performed using a haemocytometer (LASEC, South Africa) and cells were seeded for microscopy and flow cytometry.

500 μ L of DMEM with 10% FBS were added to the eight well NuncTM chamber cover glass slides (Nalge Nunc, Rochester, NY). For each well 15×10^3 cells (15 μ L) were seeded, resuspended and allowed to plate for 24 hrs at 37°C in an incubation chamber. DMEM was removed from the plates followed by rinsing 3 X with ice cold 1 X PBS. Propidium iodide was added at a ratio of 1:200 of the working stock solution to each well. These were incubated at 37°C in the dark for 20 minutes. The dye was removed and cells were rinsed thoroughly with 1 X PBS four to five times. A methanol/ acetone fixative in a ratio 1:1 was added and incubated at 4°C for 10 minutes then

removed. Cells were left to air-dry for a further 20 minutes followed by rinsing 3 X with 1 X PBS. 5% donkey serum was added for 20 minutes in a black box, and the serum was drained and Annexin-FITC primary antibody was added at a dilution of 1:200 and incubated for 90 minutes. After rinsing 3 times with 1 X PBS Annexin-FITC secondary antibody was added (1:200) and incubated for 30 minutes at room temperature.

For nuclear identification, the cells were then further stained with Hoechst dye in PBS at a ratio of 1:200 for the last 10 min and removed. 100 μ L of 1 X PBS was added to the cells and viewed using an inverted microscope. Thereafter cells were viewed using an Olympus Cell^R fluorescence 1 X 81 inverted microscope (Olympus Biosystems, Germany) using an F-view II camera (Olympus Biosystems, Germany) for image acquisition and Cell^R software (Olympus Biosystems, Germany) for processing images. The temperature of the microscope system was maintained at 37°C for live cell imaging using a Solent Scientific microscope incubator chamber (Solent Scientific, UK). The green intensity of all cells expressing Annexin V FITC signal was measured, generating a numerical value corresponding to the degree of apoptosis. Three independent experiments were conducted and 3 images per experiment acquired. Thus an n=9 was generated for each experiment.

d) Staining for mitochondrial membrane potential

Cells undergoing programmed cell death are identified by a disrupted mitochondrial physiology, this disruption results in reduced mitochondrial membrane potential (Kumar and Sitawasad 2009; Kroemer *et al.*, 2007). Inner mitochondrial permeabilisation refers to the formation of channels or pores that leads to dissipation of the mitochondrial membrane potential across the

inner mitochondria. Under normal physiological conditions the mitochondrial membrane potential ranges between 120- 180 mV (Kroemer *et al.*, 2007). Lipophilic cations accumulate in the matrix of mitochondria and this is facilitated by the mitochondrial membrane potential. Several cationic fluorochromes are used in measurement of the mitochondrial membrane potential, including chloromethyl-X-rosamine (Mito-Tracker Red); tetramethyl rhodamine methyl ester (TMRM) and 5,5,6,6-tetrachloro-1,1,3,3- tetraethyl benzimidazol carbocyanine iodide (JC-1) (Kumar and Sitawasad 2009; Kroemer *et al.*, 2007; Wang *et al.*, 2009). JC-1 was employed in our study and is a first J aggregate-forming cationic dye; it penetrates live cell plasma membrane as monomers (Wang *et al.*, 2009).

i) Seeding and staining for microscopy

500 μ L of DMEM supplemented with 10% FBS were added to the eight well Nunc[™] chamber cover glass slides (Nalge Nunc, Rochester, NY). For each well 15×10^3 cells (15 μ L) were seeded, resuspended and allowed to plate for 24 hrs at 37°C in an incubation chamber. DMEM was removed by a suction pump followed by rinsing 3 X with 1X PBS. 0.5 ml JC-1 dye in DMSO was added from the working stock solution. For a working solution 1 X assay buffer and JC-1 for 25 flow samples to each well covered in foil and incubated for 10 -15 minutes at 37°C in CO₂ incubator. Following incubation period the cells were washed with 1 X Assay buffer by adding 100 μ l of the assay buffer to each well and resuspending 3-4 times using a pipette. To avoid stressing the cell, 100 μ L assay buffer was added to the cells and viewed using a light microscope. Cells were then viewed using a Olympus Cell[^]R fluorescence 1 X 81 inverted microscope (Olympus Biosystems, Germany) using an F-view II camera (Olympus Biosystems, Germany) for image acquisition and Cell[^]R software (Olympus Biosystems, Germany) for

processing images. The temperature of the microscope was maintained at 37°C for live cell imaging using a Solent Scientific microscope incubator chamber (Solent Scientific, UK). The ratio of red/ green fluorescence measured at 590 nm and 530 nm respectively, generating a numerical value corresponding to JC-1 aggregate. Three independent experiments were conducted and 3 images per experiment acquired. Thus an n=9 was generated for each experiment.

ii) Seeding and staining for flow cytometer

T25 flasks were used to seed approximately 1×10^5 cells (100 μ L) in each flask containing 5ml of DMEM in 10 % FBS. Seeding was performed for all different treatment groups (0, 20 and 50 μ M OA) under normoglycaemic (5.5 mM) and hyperglycaemic (33 mM) conditions. At the end of the experimental protocol DMEM was removed using a pipette and the cells were washed 3 times with 1 X PBS (300 μ L). To dislodge cardiomyoblasts from the flasks, cells were trypsinised with 2ml trypsin for 3min followed by 4ml DMEM in 10 % FBS and centrifuged into a pellet. Trypsin/DMEM mixture was discarded and rinsed 3 X with 1X PBS. 0.5 ml JC-1 dye in DMSO was added from the working stock solution. For a working solution 1 X assay buffer and JC-1 for 25 flow samples were added to each well covered in foil and incubated for 10 -15 minutes at 37°C in CO₂ incubator. Following incubation period the cells were washed with 1 X Assay buffer by adding 100 μ l of the assay buffer to each well and resuspended 3-4 times using a pipette. The cells were then run through FACS Aria flow cytometer (Becton-Dickinson, CA) and population data obtained.

Four independent experiments were conducted for each condition investigated. The mean of the fluorescence of a cell population represented the numerical value of the experiment which was used for analysis.

3.3 Statistical analysis

All data were expressed as means \pm standard error of the mean (S.E.M). Statistical analysis was done using GraphPad InStat Software (version 4.00, GraphPad Software, San Diego, California, USA) using one-way analysis of variance (ANOVA), followed by Turkey-Kramer multiple comparison test multiple comparison test. A p value < 0.05 was considered significant.

3.4 Results

3.4.1 Caspase-3 assay

Hyperglycaemia has been shown to induce apoptosis in the diabetic heart (Cai *et al.*, 2002).

Here, we investigated the effects of oleanolic acid on apoptosis in glucose treated cells. Exposure of H9C2 cells to high glucose for 54 hours and 72 hours showed a marked increase in caspase-3 enzyme activity, respectively (n=5; p< 0.001 vs. 5.5 mM glucose group) (Fig 18 A and Fig 18 B).

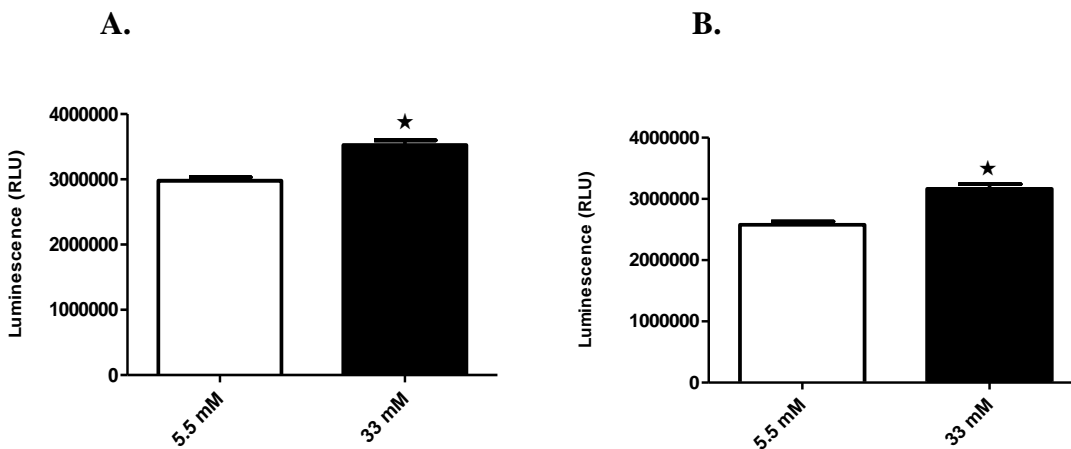


Figure 18: Caspase activity for H9C2 cells treated with high glucose. Luminescence quantification using luminometer following exposure of H9C2 cells to high glucose for (A) 54 hrs and (B) 72 hrs, as detected by *Caspase-Glo*[®] 3/7 assay described in section 3.2 of this chapter. Values are expressed as mean \pm SEM (n=5). * p < 0.001 vs. 5.5 mM glucose group.

Oleanolic acid has been shown to induce apoptosis in various models of human liver cancer cells using 4 μM and 8 μM OA, respectively (Yan *et al.*, 2010). To examine the effects of oleanolic acid in H9C2 cell lines, the cells were treated with 20 μM and 50 μM OA for 6 hours. Low glucose-treated H9C2 cell lines showed a dose-dependent reduction in caspase-3 enzymatic activity reflected by a moderate reduction in luminescence in relative light units (RLU) by $28 \pm 1.34\%$ ($n=5$; $p < 0.001$ vs. 5.5 mM glucose group and $44 \pm 1.13\%$ ($n=5$; $p < 0.001$ vs. 5.5 mM glucose group for both 20 μM and 50 μM OA (Figure 19 A). Similar effects were observed with the high glucose-treated cells. Here, luminescence was reduced by $25 \pm 2.38\%$ and $43 \pm 3.7\%$ ($n=5$; $p < 0.001$ vs. 33 mM glucose control (Fig 19 B).

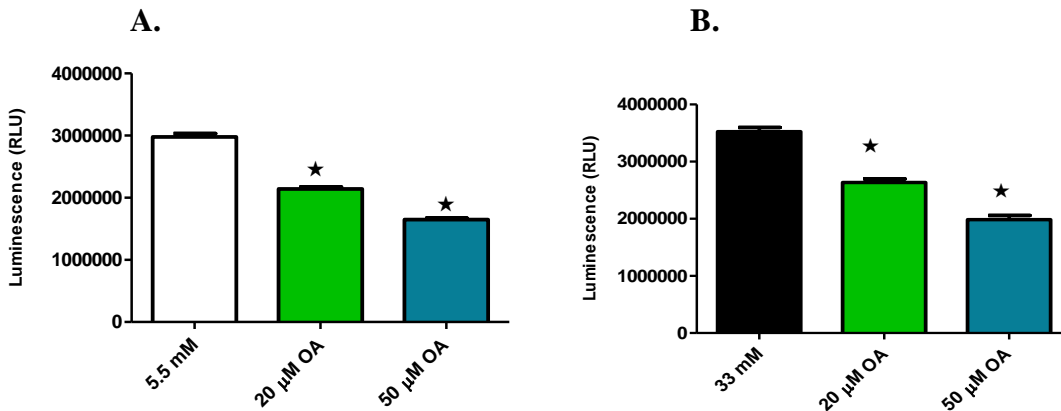


Figure 19: Effects of 6 hr OA treatment on caspase activity in H9C2 cell lines. Luminescence quantification for (A) normoglycaemic (B) hyperglycaemic cells as detected by *Caspase-Glo*[®] 3/7 assay described in section 3.2 of this chapter. Values are expressed as mean \pm SEM ($n=5$). * $p < 0.001$ vs. 5.5 mM and 33mM control groups, respectively.

We further elucidated the apoptotic effects of oleanolic acid in H9C2 cells, the cells were treated with 20 μ M and 50 μ M OA, respectively, for 24 hours. Low glucose-treated H9C2 cells showed a dose-dependent reduction in caspase-3 activity as reflected by a significant reduction on luminescence in relative light units (RLU) by $28 \pm 1.56\%$ and by $43 \pm 2.87\%$, respectively (n=5; p< 0.001 vs. 5.5 mM glucose group) for both 20 μ M and 50 μ M OA (Fig 20A). Subsequently, the high glucose-treated cells showed a significant decrease in luminescence by $19.95 \pm 2.47\%$ and by $43.67 \pm 4.15\%$, respectively (n=5; p< 0.001 vs. 33 mM glucose control) (Fig 20B).

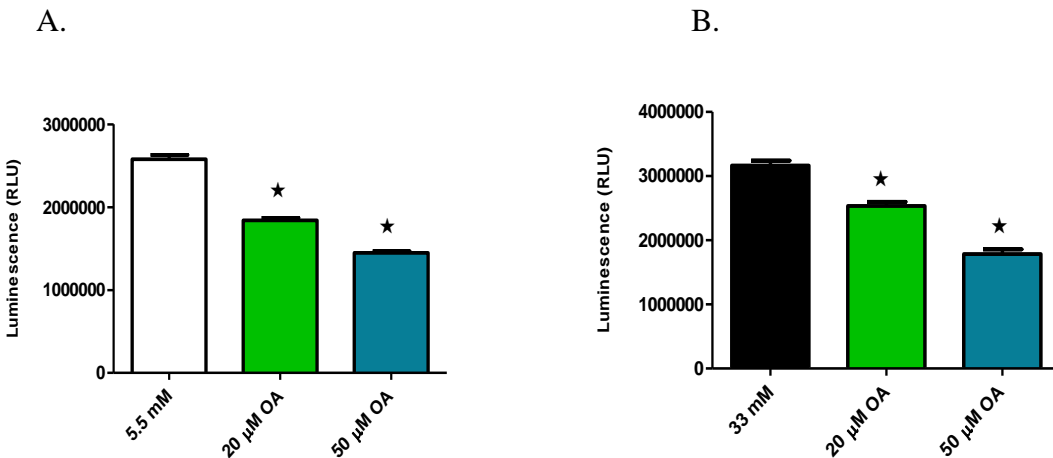


Figure 20: Effects of 24 hr OA treatment on caspase activity in H9C2 cell lines. Luminescence quantification for A) normoglycaemic B) hyperglycaemic cells as detected by *Caspase-Glo*[®] 3/7 assay described in section 3.2 of this chapter. Values are expressed as mean \pm SEM (n=5). * p< 0.001 vs. control non treated group.

3.4.2 Western blots for Caspase-3

We also employed Western blotting to quantify caspase-3 as a marker of apoptosis. Treatment of low glucose exposed cells with 20 μ M and 50 μ M OA showed a modest reduction in caspase-3 protein expression by $14.3 \pm 4.9\%$ and by $13.7 \pm 2.4\%$, respectively ($n=4$; $p < 0.05$ vs. 5.5 mM glucose (Fig 21 A)).

Exposure of H9C2 cells to high glucose for 54 hours had no significant difference on caspase 3 protein expression as compared to the normal glucose treated cells ($n=4$). For the 20 μ M OA treatment, oleanolic acid had no significant changes in caspase-3 expression in high glucose exposed H9C2 cells. However, 6 hour treatment with 50 μ M OA showed a marked reduction in caspase-3 expression by $19.6 \pm 7.3\%$ ($n=4$; $p < 0.05$ vs. 5.5 mM glucose) (Fig 21 B) in high glucose exposed H9C2 cells.

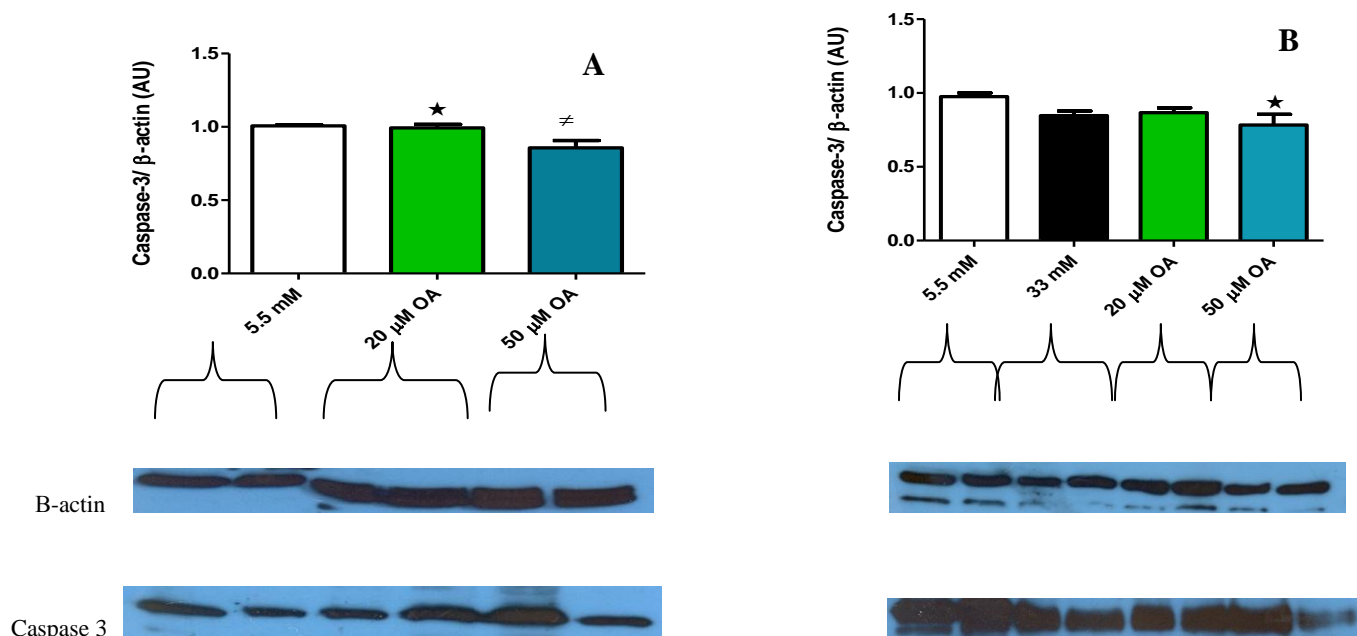


Figure 21: Effect of 6 hr OA treatment on caspase-3 protein in A) normal and B) high glucose exposed H9C2 cells. Caspase-3 quantification was determined as described earlier. The results are presented as the ratio of caspase-3 / β -actin in arbitrary units (AU). Values are expressed as means \pm SEM (n=4). * p < 0.05 vs. control, # p < 0.05 vs. 20 μ M OA treatment.

24 hours treatment of H9C2 cells with 20 μ M and 50 μ M OA showed anti-apoptotic effect of oleanolic in H9C2 cells exposed to low glucose. Here, caspase-3 protein expression was reduced to $14.3 \pm 4.5\%$ and $19.7 \pm 3.5\%$ ($n=4$; $p < 0.005$ vs. 5.5 mM glucose group) (Fig 22 A). High glucose did not induce apoptosis in H9C2 cell lines following 24 hour exposure (Fig 22 B). No significant differences were observed between 5.5 mM and 33 mM glucose treated groups (Fig 22 B). In addition, 20 μ M and 50 μ M OA concentrations showed no significant changes in the high glucose exposed H9C2 cells following 24 hours treatment with the bioactive compound (Fig 22 B).

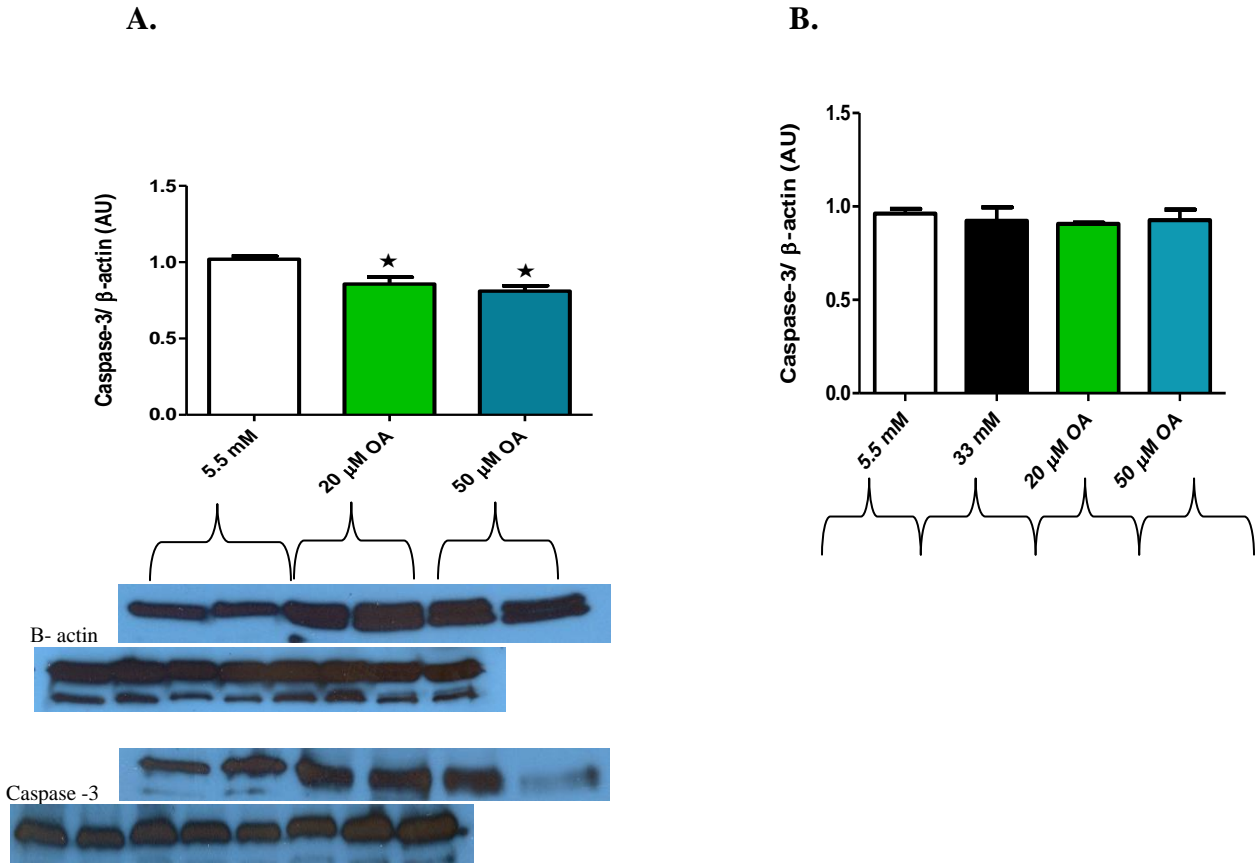


Figure 22: Effect of 24 hour OA treatment on caspase-3 protein expression in (A) normoglycaemic and (B) hyperglycaemia exposed H9C2 cells. Caspase-3 protein expression was quantified as described before. The results are presented as the ratio of caspase-3/ β-actin in arbitrary units (AU). Values are expressed as means ± SEM (n=4). * p< 0.05 vs. control groups.

3.4.3 Mitochondrial membrane potential

The effects of high glucose on the myocardium include mitochondrial membrane depolarisation due to increased oxidative stress leading to programmed cell death (Allen *et al.*, 2005). JC-1 ratio was measured using microscopy and flow cytometry as a measure of mitochondrial membrane potential. Microscopic analysis of H9C2 cells exposed to low glucose showed a $2 \pm 0.5\%$ ($n=9$ $p < 0.05$ vs. 5.5 mM glucose control) and $3.7 \pm 1.2\%$ ($n=9$) decrease in the JC-1 ratio following 6 hours treatment with both 20 μM and 50 μM OA (Fig 23 A). In parallel, flow cytometry analysis was conducted under similar treatment conditions. We found no significant changes for flow cytometric analysis (Fig 23 B).

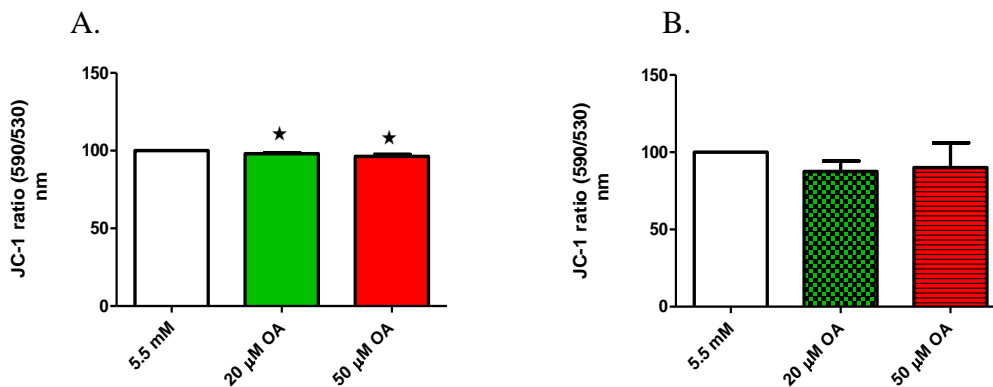


Figure 23: Effect of 6 hrs OA treatment on mitochondrial membrane potential in low glucose exposed H9C2 cells. Bar graphs represent (A) microscopic and (B) flow cytometric analyses. The results are presented as the ratio of red / green fluorescent signal measured at 590nm and 530 nm. Values are expressed as means \pm SEM ($n=9$ for Fig 23 A and $n= 4$ for Fig 23 B). * $p < 0.05$ vs. 5.5 mM glucose control.

We further investigated the effects of treatment of high glucose exposed cells with oleanolic acid for 6 hours. Here, we found no significant changes in the JC-1 ratio using the microscope (Fig 24 A) and flow cytometry (Fig 24 B) analysis.

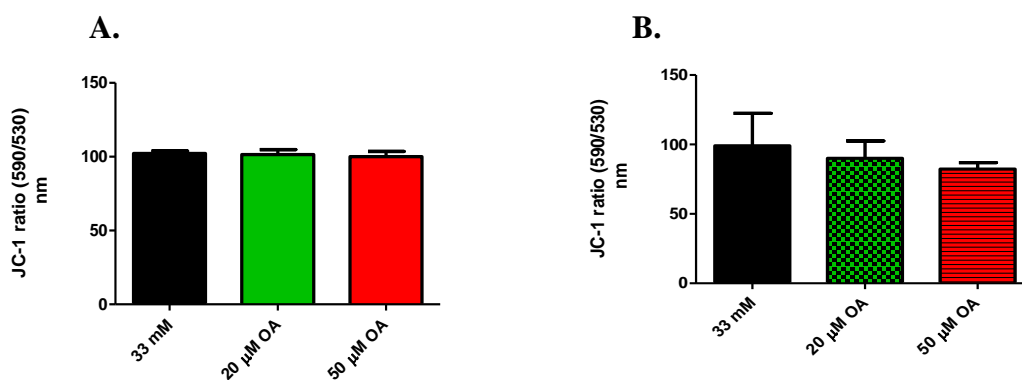


Figure 24: Effects of 6 hrs OA treatment on mitochondrial membrane potential in high glucose treated H9C2 cells. Bar graphs represents (A) microscopic and (B) flow cytometric analyses for the 6 h treated time points. Mitochondrial membrane potential was measured by JC-1 fluorescent assay. The results are presented as the ratio of red / green fluorescent signal measured at 590 nm and 530 nm. Values are expressed as means \pm SEM (n=9 for Fig 24 A and n= 4 for Fig 24 B).

Microscopic analysis of H9C2 cells initially exposed to low glucose followed by treatment with 20 μ M and 50 μ M OA, respectively, for 24 hours did not produce statistically significant changes for mitochondrial membrane potential (Fig 25 A) . In parallel, flow cytometric analyses (Fig 25 B) of 20 μ M and 50 μ M OA showed no significant changes in low glucose treated group in comparison to their control groups.

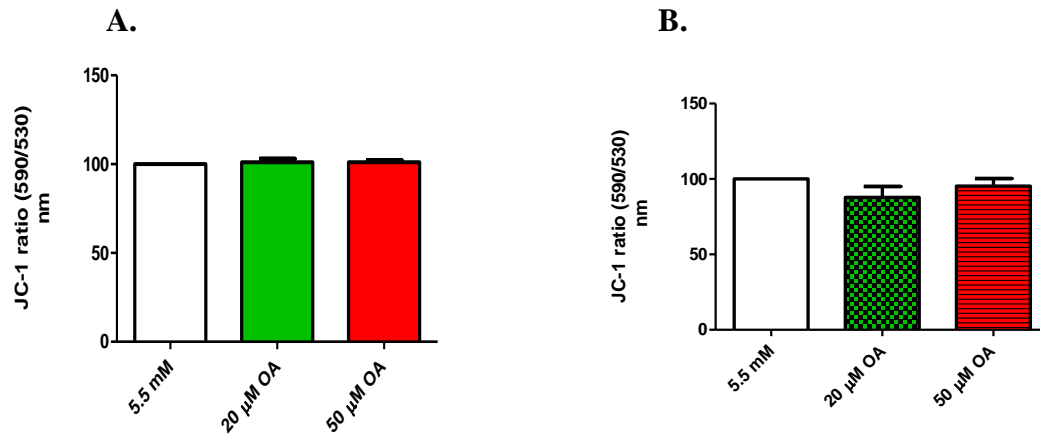


Figure 25: Effects of 24 hrs OA treatment on mitochondrial membrane potential in normoglycaemic treated H9C2 cells. Graphs represents (A) microscopic and (B) flow cytometric analysis for the 24 h treated time point. Mitochondrial membrane potential was measured by JC-1 fluorescent assay. The results are presented as the ratio of red / green fluorescent signal measured at 590 nm and 530 nm. Values are expressed as means \pm SEM (n=9 for Fig 25 A and n= 4 for Fig 25 B).

Treatment of high glucose-exposed cells with 20 μ M and 50 μ M OA for 24 hours had no effect on mitochondrial membrane potential as measured by qualitative and quantitative analyses (Fig 26 A and 26 B)

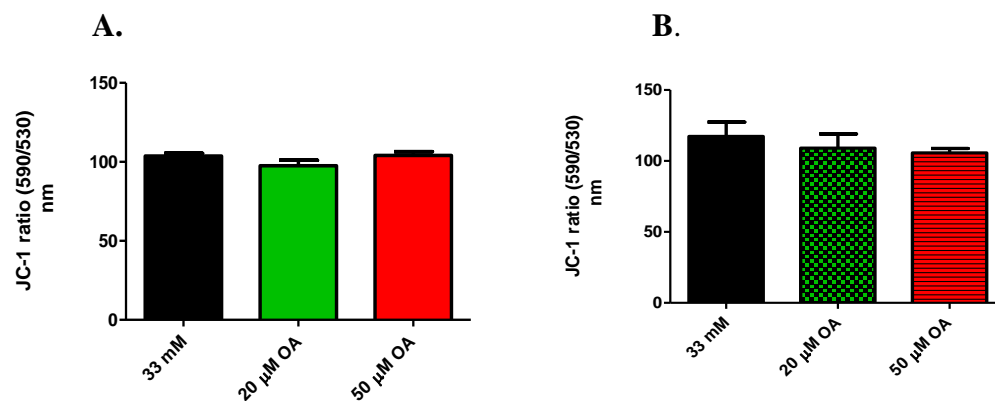


Figure 26: Effects of 24 hrs OA treatment on mitochondrial membrane potential in hyperglycaemia treated H9C2 cells. Bar graphs represents (A) microscopic and (B) flow cytometric analysis for 24 hr treatment time point. Mitochondrial membrane potential was measured by JC-1 fluorescent assay. The results are presented as the ratio of red / green fluorescent signal measured at 590 nm and 530 nm. Values are expressed as means \pm SEM (n=9 for Fig 26 A and n= 4 for Fig 26 B).

3.4.4 Annexin V- FITC staining

Annexin V- FITC was measured qualitatively as a marker of apoptosis. Treatment of H9C2 cells with high glucose for 54 hours (Fig 27 A) and 72 hours (Fig 27 B) had no significant effects on Annexin V-FITC staining compared to low glucose control groups.

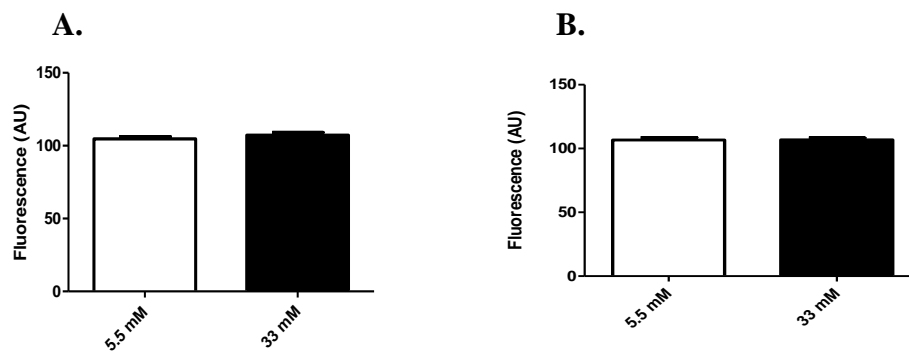


Figure 27: Effects of OA treatment on apoptosis in H9C2 cell line. Green fluorescence quantification of cells exposed to high glucose for (A) 54 hrs and (B) 72 hrs. Fluorescent quantification using Annexin V-FITC and PI staining for microscopic analysis. Values are expressed as mean \pm SEM (n=9).

Initially 6 hours treatment of H9C2 cells with 20 μ M and 50 μ M OA had no significant effect on FITC staining of H9C2 cells exposed to low glucose conditions (microscopic analysis) (Fig 28 A). No changes were observed in cells exposed to high glucose environment with the 20 μ M OA treatment (Fig 28 B). However, 50 μ M OA reduced the FITC signal in high glucose treated-cells (n=9, p< 0.05 vs. high glucose control) (Fig 28 B).

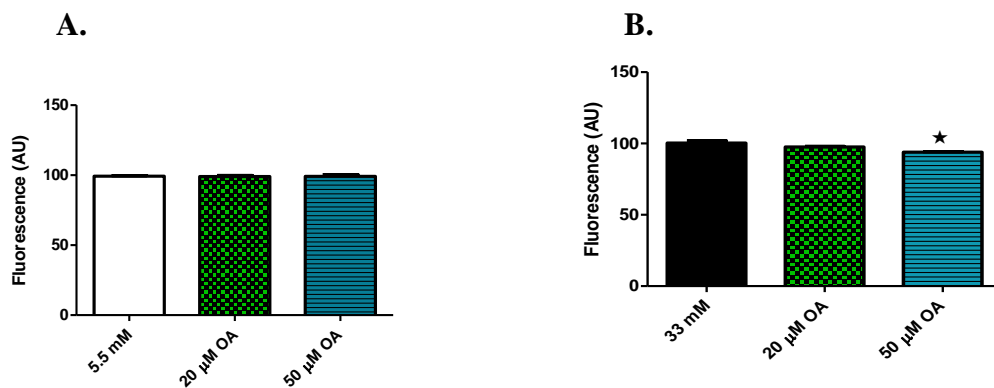


Figure 28: Effects of 6 hr OA treatment on apoptosis in H9C2 cell lines. Green fluorescence quantification of cells treated under (A) normoglycaemic and (B) hyperglycaemic conditions. Fluorescence quantification for Annexin V-FITC and PI staining using microscopic analysis. Values are expressed as mean \pm SEM (n=9). * p < 0.05 vs. 5.5 mM glucose group.

In parallel, we examined the effects of 24 hour OA treatment on FITC staining in H9C2 cells. Here, low glucose exposed H9C2 cell lines showed no significant difference with the 20 μ M OA treated group in comparison to 5.5 mM glucose control group. However, the 50 μ M OA treated group showed a $6.8 \pm 3\%$ decrease ($n=9$; p value of 0.08) vs. 5.5 mM glucose control (Fig 29A). Subsequently, H9C2 cells exposed to high glucose conditions showed a reduction in FITC fluorescent signal, i.e. $9.3 \pm 2.3\%$ and $8.9 \pm 1.1\%$ ($n=9$; $p < 0.05$ vs. 33 mM glucose,) following 24 hours of treatment with 20 μ M and 50 μ M OA, respectively (Fig 29B).

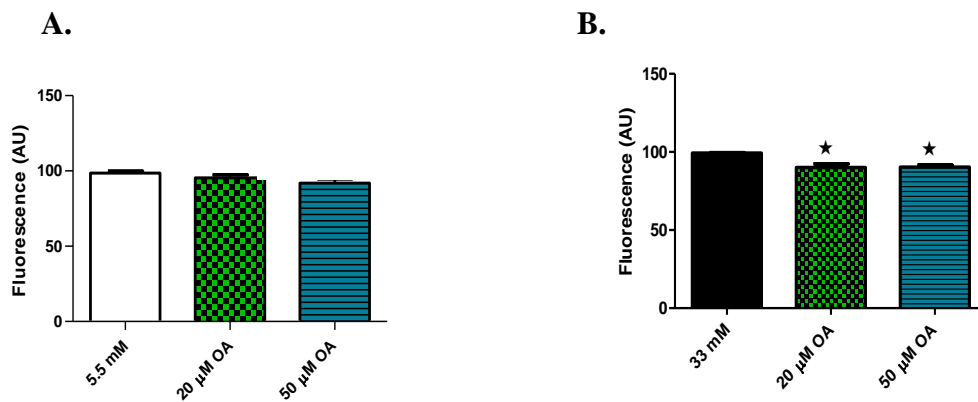


Figure 29: Effects of 24 hr OA treatment on apoptosis in H9C2 cell lines. Green fluorescence quantification of cells treated under (A) normoglycaemic and (B) hyperglycaemic conditions. Fluorescence quantification using Annexin V-FITC and PI staining for microscopic analysis. Values are expressed as mean \pm SEM ($n=9$). * $p < 0.05$ vs. 5.5 mM glucose group.

3.5 Discussion

Apoptosis or programmed cell death is observed both in physiological and pathophysiological conditions (Sharifi *et al.*, 2009). Physiological programmed cell death is required for elimination of cells that have lost growth control (Juan, 2006). However, in the myocardium apoptosis is detrimental and contributes to the onset of the diabetic cardiomyopathy and subsequently heart failure (Kumar and Sitasawad 2009). In DM, hyperglycaemia has been shown to induce apoptosis in the myocardium through ROS generation (Rajamani and Esoop 2010; Kumar and Sitasawad, 2009; Cai *et al.*, 2002).

In the current study treatment of the cardiomyocytes with high glucose increased caspase-3/7 activity. However, high glucose exposure did not result in any significant differences for other apoptotic markers e.g. Caspase-3 (Western blotting), Annexin V immunohistological staining, and mitochondrial membrane potential evaluation (6 and 24 hour timepoints).. We found that 54 hours and not 72 hours of hyperglycaemia resulted in increased ROS production in heart cells. However, in this study, we did not perform the cell viability assay to establish cell densitometry which could have accounted for the non significant changes observed at 72 hours (Mosman, 1983; Chiba *et al.*, 1997; Stephanou *et al.*, 2000).

3.5.1 Annexin V-FITC staining

Although mitochondrial membrane destruction is a basic indicator of cell death, it does not necessarily imply that preceding mechanism leads to cell death. Another approach is the employment of Annexin V – here loss of phospholipids asymmetry is detected experimentally by Annexin V binding to phosphatidyl serine (PS). This occurs through externalization of PS which

is an early event in apoptosis that occurs while the plasma membrane is relatively intact (Dallack *et al.*, 2008; Wang 2001)

Low glucose exposed cells displayed no cell death following 6 hours treatment using both the 20 μ M and 50 μ M OA doses. However, following 24 hours of OA treatment cells exhibited a trend towards increased death (p value of 0.08). However, we believe since this is not statistically different that it has no biological significance. Interestingly, 6 hour treatment with 50 μ M OA reduced fluorescence in high glucose exposed cells. As mentioned earlier, no significant changes were observed with the 33 mM glucose treated groups compared to the 5.5 mM glucose control group (for both 54 and 72 hour time points). Of note, decreased apoptosis for both 20 and 50 μ M OA doses (high glucose culturing conditions) is promising and supports an anti-apoptotic role for the OA compound. In support, previous studies by Teodoro showed that OA was most effective at the 50 μ M OA concentration - both under basal and insulin stimulated states in (INS-1 832/13) pancreatic β -cells (Teodoro *et al.*, 2008).

3.5.2 Mitochondrial membrane potential

The triterpenoids OA and UA have been shown to cause loss of mitochondrial membrane potential via disturbance of mitochondria membrane permeability (Yan *et al.*, 2010). Findings of this study where H9C2 cell lines cultured in low glucose medium showed no significant changes in membrane potential for both 6 and 24 hours after treatment with oleanolic acid. High glucose causes reduced membrane potential, a study conducted in 2009 with Human umbilical vein endothelial cells (Huvec) showed a marked reduction in mitochondrial potential following high glucose exposure (25 mM glucose) (Kumar and Sitasawad, 2009; Li *et al.*, 2009). OA

depolarised mitochondrial membrane potential ($\Delta\psi$) in cardiomyocytes subjected to ischemia (Wang *et al.*, 2009). In human derived cervical cells (HeLa) cells the oleanolic acid derivative was reported to reduce $\Delta\psi$ (Sun *et al.*, 2006). In our study exposure of cells with high glucose environment showed no significant changes in mitochondrial membrane potential as measured with the JC-1 lipophilic dye in comparison to low glucose treated control group. Our investigational compound did not have any significant effects on the high glucose treated cells; this is similar to the study conducted with two triterpenes (OA and UA) in human normal liver (L-02) cell line on apoptotic markers (Yan *et al.*, 2010). Therefore disruption of mitochondrial membrane potential may not always be present in apoptosis.

3.5.3 Western blots

Caspase activity can be demonstrated by Western blotting by using specific antibodies against caspase. Proteolytic cleavage and activation of effector caspases-3 can be observed by Western blotting. Caspase-3 is involved in downstream process in apoptosis (Sharifi *et al.*, 2009). OA has been shown to induce apoptosis in human liver cancer cell lines (Yan *et al.*, 2010). Our study showed that treatment of normal glucose exposed H9C2 cell lines with OA resulted in a reduction in caspase-3 protein expression. These effects were observed both at 6 and 24 hour time points. Therefore OA in low glucose treated H9C2 cell lines may have cardioprotective effects.

High glucose treatment of H9C2 cell lines has been shown to up regulate caspase-3 as an effector caspase in apoptosis (Rajamani and Essop, 2010). Our findings, however, showed no significant increases in caspase-3 protein when compared to the control groups. Therefore no apoptosis was observed in our model. This could be attributed to low sample size (n= 3-4). We believe that

increased sample size may have generated better statistical comparisons. Absence of apoptosis could also be attributed to the sensitivity of the probed substance. In a study with hepatocyte derived cellular carcinoma cell line (Huh7cells) where DNA fragmentation was quantified, this yielded more significant results on the apoptotic marker whereas in our study we probed for protein expression which may be less sensitive (Yan,*et al.*, 2010). Interestingly, 6 hour treatment with 50 μ M OA of H9C2 cells exposed to high glucose showed a reduction in caspase-3 proteins. However, this effect was not observed following treatment with oleanolic acid for 24 hours. Interestingly, these findings coincide with decreased FITC signal following treatment of high glucose exposed cells with 50 μ M OA for 6 hours (Fig 28 B). This reduction in FITC signal observed at the 6 hour time point may indicate the presence of apoptosis.

Technique sensitivity may also have a role in the absence of apoptosis in western blot analysis and annexin V-FITC staining which was immunohistochemically.

Western blot techniques have the disadvantage of measuring enzyme activity in a cell population and not in individual cells. This limitation is overcome by staining cells with specific antibodies (Fink and Cookson 2005). The caspase glo kit enzymatic activity assay produced significant results confirming the induction of apoptosis by high glucose induced oxidative stress this was concentration and dose dependent as shown by Cai (2002).

3.5.4 Caspase-3

Caspase-3 activity is detectable after the cell passes through a crucial commitment phase of apoptosis, during which time the apoptosome, composed of oligomerized Apaf-1/cytochrome

c/procaspase-9/(dATP/ATP), is assembled, providing the necessary components to advance a self-destructive cascade and ensuring cell death (Segal and Beem 2001). A more specific and comprehensive understanding of the mechanisms responsible for cell death requires delineation of the individual enzymatic and biochemical steps of execution (Yan *et al.*, 2010). Increased activity of caspases in cells may enhance apoptosis; this was observed in a study conducted by Yan *et al.*, 2010. Previous studies have showed that treatments with oleanolic acid or ursolic acid markedly elevated the activity of caspase-8, an upstream initiator, and caspase-3, a downstream effector in L-02 cancerous cells (Yan *et al.*, 2010). Contrary to this study, we found that OA reduced activity of caspase 3/7 in low glucose and high glucose exposed cells. The results observed with the caspase-glo assay confirm the anti- apoptotic effects of OA in H9C2 cells.

In conclusion, this study found that exposure of H9C2 cells to a high glucose environment increases oxidative stress, which in turn activated caspases and the induction of programmed cell death. We found that oleanolic acid exerts anti-apoptotic effects by reducing caspase-3 activity. Thus oleanolic acid shows great promise as a novel therapeutic agent, i.e. may alleviate cardiovascular complications associated with diabetes mellitus.

Chapter 4

4.1 General Discussion and Conclusion

The aim of the present study was to investigate whether plant derived oleanolic acid exerts anti-oxidant and anti-apoptotic effects in H9C2 cells exposed to a high glucose environment. Oxidative stress is one of early events that occur in diabetic cardiomyopathy and ROS is one of the main triggers of programmed cell death in the myocardium.

Exposure of H9C2 cells to high glucose environment for 54 hours increased ROS fluorescence. However, these effects were not changed following exposure to high glucose for 72 hours. We speculate that the cells exposed to high glucose for 72 hours did not exhibit significant fluorescence due to reduced cell density. However, our study showed that OA possesses antioxidative effects in low and high glucose-exposed cells together with the ability to decrease hyperglycaemia-induced apoptosis.

We further investigated the effects of oleanolic acid on programmed cell death markers. Here, we showed that treatment of the cardiomyocytes with high glucose increased caspase 3/7 activity, suggesting hyperglycaemia-induced cell death. However, the high glucose-induced caspase activity was abolished following treatment with OA. Likewise treatment with OA reduced Annexin- FITC signal in cells exposed to high glucose levels. The externalisation of phosphatidyl-serine is an early event in apoptosis, occurring while the plasma membrane is intact and this was measured by Annexin-FITC staining (Dallack *et al.*, 2008). Proteolytic cleavage and activation of effector caspase-3 is also observed during induction of programmed cell death. In this study we showed that OA inhibited externalisation of phosphatidyl serine and caspase-3 activation. Caspase-3 is an effector caspase involved in the downstream pathway of apoptosis

(Sharifi *et al.*, 2009) and its activity is only detectable after the cell passes through a crucial commitment phase of apoptosis.

In conclusion our results suggest that OA possesses antioxidant and anti-apoptotic properties that may serve as unique therapeutic strategies for diabetes and the diabetic cardiomyopathy.

4.2 Limitations and Recommendations for Future Studies

For the present study we did not use ROS-specific dyes to measure oxidative stress – this was due to financial constraints. Investigation into the effects of oleanolic acid on ROS generation using ROS-specific dyes should establish the exact mechanism of action of the bioactive compound. Furthermore, the use of Annexin kit for the detection of apoptosis is highly recommended. For our study we used immunohistochemical staining with antibodies specific for caspase-3. However, the Annexin kit is sensitive and should also add more weight to our current findings.

Despite these limitations we are of the opinion that our study opens up exciting therapeutic possibilities to treat diabetes and also diabetes-related heart diseases. The next stage of investigation will be to test whether these interesting findings are able to result in functional changes *in vivo* e.g. in response to an ischaemic insult.

Chapter 5

5.1 References

1. A´lvarez-Barrientos A, Arroyo J, ´Sar nombela RC and Sa´nchez-pe´rez M: Applications of flow cytometry to clinical microbiology. *Clin Micro Rev*: 167–195, 2000.
2. Abdel-Rahman MK and El-Megeid AA: Hepatoprotective Effect of Soapworts (*Saponaria officinalis*), Pomegranate Peel (*Punica granatum* L) and Cloves (*Syzygium aromaticum* linn) on Mice with CCl₄ Hepatic Intoxication. *World J of Chem* 1: 41-46, 2006.
3. Agbaje EO, Adeneye AA, and Daramola AO: Biochemical and toxicological studies of aqueous extract of *syzygium aromaticum* (l.) merr. and perry (myrtaceae) in rodents. *Afr J Trad Chem* 6: 241 – 254, 2009.
4. Alberti KG and Zimmet PZ: Definition, diagnosis and classification of diabetes mellitus and its complications. *Part 1: diagnosis and classification of diabetes mellitus provisional report of a WHO consultation*. *Diabet Med* 15: 539-53, 1998.
5. Allen DA, Yaqoob MM, Steven M, and Harwood SM: Mechanisms of high glucose-induced apoptosis and its relationship to diabetic complications. *J of Nutr Biochem* 16: 705–713, 2005.
6. Armstrong JS: Mitochondrial membrane permeabilization: the sine qua non for cell death. *Bio Essays* 28: 253–260, 2006.
7. Aronson D and Rayfield EJ: How hyperglycemia promotes atherosclerosis: molecular Mechanisms. *Cardiovasc Diabetol* 1: 1-10 2002.
8. Arulyan N, Rangasamy S, James E, and Pitcha D: A database for medicinal plants used in treatment of diabetes and its secondary complications. *Bioinformation* 2: 22-23, 2007.
9. Ashgar O, Al-sunni A, Khavandi K, Khavandi A, Withers S, Greenstein A, Heagerty AM, and Malik RA: Diabetic cardiomyopathy. *Clin Scie* 116: 741-760, 2009.
10. Avogaro A, de Kreutzenberg SV, Negut C, Tiengo A, and Scognamiglio P: Diabetic cardiomyopathy: A metabolic perspective. *Am J Cardiol* 93: 13A-16A, 2004.
11. Bai X, Qiu A, Guan J and Shi Z: Antioxidant and protective effect of an oleanolic acid enriched extract of *A. deliciosa* root on carbon tetrachloride induced rat liver injury. *Asia Pac J Clin Nutr* 16: 169-173, 2007.

12. Ballano E, Omerovic E, Svensson H, Waagstein F, and Fu M: Cardiac remodelling rather than myocardial energy metabolism is associated with cardiac dysfunction in diabetic rats. *Int J of Cardiol* 114: 195-201, 2007.
13. Banerjee S, Panda CK and Das S: Clove (*Syzygium aromaticum L*, a potential chemopreventive agent for lung cancer. *Carcinogenesis* 27: 1645–1654, 2006.
14. Barnard RJ and Youngren JF: Regulation of glucose transport in skeletal muscle. *Federation of Am Soc for Exp Biol Journal* 6: 3238-324, 1992.
15. Bar-Tana J: Peroxisome proliferator-activated receptor gamma (PPAR γ) activation and its consequences in humans. *Toxicol Lett* 120: 9, 2001.
16. BD Biosciences. Introduction to Flow Cytometry: A Learning Guide. Manual Part: 11-11032, 2000.
17. Belke DD, Betuing S, Martin J, Graveleau C. Young ME, Pham M, Zhang D, Donald RC, McClain C, Litwin SE, Taegtmeier H, Severson D, Kahn C, Rand E, and Abel D: Insulin signaling coordinately regulates cardiac size, metabolism, and contractile protein isoform expression. *J Clin Invest* 109: 629–639, 2002.
18. Bisset N: *Hearbal Drugs and Phytopharmaceuticals*. Stuttgart, Germany, CRC Press, 130-131, 1994.
19. Bonnefont-Rousselot D: Glucose and reactive oxygen species. *Curr Opin Clin Nutr Metab Care* 5: 561-568, 2002.
20. Bouché C, Serdy S, Kahn CR, and Goldfine AB: The cellular fate of glucose and its relevance in Type 2 diabetes. *Endo Rev* 25: 807-830, 2004.
21. Boudina S and Abel ED: Diabetic Cardiomyopathy Revisited. *Circulation* 115: 3213-3223, 2007.
22. Bradford MM: A rapid and sensitive method for the quantification of microgram quantities of protein utilizing the principle of protein-dye binding. *Anal Biochem* 72: 248-254, 1976.
23. Brownlee, M., *Biochemistry and molecular cell biology of diabetic complications*. Nature 414: 813-20. 2001.
24. Brownlee M. Banting Lecture 2004: The pathobiology of dibetic complications; a unifying mechanism. *Diabetes* 54: 1615-1625, 2005.

25. Brun RP, Tontonoz P, Forman BM, Ellis R, Chen J, Evans RM and Spiegelman BM: Differential activation of adipogenesis by multiple PPAR isoforms. *Genes and Development* 10: 974–984, 1996b.
26. Buchanan TA and Xiang AH: Gestational diabetes mellitus. *Diabetes* 115: 2796-803, 2005.
27. Buchanan TA, Xiang AH, Peters RK, Kjos SL, Marroquin A, Goico J, Ochoa C, Tan S, Berkowitz K, Hodis HN and Azen S: Preservation of pancreatic β -Cell function and prevention of type 2 diabetes by pharmacological treatment of insulin resistance in high-risk Hispanic women. *J of the Amer Diabet* 51: 2796-2803, 2002.
28. Cai L and Kang YJ: Oxidative stress and diabetic cardiomyopathy. *Cardiovasc. Toxicol* 3: 181-193, 2001.
29. Cai L, Li W, Wang G, Guo L, Jiang Y and Kang YJ: Hyperglycemia-induced apoptosis in mouse myocardium. Mitochondrial cytochrome c- mediated caspase-3 activation pathway. *Diabetes* 51: 1938-1, 2002.
30. Carr DB and Gabbe S: Gestational diabetes; detection, management, and implications. *Clin Diabetes* 16: 4–11, 1998.
31. Carvalho E, Kotani K, Peroni OD and Kahn BB: Adipose-specific overexpression of GLUT4 reverses insulin resistance and diabetes in mice lacking GLUT4 selectively in muscle. *Am J Physiol Endocrinol Metab* 289: E551–E561, 2005.
32. Chiba K, Kawakami K and Tohyama K: Simultaneous Evaluation of Cell Viability by Neutral Red, MTT and Crystal Violet Staining Assays of the Same Cells. *Toxicology in Vitro* 12: 251-258, 1998.
33. Chumakova OS, Zateřshchikov DA, Sidorenko BA: Apolipoprotein B: structure, function, gene polymorphism, and relation to atherosclerosis. *Kardiologija* 45: 43–55, 2006.
34. Couch RD, Browning RG, Honda T, Gribble GW, Wright DL, Sporn MB and Anderson AC: Studies on the reactivity of CDDO, a promising new chemopreventive and chemotherapeutic agent: implications for a molecular mechanism of action. *Bioorg. Med. Chem. Lett.* 15: 2215–2219, 2005.

35. Dallak MM, Mikhailidis DP, Haidara MA, Bin-Jalialh MI, Tork OM, Rateb MA, Yassin HZ, Al-refaie ZA, Ibrahim IM, Elawa SM, Rashed LA and Afifi NA: Oxidative Stress as a Common Mediator for Apoptosis Induced-Cardiac Damage in Diabetic Rats. *Cardiovas Medicine J* 2: 70-78, 2008.
36. DeWitt DE and Dugdale DC: Using new strategies in the treatments of diabetes: Clinical application. *JAMA* 289: 2265-2269, 2003.
37. Dhatariya K: People with type 1 diabetes using short acting analogue insulin are less dehydrated than those with using human soluble insulin prior to onset of diabetic ketoacidosis. *Medical Hypo* 71: 706–708, 2008.
38. Dinneen SF: What is diabetes? *Medicine*: 45-46, 2006.
39. Du X, Matsumura T, Edelstein D, Rossetti L, Zsengellér Z, Szabó C and Brownlee M: Inhibition of GAPDH activity by poly(ADP-ribose) polymerase activates three major pathways of hyperglycemic damage in endothelial cells. *J Clin Invest* 112: 1049-57, 2003.
40. Ducorps M, Ndong W, Jupkwo B, Belmejdoub G, Thiolet C, Mayaudon H and Bauduceau B: Diabetes in Cameroon. Classification difficulties in Africa. *Medicin Trop* 56: 264–270, 1996.
41. Dzubak P, Hajduch M, Vydra D, Hustova A, Kvasnica M, Biedermann D, Markova L, Urban M, and Sarek J: Pharmacological activities of natural triterpenoids and their therapeutic implications. *Nat Prod Rep* 23: 394-411, 2006.
42. Essop MF: Cardiac metabolic adaptations in response to chronic hypoxia. *J Physiol* 584: 715–726, 2007.
43. Fang ZY, Prins JB and Marwick TH: Diabetic Cardiomyopathy: Evidence, Mechanisms, and Therapeutic Implications. *Endo Rev* 25: 543-547, 2004.
44. Feuvray D and Darmellah A: Diabetes-related metabolic perturbations in cardiac myocyte. *Diabetes and Metab* 34: S3-S9, 2008.
45. Fink SL and Cookson BT: Apoptosis, Pyroptosis, and Necrosis: Mechanistic Description of Dead and Dying Eukaryotic Cells. *Infection and Immun* 73: 1907-1916, 2005.
46. Finkel T and Holbrook NJ. Oxidants, oxidative stress and the biology of ageing. *Nature* 408: 239–247, 2000.

47. Finkel T, Holbrook NJ: Oxidants, oxidative stress and the biology of ageing. *Nature* 408: 239–247, 2000.
48. Fiordaliso F, Cuccovillo I, Bianchi R, Bai A, Doni M, Salio M, De Angelis N, Ghezzi P, Latini R and Masson S: Cardiovascular oxidative stress is reduced by an ACE inhibitor in a rat model of streptozotocin-induced diabetes. *Life Sci* 79: 121–129, 2006.
49. Fong D: Changing times for the management of diabetic retinopathy. *Survey of ophthalmology* 47: S238-S245, 2002.
50. Frustaci, A, Kajstura J, Chimenti C, Jakoniuk I, Leri A, Maseri A, Nadal-Ginard B, and Anversa P.: Myocardial cell death in human diabetes. *Circ Res* 87: 1123-1132, 2000.
51. Fuentes O and Alarcón J: *Bauhinia candicans* stimulation of glucose uptake in isolated gastric glands of normal and diabetic rabbits. *Fitoterapia* 77: 271-275, 2006.
52. Garau C, Cummings E, Phoenix DA and Singh J: Beneficial effect and mechanism of action of *Momordica charantia* in the treatment of diabetes mellitus: A mini review. *Inter J of Diab and Metabol* 11:46-55, 2003.
53. Ghosh D, Thejomoorthy P and Veluchamy K: Anti-inflammatory and analgesic activities of oleanolic acid 3-/3-glucoside (RDG-1) from *Randia dumetorum* (Rubiaceae). *Indian J of Pharmacol* 15: 331-342, 1981.
54. Gill C, Mestrlil R and Samali A: Losing heart: the role of apoptosis in the heart disease-a novel therapeutic target? *Federal of European biochem soc J* 16: 135-146, 2002.
55. Goetz ME and Luch A: Reactive species: A cell damaging rout assisting to chemical carcinogens. *Cancer Letters* 266: 73–83, 2008.
56. Greenspan FS and Gardner DG: Basic and clinical endocrinology. 7th Ed Medical Publishing Division pg. 669, 2004.
57. Hafer K, Iwamoto KS and Schiest RH: Technical Advance; Refinement of the Dichlorofluorescein Assay for Flow Cytometric Measurement of Reactive Oxygen Species in Irradiated and Bystander Cell Populations. *Radiation Research* 169: 460–468, 2008.
58. Hall AP and Davies MJ: Assessment and management of diabetes mellitus. *Acute care:* 224-229, 2008.
59. Hannan JMA, Marenah L, Ali L, Rokeya B, Flatt PR and Abdel-Wahab YH: Insulin secretory actions of extracts of *Asparagus racemosus* root in perfused pancreas, isolated

- islets and clonal β -cells. *J of Endocrinol* 192: 159-168, 2007.
60. Hansson GK: Inflammation, Atherosclerosis, and Coronary Artery Disease. *N Engl J Med* 352: 1685-1695, 2005.
 61. Hayat SA, Patel B, Khattar RS and Malik RA: Diabetic cardiomyopathy: mechanisms, diagnosis and treatment. *Clin Sci* 107: 539-557, 2004.
 62. He A, Wang J, Gui C, Jiang Y, Sun Y and Chen T: Changes of mitochondrial pathway in hypoxia/ reoxygenation induced cardiomyocytes apoptosis. *Folia Histochemica ET Cytobio* 45: 397-400, 2007.
 63. He X, Chen MG and Ma Q: Activation of Nrf2 in defense against cadmium-induced oxidative stress. *Chem Res Toxicol.* 21: 1375–1383, 2008.
 64. Heginbotham A, Millay V and Quick M: The Use of Immunofluorescence Microscopy (IFM) and Enzyme-linked Immunosorbent Assay (ELISA) as Complementary .Techniques for Protein Identification in Artists' Materials. WAG Postprints—Portland, Oregon A, 2004.
 65. Hostettmann K and Marston A: Chemistry and Pharmacology of Natural Products: Saponins. Cambridge University Press, UK, 1995.
 66. Hotchkiss RS and Nicholson DW: Apoptosis and caspases regulate death and inflammation in sepsis. *Nature Rev Immunol* 6: 813-822, 2006.
 67. Hsu JH, Wu YC, Liu IM and Cheng JT: Release of acetylcholine to raise insulin secretion in Wistar rats by oleanolic acid one of the active principles contained in *Cornus officinalis*. *Neurosa Cell* 404: 112-116, 2005.
 68. Hue L *et al*: Regulation of glucose metabolism in cardiac muscle. *Biochem Soc Trans*, 2 311-4.1995
 69. Huang TH, Peng G, Kota BP, Li GQ, Yamahara J, Roufogalis BD and Li Y: Pomegranate flower improves cardiac lipid metabolism in a diabetic model: role of lowering circulating lipids. *Brit J of Pharmacol* 145: 767-774, 2005.
 70. Huss JM and Kelly DP: Mitochondrial energy metabolism: a question of balance. *J. Clin, Invest* 115: 547-555, 2005.
 71. Itakura H, Matsumoto A: Apolipoprotein B. *Nippon Rinsho* 52: 3113–8, 1995
 72. Johansen JS, Harris AK, Rychly DJ and Ergul A: Oxidative stress and the use of antioxidants in diabetes: Linking basic science to clinical practice. *Cardiovasc Diabetol* 4: 5, 2005.

73. Juan M, Park M, Lee HC, Kang YH, Kang ES and Kim SK: Antidiabetic agents from medicinal plants. *Curr Medici Chem* 13: 1203-1218, 2006.
74. Jung SJ, Kim DH, Hong YH, Lee JH, Song HN, Rho YD and Baek NI: Flavonoids from the flower of *Rhododendron yedoense* var. *poukhanense* and their antioxidant activities. *Arch. Pharm. Res* 30: 146-150, 2007.
75. Kaczmarczyk SJ, Andrikopoulos S, Favaloro J, Domenighetti AA, Dunn A, Ernst M, Grail MD, Fodero-Tavoletti M, Huggins CE, Delbridge LM Zajac JD and Proietto J: Threshold effects of glucose transporter-4 (GLUT4) deficiency on cardiac glucose uptake and development of hypertrophy. *J of Molec Endocrinol* 31: 449–459, 2003.
76. Khan MA, St Peter JV, Xue JL: A prospective, randomized comparison of the metabolic effects of pioglitazone or rosiglitazone in patients with Type 2 diabetes who were previously treated with troglitazone. *Diabetes Care* 25:708–711, 2002
77. Khan SA. Bitter gourd (*Momordica charantia*): A potential mechanism in anti-carcinogenesis of colon. *World J Gastroenterol* 13:1761-2, 2007.
78. Khavandi K, Khavandi A, Asghar O, Greenstein A, Withers S, Heagerty AM and Malik. RA: Diabetic cardiomyopathy – a distinct disease? *Best Practice and Research Clinical Endocrinology and Metabolism* 23: 347–360, 2009.
79. King GL and Loeken MR: Hyperglycemia-induced oxidative stress in diabetic complications. *Histochem Cell Biol* 122: 333–338, 2004.
80. Kodowaki T: Insights into insulin resistance and type 2 diabetes from knockout mouse models. *J of Clin Invest* 106: 459-465, 2000.
81. Kroemer G, Galluzi L and Brenner C: Mitochondrial permeabilization in cell death. *Physiol Rev* 87:99-163, 2007.
82. Kudzma DJ: Effects of thiazolidinediones for early treatment of type 2 diabetes mellitus. *American J of Managed Care* 8: S472-S482, 2002.
83. Kumar S and Sitasawad SL: N-acetylcysteine prevents glucose/glucose oxidase-induced oxidative stress, mitochondrial damage and apoptosis in H9C2 cells. *Life Scie* 84: 328–336, 2009.
84. Kuyvenhoven JP and Menders AE: Oxidative stress and diabetes mellitus. Pathogenesis of long term complications. *European J of Med* 10: 9-19, 1999.

85. Lashin O and Romani A: Mitochondria respiration and susceptibility to ischemia-reperfusion injury in diabetic hearts. *Arch Biochem Biophys* 420: 298-304, 2003.
86. Lashin OM, Szweda P, Szweda LI and Romani AM: Decreased complex II respiration and HNE-modified SDH subunit in diabetic heart. *Free Radical Biol Med* 40: 886-96, 2006.
87. Lee HK, Nam GW, Kim SH and Lee SH: Phytocomponents of triterpenoids, oleanolic acid and ursolic acid, regulated differently the processing of epidermal keratinocytes via the PPAR- α pathway. *Exper Dermatol* 15: 66-76, 2006.
88. Levrant S, Vannary-Bouchiche C, Pesse B, Pacher P, Fehl F and Waeber B: Peroxynitrite is a major trigger of cardiomyocytes apoptosis in-vivo and in-vitro. *Free Radio Biol Med* 41: 886-895, 2006.
89. Liu J: Pharmacology of oleanolic acid and ursolic acid. *J of Ethnopharmacol* 49: 57-68, 1995.
90. Liu L and Wang X: Improved Dissolution of Oleanolic Acid with Ternary Solid Dispersions. *AAPS Pharm Sci Tech* 8: 113-125, 2007.
91. Lopaschuk GD, Folmes CDL, Stanley WS: Cardiac Energy Metabolism in Obesity. *Circ Research* 101:335-347, 2007.
92. Mahato SB and Kundu AP: ^{13}C NMR Spectra of pentacyclic triterpenoids-a complication and some salient features. *Phytochemistry* 37: 1517-1573, 1994.
93. Mahley RW, Innerarity TL, Rall SC, Weisgraber KH: Plasma lipoproteins: apolipoprotein structure and function. *J. Lipid Res.* 2: 1277-94, 1985.
94. Mahomed IM and Ojewole JA: Hypoglycemic effect of *Hypoxis hemerocallidea* corm (African Potato) aqueous extract in rats. *Methods Find Exp Pharmacol* 25: 617-23, 2003.
95. Maiti R, Das UK and Ghosh D: Attenuation of hyperglycaemia and hyperlipidaemia in streptozotocin-induced diabetic rats by aqueous extract of seed *Tamarindus indica*. *Biol and Pharmacol Bulletin* 2: 1172-1176, 2005.
96. Mapanga RF, Tufts MA, Shode FO and Musabayane CT: Renal effects of plant-derived oleanolic acid in streptozotocin-induced diabetic rats. *Renal Fail* 31: 481-491, 2009.
97. McCune LM and Johns T: Antioxidant activity in medicinal plants associated with the symptoms of diabetes mellitus used by the indigenous peoples of the North American boreal forest. *Journal of Ethnopharmacol* 82: 197-205, 2002.

98. Meng X, Li ZM, Zhou YJ, Cao YL and Zhang J: Effect of the antioxidant alphalipoic acid on apoptosis in human umbilical vein endothelial cells induced by high glucose. *Clin Exp Med* 8: 43–49, 2008.
99. Miller EJ, Li J, Leng L, McDonald C, Atsumi T, Bucala R and Young LH: Macrophage migration inhibitory factor stimulates AMP-activated protein kinase in the ischaemic heart. *Nature* 451: 578–582, 2008.
100. Mishra TK and Rath PK: Diabetic Cardiomyopathy: Evidences, Pathophysiology, and therapeutic considerations. *JACM* 6: 312-318, 2005.
101. Mosmann T: Rapid colorimetric assay for cellular growth and survival: application to proliferation and cytotoxicity assays. *J Immunol Methods* 65: 55–63, 1983.
102. Musabayane CT, Bwititi PT and Ojewole JAO: Effects of oral administration of some herbal extracts on food consumption and blood glucose levels in normal and streptozotocin-treated diabetic rats. *Methods Find Exp Clin Pharmacol* 28: 223-228, 2006.
103. Musabayane CT, Mahlalela N, Shode FO, Ojewole JAO: Effects of *Syzygium cordatum* (Hochst.) [Myrtaceae] leaf extract on plasma glucose and hepatic glycogen in streptozotocin-induced diabetic rats. *J of Ethnopharmacol* 97: 485–490, 2005.
104. Nuttall SL, Kendal MJ and Martini U: Antioxidant therapy for prevention of cardiovascular disease. *J Med* 92: 239-244, 1999.
105. Ojewole JA, Kamadyaapa DR and Musabayane CT: Some *in vitro* and *in vivo* cardiovascular effects of *Hypoxis hemerocallidea* fisch and ca mey (hypoxidaceae) corm (African Potato) aqueous extract in experimental animal models. *Cardiovasc J S Afr* 17: 166-71, 2006.
106. Opie LH: Metabolism of the heart in health and disease. II. *Am Heart Journal* 77: 100–122, 1969.
107. Ormerod MG: The Study of Apoptotic cells by flow cytometry: *Leukemia* 12, 27 1013-25, 1998.
108. Orwa C, Mutua A, Kindt R, Jamnadass R and Anthony S: *Agro Forest Tree Database: A tree reference and selection guide version 4.0*. 2009.
109. Ovesn'a Z, Kozics K, and Darina Slameřnov'a D: Protective effects of ursolic acid and oleanolic acid in leukemic cells. *Mutation Research* 600: 31–137, 2006.

110. Pacher P, Bechman JS and Liaudet L: Nitric oxide and peroxynitrite in health and disease. *Physiol Rev* 87: 315-424, 2007.
111. Palters A, Ruch M: Davidson's diabetes mellitus: diagnosis and treatment. 5th ed. Souder's. pg 1, 53 and 133, 2004.
112. Park M, Ryu S, Kim DK, Lim J, Lee Z and Kim K: Fas-associated factor-1 mediates chemotherapeutic-induced apoptosis via death effector filament formation. *Int. J. Cancer* 115: 412–418, 2005.
113. Pinent M, Blay M, Bladé MC, Salvadó MJ, Arola L and Ardé: Grape seed-derived procyanidins have an anti-hyperglycaemic effect in streptozotocin-induced diabetic rats and insulin-mimetic activity in insulin-sensitive cell lines. *Endocrinology*; 145: 4985-4990, 2004.
114. Poornima IG, Parikh P, Shannon RP: Diabetic Cardiomyopathy: The Search for a Unifying Hypothesis. *Circ. Res* 98:596-605, 2006.
115. Prasad RC, Herzog B, Boonec B, Simsc L and Waltner-Lawa M: An extract of *Syzygium aromaticum* represses genes encoding hepatic gluconeogenic enzymes. *J Ethnopharmacol.* 96: 295-301, 2005.
116. Prince PS, Menon VP and Pari L: Hypoglycaemic activity of *Syzygium cumini* seeds: effect on lipid peroxidation in alloxan diabetic rats. *J of Ethnopharmacol* 61: 1-7, 1998.
117. Prosch H, Grois N, Prayer D, Waldhauser F, Steiner M, Minkov M and Gadner H: Central diabetes insipidus as presenting symptom of Langerhans cell histiocytosis. *Pediatr Blood Cancer* 43: 594-599, 2004.
118. Raff M: Cell suicide for beginners. *Nature* 396: 119-122, 1998.
119. Rajamani U and Essop MF: Hyperglycemia-mediated activation of the hexosamine biosynthetic pathway results in myocardial apoptosis. *Am J Physiol Cell Physiol* 299: C139–C147, 2010.
120. Rao AA: Identification of Biomarkers for Type 2 Diabetes and Its Complications: A Bioinformatic Approach, 1-25, 2007.
121. Rao BK and Rao CH: Hypoglycemic and antihyperglycemic activity of *Syzygium alternifolium* (wt) Walp seed extracts in normal and diabetic rats. *Phytomedicine* 8: 88-93, 2001.

122. Rastogi RP, Rajeshwar R, Sinha P: Apoptosis: Molecular mechanisms and pathogenicity: Excli Journal 8:155-181, 2009.
123. Rastogi RP, Sinha RRP: Apoptosis: Molecular mechanisms and pathogenicity. EXCLI J 8:155-181, 2009.
124. Regula KM, Ens K and Kirshenbaum LA: Mitochondria-assisted cell suicide: a license to kill. J of Mol and Cell Cardiol 35: 559–567, 2003.
125. Rodrigues B, Cam MC and McNeill JH: Myocardial substrate metabolism: implications for diabetic cardiomyopathy. J Mol Cell Cardiol 27: 169-179, 1995.
126. Rolo AP and Palmeira CM: Diabetes and mitochondrial function: Role of hyperglycemia and oxidative stress. Toxicol and App Pharmacol 212:167-178, 2006.
127. Rotondo D and Davidson J: Prostaglandin and PPAR control of immune cell function. Immunol 105: 20-22, 2002.
128. Rubler S, Dlugash J, Yuceoglu YZ, Kumral T, Branwood AW and Grishman A: New type of cardiomyopathy associated with diabetic glomerulosclerosis. Am J Cardiol 30: 595–602, 1972.
129. Sardão VA, Oliveira PJ, Holy J, Oliveira CR and Wallace KB. Vital imaging of H9c2 myoblasts exposed to *tert*-butylhydroperoxide – characterization of morphological features of cell death *BMC Cell Biology*, 8:11. 2007.
130. Sadeghi MM: The pathobiology of the vessel wall: Implications for imaging. J of Nucl Cardiol 13: 402-414, 2006.
131. Scalbert A, Johnson IT, and Saltmarsh M: Polyphenols: antioxidants and beyond. Am J Clin Nutr 81: 215S–217S, 2005.
132. Schulze-osthoff S, Ferrari D, Los M, Wesselborg S and Peter ME: Apoptosis signaling by death receptors. Eur J Biochem 254: 439-459, 1998.
133. Segal MS and Beem E: Effect of pH, ionic charge, and osmolality on cytochrome *c*-mediated caspase-3 activity. Am J Physiol Cell Physiol 281: C1196–C1204, 2001.
134. Senthil S, Sridevi M and Pugalendi KV: Cardioprotective effects of oleanolic acid on isoprenol- induced myocardial ischemia in rats. Toxicol Pathol 35: 418-423, 2007.
135. Sharifi AM, Eslami H, Larijani B and Davoodi J: Involvement of caspase-8, -9, and -3 in high glucose-induced apoptosis in PC12 cells. Neurosci Lett 45: 47-51, 2009.

136. Sharma V and McNeil JH: Diabetic cardiomyopathy. Where are we 20 years later? *Can J Cardiol* 22: 305-308, 2006.
137. Shirpoor A, Salamib S, Khadem-Ansarib MH, Ilkhanizadeh C: Cardioprotective effect of vitamin E: rescues of diabetes-induced cardiac malfunction, oxidative stress, and apoptosis in rat. *J of Diabetes and Its Compl* 23: 310–316, 2009.
138. Shishodia S, Majumdar S, Banerjee S and Aggarwal BB: Ursolic acid inhibits nuclear factor-kappa B activation induced by carcinogenic agents through suppression of IkappaB alpha kinase and p65 phosphorylation: correlation with down-regulation of cyclo-oxygenase 2, matrix metalloproteinase 9, and cyclin D1. *Cancer Research*; 63: 4375-4383, 2003.
139. Smart RC and Hodgson E: *Molecular and Biochemical Toxicology*. 4th ed. Hoboken, New Jersey: John Wiley and Sons, Inc. 119-120, 295-296, 310, 555, 587, 693-702, 2008.
140. Somova L, Shode FO, Nadar A and Rammana P: Antihypertensive, anti-atherosclerotic and antioxidant activity of triterpenoids isolated from *Olea europea* subspecies *Africana* leaves. *J Ethnopharmacol* 84: 299-305, 2003.
141. Somova LO, Nadar A, Rammanan P and Shode FO: Cardiovascular, antihyperlipidemic and antioxidant effects of oleanolic and ursolic acids in experimental hypertension. *Phytomedicine* 10: 115-121, 2003.
142. Stangeland T, Dhillion SS and Reksten H: Recognition and development of traditional medicine in Tanzania. *J of Ethnopharmacol* 117: 290-299, 2008.
143. Stenbit AE, Tsao T, Li J, Burcelin R, Geenen D, Factor SM, Houskecht K, Katz EB and Charron M. GLUT 4 heterozygous knockout mice develop muscle insulin resistance and diabetes. *Nature Med* 3: 1096-1011, 1997.
144. Stephanou A, Brar B, Liao Z, Scarabelli T, Knight RA and Latchman DS: Distinct initiator caspases are required for the induction of apoptosis in cardiac myocytes during ischaemia versus reperfusion injury. *Cell Death Differ*. 8: 434–435, 2001.
145. Stephens JW, Khanolkar MP and Bain SC: The biological relevance and measurement of plasma markers of oxidative stress in diabetes and cardiovascular disease. *Atherosclerosis* 202: 321-329, 2009.

146. Sun H, Zheng Q and Tu J: Induction of apoptosis in HeLa cells by 3 β -hydroxy-12-oleanen-27-oic acid from the rhizomes of *Astilbe chinensis*. *Bioorganic Medicinal Chemistry* 14: 1189–1198, 2006.
147. Teixeira CC, Pinto LP, Kessler FH, Knijnik L, Pinto CP, Gastaldo GJ and Fuchs FD: The effect of *Syzygium cumini* (L.) skeels on post-prandial blood glucose levels in non-diabetic rats and rats with streptozotocin-induced diabetes mellitus. *J of Ethnopharmacol* 56 :209–213, 1997.
148. Teodoro T, Zhang L, Alexander T, Yue J, Vranic M and Volchuk A: Oleanolic acid enhances insulin secretion in pancreatic β -cells. *FEBS* 582:1375-1380, 2008.
149. Tiwari AK and Rao JM: Diabetes mellitus and multiple therapeutic approaches of phytochemicals: Present status and future prospects. *Curr Sci* 83:30-38, 2002.
150. Trost S and LeWinter M: Diabetic cardiomyopathy. *Curr Treat Opt Cardiovasc Med* 3: 481–492, 2001.
151. Van Wyk BE, Van Oudtshoorn B, Gericke N: Medicinal plants of South Africa. 1st ed. Briza Publications, South Africa. 1-302,1997.
152. Wang GW, Klein JB and Kang YJ: Metallothionein inhibits doxorubicin-induced mitochondrial cytochrome c release and caspase-3 activation in cardiomyocytes. *J Pharmacol Exp Ther* 298:461-468, 2001.
153. Wang H, Wang Z, Gou W: Comparative determination of ursolic acid and oleanolic acid of *Macrocarpium officinalis* (Sieb. et Zucc.) Nakai by RP-HPLC. *Indust Crops and Prod* 28: 328–332, 2008.
154. Wang J, Ma H, Zhang X, He L, Gao X, Ren J and Li J: A novel AMPK activator from Chinese herb medicine and ischemia phosphorylate the cardiac transcription factor FOXO. *Int Physiol Pathophysiol Pharmacol* 1: 116- 126, 2009.
155. Wang J, Song Y, Wang Q, Kralik P and Epstein M: Causes and characteristics of diabetic cardiomyopathy. *The Rev Diabetic Studies* 3: 108-117, 2006.
156. Wang X, Ye X , Liu R, , Chen H, Bai H, Liang X, Zhang X, Wang Z, Li W and Hai C: Antioxidant activities of oleanolic acid in vitro: Possible role of Nrf2 and MAP kinases. *Chemico-Biological Interactions* 184: 328–337, 2010.
157. Wang X: The expanding role of mitochondria in apoptosis. *Genes and Develop* 15:2922–2933, 2001.

158. Wiernsperger NF: Is non-insulin dependent glucose uptake a therapeutic alternative? Part 1: Physiology, mechanisms and role of non-insulin dependent glucose uptake in type 2 diabetes. *Diabetes Metabol* 31: 415-426, 2005.
159. William MD, Salle D and Robinson M: Diabetic ketoacidosis in toddler with a diaper rash. *Ame J of Emerg Med* 26: 834.e1–834.e2, 2008.
160. Wold LE, Ceylan-isik AF and Ren J: Oxidative stress and stress signaling: menace of diabetic cardiomyopathy. *Acta Pharmacol Sinica* 26: 908-917, 2005.
161. World Health Organisation (WHO). *The World Health Report 2002: Working Together for Health*, 2002.
162. Yan S, Huang C, Wua S and Yin M: Oleanolic acid and ursolic acid induce apoptosis in four human liver cancer cell lines. *Toxico in Vitro* 24: 842–848, 2010.
163. Yoshikawa M and Matsuda H: Antidiabetogenic activity of oleanolic acid glycosides from medicinal foodstuffs. *Biofactors* 13:231–237, 2000.
164. Young ME, McNulty P, Taegtmeyer H. Adaptation and Maladaptation of the heart in diabetes: part II: potential mechanisms. *Circulation* 105: 1861–1870, 2002.
165. Zhang DX, Fryer RM, Hsu AK, Zou AP, Gross GJ and Campbell WB: Production and metabolism of ceramide in normal and ischemic-reperfused myocardium of rats. *Basic myocardium of rats. Basic Res Cardiol* 96: 267-74, 2001.